Mechanisms of HIV-associated neurotoxicity: Tat-induced synapse loss and recovery

A DISSERTATION SUBMITTED TO
THE FACULTY OF THE GRADUATE SCHOOL
OF THE UNIVERSITY OF MINNESOTA
BY

ANGELA HAIJUNG BRUNNER

IN PARTIAL FULFILLMENT OF THE REQUIREMENTS
FOR THE DEGREE OF
DOCTOR OF PHILOSOPHY

STANLEY A. THAYER, ADVISOR

MAY, 2013

Acknowledgements

Thank you, first and foremost, to my advisor, Dr. Stanley Thayer. Your guidance and mentorship throughout my career were invaluable. You were a patient, kind, genuine, and professional leader, and I would never have become the scientist I am today without such an exceptional role model. You show every day what it means to not only be a scientist of integrity, but also a good and compassionate person, and I consider myself exceedingly lucky to have had you as my teacher.

Thank you to the wonderful members of my thesis committee: my chair, Dr. Kevin Wickman, Dr. Jonathan Marchant, and Dr. Lorene Lanier. Your time, constructive support, and genuine and caring guidance were immensely appreciated in all aspects of my work. Thank you for helping to make me a better scientist.

Thank you to all the members of the Thayer lab, both past and present, for your advice, camaraderie, coffee breaks, and friendship. In particular, my thanks go out to Dr. Hee Jung Kim, who mentored me through my first years as a student and taught me how to navigate the lab.

A special thank you to the members of my graduate school cohort, Tiffany, Daniel, Jeff, Mike, Jerid, Katya, and Kelsey. You made the trials of graduate school easier to bear, and the victories that much more special.

Thank you to all my friends and family, who cheered me on and supported me for all these years. A special thanks to my father, the original Ph.D., who has always encouraged me to do my best in life.

And finally, I have to thank my husband Mike, who followed my scientific dreams to Minnesota, believed in my abilities, and endured the journey with me. I could never have done it without your unfailing love and support.

The work in this dissertation would not be possible without financial contributions from multiple sources. Dr. Thayer is supported by NIH grant R37 DA 07304. I have been supported by NIDA grant T32 DA07234, as well as multiple fellowships from the University of Minnesota Graduate School.

Abstract

HIV infection is a worldwide pandemic. A debilitating neurological consequence of HIV infection is progressive cognitive decline, known as HIV-associated neurocognitive disorders (HAND). HAND afflicts up to 50% of all HIV patients to varying degrees, and as survival of HIV patients improves with current antiretroviral therapies, the prevalence of HAND is also increasing. This, coupled with the lack of current effective HAND therapies, creates a dire need to understand the mechanisms underlying the cognitive decline associated with HIV. HAND symptoms correlate closely with processes of neuronal injury, which are early events that precede overt neuronal death. One such injurious process is synapse loss. The HIV protein transactivator of transcription (Tat) is a neurotoxic viral protein released from infected cells into the central nervous system. Tat contributes to the pathologies seen in HAND patients, and induces loss of excitatory synapses between rat hippocampal neurons in culture. Using an innovative live cell imaging assay, our laboratory has previously shown that Tat induces reversible synapse loss via a pathway that is distinct from cell death.

In this dissertation, I outline three studies that stem from the current knowledge involving Tat-induced synapse loss. First, I assessed how subunit selectivity influenced N-methyl-D-aspartate (NMDA) receptor activity on the toxic effects of Tat. A pharmacological study showed that GluN2A-containing NMDA receptors had distinct and opposing effects as compared to GluN2B-containing NMDA receptors when modulating Tat-induced cell death, as well as Tat-induced synapse loss and subsequent synapse recovery. Intriguingly, inhibition of GluN2B-containing NMDA receptors induced synapse recovery after Tat-induced synapse loss, indicating a role for tonic suppression of recovery by GluN2B-containing receptors.

Second, I determined the effects of Tat exposure on presynaptic terminals. Tat

induced loss of presynaptic terminals concurrent with loss of postsynaptic densities. This loss of presynaptic terminals was dependent on postsynaptic mechanisms, and the integrity of postsynaptic densities was required to maintain the presence of presynaptic terminals after Tat exposure. Tat-induced loss of presynaptic terminals was reversible, and this reversal was dependent on postsynaptic activity as well.

Finally, I determined the molecular mechanisms of synapse recovery downstream of GluN2B-containing NMDA receptors. After Tat-induced synapse loss, GluN2B-containing NMDA receptors were persistently activated, suppressing synapse recovery by activation of neuronal nitric oxide synthase. The subsequent production of nitric oxide stimulated cGMP production by soluble guanylyl cyclase. Protein kinase G was activated and phosphorylated an actin-associated protein during persistent Tat exposure.

These studies elucidated important information regarding the mechanisms by which HIV Tat exerts its neurotoxic effects, emphasizing the importance of subunit composition when determining toxic or beneficial effects of NMDA receptor activation as well as unmasking the importance of the postsynaptic density as the central target of Tat's effects. Furthermore, these studies highlight the reversibility of synapse loss and uncover a new role for the canonical NO/cGMP/PKG pathway in modulating synapse recovery downstream of GluN2B-containing NMDA receptors. Tat-induced synapse loss and subsequent recovery can correlate to symptoms of cognitive decline seen in HAND. Targeting these mechanisms can shed new light on therapeutic strategies to treat HAND patients.

Table of Contents

List of Figures

Abbreviations

AIDS, Acquired Immunodeficiency Syndrome

ANOVA, analysis of variance

BAPTA-AM, 1,2-bis(o-aminophenoxy)ethane- N,N,N',N'-tetraacetic acid, acetoxymethyl ester

BSA, bovine serum albumin

Ca^{2+}, calcium

CDK9, cyclin dependent kinase 9

cDNA, complementary deoxyribonucleic acid

cGMP, cyclic guanosine monophosphate

CNS, central nervous system

CO_2, carbon dioxide

DMEM, Dulbecco's Modified Eagle's Medium

DNA, deoxyribonucleic acid

FBS, fetal bovine serum

FITC, fluorescein isothiocyanate

GFP, green fluorescent protein

HAART, highly active antiretroviral therapies

HAND, HIV-associated neurocognitive disorders

HEPES, hydroxyethyl piperazineethanesulfonic acid

HHSS, HEPES-Hanks salt solution

HIV, Human Immunodeficiency Virus type 1

HS, horse serum

L-NAME, L-NG-nitroarginine methyl ester

LRP, low density lipoprotein receptor-related protein

mRNA, messenger ribonucleic acid

NMDA, N-methyl-D-aspartate

NMDAR, N-methyl-D-aspartate receptor

nNOS, neuronal nitric oxide synthase

NO, nitric oxide

PI, propidium iodide

PKG, protein kinase G

PSD, postsynaptic density

PSD95, postsynaptic density protein 95

RAP, receptor-associated protein

RNA, ribonucleic acid

SEM, standard error of mean

sGC, soluble guanylyl cyclase

Syn, synaptophysin

TAK, transactivator kinase complex

TAR, Tat activation region

Tat, transactivator of transcription

TRITC, tetramethylrhodamine isothiocyanate

VASP, vasodilator-associated phosphoprotein

Summary of Published Manuscripts

1. Shin A.H., Kim H.J., and Thayer S.A. (2012) Subtype selective NMDA receptor antagonists induce recovery of synapses lost following exposure to HIV-1 Tat. Br J Pharmacol, Jun; 166(3):1002-17.

2. Shin A.H., and Thayer S.A. (2013) HIV-1 Tat induces excitotoxic loss of presynaptic terminals in hippocampal cultures. Mol Cell Neuroscience, Jan; 54: 22-29.

Chapter One:

Introduction

I. HIV virology and pathogenesis

Over 30 million people worldwide are currently infected with human immunodeficiency virus type 1 (HIV) (UNAIDS, 2010). HIV is a lentivirus from the family *Retroviridae,* a large group of single stranded RNA viruses (Morse et al., 2003). The viral structure of HIV is comprised of a lipid envelope that encases a dense core. Associated with this core is a capsid and nucleocapsid that contain duplicate copies of the HIV RNA genome, an approximately 10 kilobyte single strand of RNA complexed with various viral proteins necessary for replication (Morse et al., 2003). This RNA genome is tightly packaged within the virion core, and protected from degradation by RNAses present in bodily fluids. As a result of this durability, the measurement of HIV RNA levels is central to monitoring disease progression and patient response to therapy (Carpenter et al., 2000). The HIV viral envelope contains the glycoproteins gp41 and gp120, which are essential for recognition of host cells that are positive for the CD4 receptor and a corresponding co-receptor, either CCR5 or CXCR4 (Wyatt et al., 1998; Greene and Peterlin, 2002). Binding of the envelope glycoproteins to the host cell receptors initiates fusion of the viral envelope with the target cell's plasma membrane via a series of conformational changes mediated by a helix coiled-coil mechanism (Chan and Kim, 1998).

The HIV viral life cycle is characterized by ten distinct steps: attachment to the host cell, viral fusion with the host membrane, uncoating of the nucleocapsid, reverse transcription of the viral RNA genome, integration of viral cDNA into the host genome, transcription of viral RNA using host machinery, translation of viral proteins, assembly and budding of immature virus, and extracellular maturation (Greene and Peterlin, 2002; Morse et al., 2003; Stevenson, 2003). There are several nonstructural HIV proteins that regulate viral replication. One of these proteins is transactivator of transcription, or Tat,

which increases the transcription rate of viral cDNA by binding to RNA polymerase (Greene and Peterlin, 2002; Stevenson, 2003). Others include viral protein R (vpr), which enhances viral replication in nonreplicating cells, and virion infectivity protein (vif), which is essential to properly assemble the viron core (Cohen et al., 1990; Goncalves et al., 1996). Once the virus has replicated, it is released into the bloodstream to target other host cells and continue the replication process. HIV viral replication and turnover in infected calls can occur as often as every two days (Perelson et al., 1996).

HIV is classified into nine separate subtypes, or clades, based on the diversity of the viral envelope: A, B, C, D, F, G, H, J, and K (Sacktor et al., 2007). The vast majority of HIV patients in the Americas, Australia, and Europe are infected with clade B, although it is distributed in varying degrees worldwide. In contrast, clade C, which comprises over 49% of worldwide HIV infections, is primarily found in southern and eastern Africa, India, Nepal, and China (Liner et al., 2007). The particular clade of HIV can affect its infectivity rates and its susceptibility to antiretroviral drugs, as well as the extent of disease progression. HIV clade B has been shown to be more neurotoxic in an *in vivo* model as compared to HIV clade C (Rao et al., 2008). Further viral classification of HIV divides the virus into two categories based on the specific host co-receptor that is required in addition of CD4 to facilitate binding of the viral envelope to the host cell, i.e., the viral tropism. T-tropic, or syncytium forming virus recognizes CXCR4, a G-protein coupled receptor. M-tropic, or macrophage-tropic virus recognizes CCR5, also a G-protein coupled receptor. Dual tropic viruses have also been found that can bind to either co-receptor in addition to CD4 (Berger et al., 1999). The genetic and tropic diversity of HIV complicate the development of effective treatment for viral infection.

HIV transmission occurs most commonly via sexual contact, sharing of contaminated needles and syringes, and transfusion of contaminated blood and other

bodily fluids (Chin and Ascher, 2000). HIV infection presents initially as an acute influenza-like illness, with symptoms such as fever, fatigue, and rash, which may persist for days to several weeks (Kahn and Walker, 1998). Subsequently, however, the infection may become asymptomatic for a period of years, until eventual progression to the late clinical stage known as Acquired Immunodeficiency Syndrome (AIDS) (Chin and Ascher, 2000; UNAIDS, 2010). AIDS is defined as the stage of HIV infection when the level of CD4-positive lymphocytes is either less than 200 cells per cubic millimeter, or less than 14% of total lymphocyte counts (Chin and Ascher, 2000). AIDS patients, due to the severity of lymphocyte depletion, are vulnerable to a spectrum of opportunistic infections, such as *pneumocystis carinii* pneumonia, Kaposi's sarcoma, and *mycobacterium* tuberculosis (Morse et al., 2003). The systemic nature of HIV-induced immunosuppression indicates that nearly all organ systems are vulnerable; dermatologic lesions, oral and gastrointestinal infections, and a range of neurological disorders are commonly seen in AIDS patients (Morse et al., 2003).

II. Treatment of HIV

The recommended therapy for patients diagnosed with HIV is to immediately begin a multi-drug regimen known as highly-active anti-retroviral therapy (HAART); without HAART, the majority of HIV patients will eventually develop AIDS (Chin et al., 2007; OARAC, 2013). HAART was introduced beginning in 1996-1998 as mainline therapy for HIV-infected patients (Kaplan et al., 2000). This therapy involves the combined administration of at least 3 separate antiretroviral drugs, including nucleoside reverse-transcriptase inhibitors, nonnucleoside reverse-transcriptase inhibitors, integrase inhibitors, and protease inhibitors (Kaplan et al., 2000; OARAC, 2013). All HIV antiretroviral drugs serve as viral inhibitors; they each target a distinct step in the HIV

viral life cycle to inhibit viral replication and infection of naïve cells. Since the advent of HAART, survival of HIV patients has drastically improved. HAART has decreased the diagnosis of opportunistic infections, decreased viral load, and increased lifespan of HIV patients (Kaplan et al., 2000; Sacktor et al., 2002; Tozzi et al., 2005b). Between 2004 and 2009, there was a 19% decline in the number of deaths of HIV patients (UNAIDS, 2010). However, there is currently no known cure for HIV infection, and since its classification in 1981 HIV and AIDS have killed over 20 million people worldwide (UNAIDS, 2010), making it one of the most devastating pandemics in human history. In addition to its many peripheral and immunological targets, HIV also infiltrates the central nervous system (CNS). HIV penetration of the CNS leads to a wide range of HIV-associated neuropathologies, producing serious and debilitating neurological impairment.

III. HIV-associated neurocognitive disorders

Cognitive symptoms associated with HIV infection are collectively known as HIV-associated neurocognitive disorders, or HAND (Antinori et al., 2007). HAND is a progressive disease that encompasses a wide spectrum of symptoms. These can range from asymptomatic neurocognitive impairment (ANI) that can only be diagnosed clinically, and mild neurocognitive disorder (MND), to HIV-associated dementia (HAD). Patients are evaluated with a range of neuropsychological tests that evaluate verbal and language skills, working and executive memory and function, information processing, and sensory perception, among others (Antinori et al., 2007; Ellis et al., 2007). Symptoms associated with HAND can impair patients' abilities to function independently on a daily basis (Heaton et al., 2004; Antinori et al., 2007). This makes HAND a significant complication of HIV infection, one that requires therapeutic intervention.

Currently, there is no consensus on a standard of treatment for patients

diagnosed with HAND, other than to continue their HAART regimen (McArthur et al., 2010). HAART has been shown to relieve HIV-associated neurocognitive symptoms and decrease their severity, albeit temporarily and with variable results (Ferrando et al., 1998; Suarez et al., 2001; Robertson et al., 2004). As a result, the number of HIV patients diagnosed with HAD has all but disappeared. However, as more and more patients live longer with HIV infection, the prevalence of patients also living with milder forms of HAND has increased, with estimates reaching as high as 50% of all HIV patients (Heaton et al., 2010). Furthermore, the initial efficacy of HAART in treating HAND symptoms eventually declines, with HAND symptoms persisting in patients whose viral loads are low (Tozzi et al., 2005b). Other CNS drugs are currently in clinical trials for efficacy in treating HAND, such as the clinically approved Alzheimer's drug memantine (Schifitto et al., 2007b; Zhao et al., 2010) and the monoamine oxidase inhibitor selegiline (Schifitto et al., 2007a), but no approved pharmacotherapies have emerged. As a result, there is currently a lack of effective therapies to treat HAND symptoms. Therefore, there is a pressing need to elucidate the mechanisms that induce HAND symptoms so that targeted treatment may be developed.

IV. Mechanisms of neuronal injury associated with HAND

The primary mechanisms by which HIV induces neurotoxicity are indirect; neurons do not express the receptors necessary for viral insertion and replication. Instead, infected neuroimmune cells such as macrophages and astroglia induce neurotoxicity in the CNS (Pulliam et al., 1991; Gendelman et al., 1994; Minagar et al., 2002). HIV-infected cells stimulate production of inflammatory cytokines such as TNFα and IL-1β, and release toxic factors and viral proteins into the extracellular space (Genis et al., 1992; Speth et al., 2001). It is these cytokines and toxins that in turn induce

neurotoxic processes, including glutamate dysregulation and excessive calcium (Ca^{2+}) influx. These processes eventually lead to neuronal death (Figure 1.1).

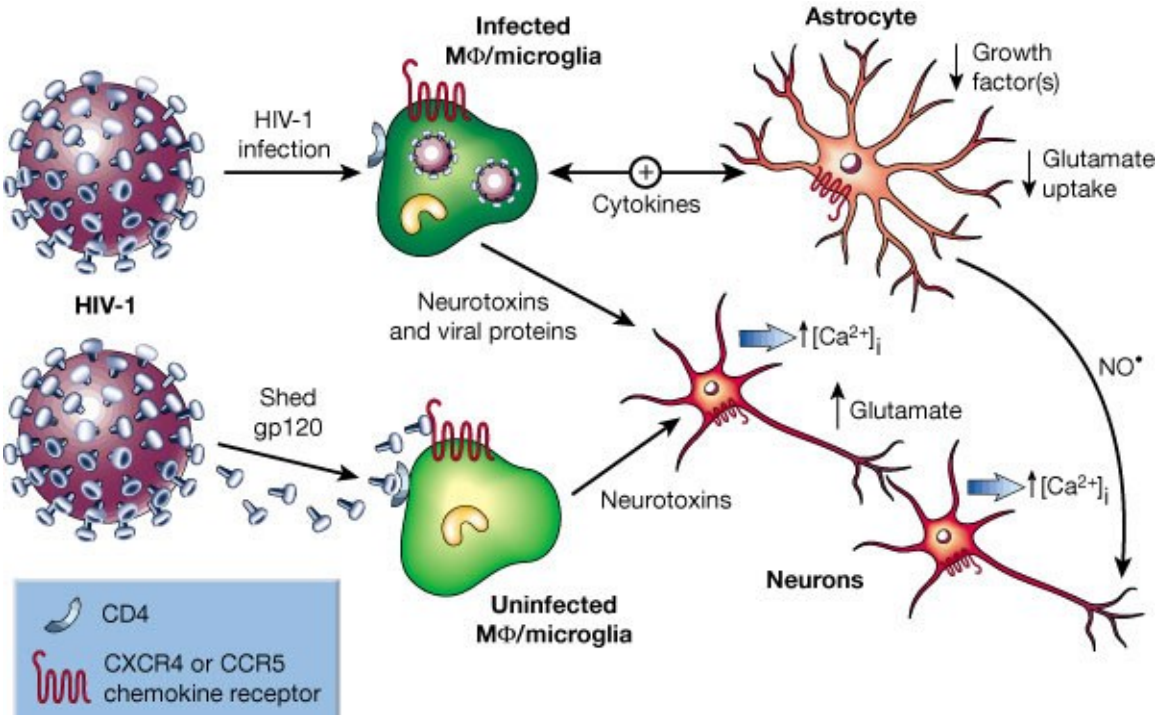

Figure 1**.1. HIV induces neurotoxicity indirectly.** HIV infects neuroimmune cells such as macrophages (MΦ) and microglia. Infected cells release cytokines and viral proteins, which are the primary mediators of calcium (Ca^{2+}) and glutamate dysregulation in neurons (Kaul et al., 2001). Reproduced with permission, © 2001, Nature Publishing Group.

While neuronal death is seen in HAND patients, clinical post-mortem studies have shown that the extent of neuronal death does not correlate with the rate and extent of cognitive decline in HAND patients (Adle-Biassette et al., 1999). Rather, it is earlier mechanisms of neuronal injury that correlate closely with HAND symptoms (Masliah et al., 1997; Everall et al., 1999; Sa et al., 2004). These injurious processes can include reduced synaptic density, pruning and beading of dendrites, and aberrant sprouting of spines, and are early events in HAND progression (Ellis et al., 2007). These irregularities in the neuronal network are disruptive to normal neuronal communication, and as a result, cognitive function. Immunohistological studies have shown that brain regions that are particularly susceptible to neuronal damage include the striatum and the hippocampus (Moore et al., 2006), areas of the brain that are particularly important for learning and memory as well as higher cognitive function. The idea that the correlative mechanisms of HAND are early events that precede overt neuronal death suggests that these injuries can be prevented or even reversed with the appropriate targeted therapies.

V. HIV Tat: a neurotoxic viral protein

There are a number of HIV proteins that have been shown to contribute to the neuronal injury seen in HAND, including the HIV transactivator of transcription (Tat). Tat was first identified in 1985 as an inductor of transcription in HIV-infected cells (Sodroski et al., 1985), and has been shown to be involved in many processes of neuronal injury, both *in vitro* and *in vivo.* It is a nonstructural viral protein that is part of the viral replication machinery and essential for viral replication (Dayton et al., 1986).

Within the viral machinery, Tat's primary role is to facilitate transcription elongation of the HIV genome. After transcription of the genome is initiated, Tat is recruited to the transcription complex, which includes the holoenzyme RNA

polymerase II, and binds to the Tat activation region (TAR) of the transcribed HIV RNA (Isel and Karn, 1999). Tat binding to TAR induces recruitment of the transactivator kinase complex (TAK), including the cyclin-dependent kinase 9 (CDK9) and cyclin T1 (Garber et al., 1998; Wei et al., 1998). CDK9 becomes constitutively active, hyperphosphorylating the C-terminal domain of RNA polymerase II and activating the transcription complex, which goes on to transcribe the rest of the HIV genome (Isel and Karn, 1999). Tat's transcriptional activities can increase synthesis of reporter genes more than 100-fold in infected cells (Sodroski et al., 1985).

In addition to its facilitation of HIV transcription, Tat is also released by HIV-infected cells and can modulate the expression levels of a host of heterologous genes, such as bcl-2 and tumor necrosis factor (Sastry et al., 1990; Zauli et al., 1995). Exogenous release and uptake of Tat protein occurs when cell death is minimal and Tat expression is high (Ensoli et al., 1993). One such mechanism by which Tat is taken up into cells is via the low-density lipoprotein receptor-related protein (LRP) (Liu et al., 2000). Tat release into the extracellular space can promote HIV pathology in cells derived from AIDS patients (Ensoli et al., 1990), and contribute to increasing viral replication in latently infected cells (Green and Loewenstein, 1988), as well as activating uninfected immune cells to increase permissivity for infection by the HIV virus (Li et al., 1997). Thus, in addition to its transcriptional activity within infected cells, extracellular Tat has pathogenic effects in the progression of HIV infection.

Exogenous Tat is also released in the CNS by infected neuroimmune cells, such as monocytes. Application of Tat protein, both *in vitro* and *in vivo*, is neurotoxic, inducing toxic rises in intracellular calcium (Bonavia et al., 2001) and direct depolarization in neurons (Magnuson et al., 1995; Cheng et al., 1998), and striatal lesions and even overt lethality in rodent models (Sabatier et al., 1991; Hayman et al., 1993). These and other

studies conclude that HIV Tat is excitotoxic to neurons (Bansal et al., 2000; Haughey et al., 2001). Furthermore, Tat protein and mRNA are found in HAND patients (Hofman et al., 1994; Wiley et al., 1996; Del Valle et al., 2000; Hudson et al., 2000). Expressing Tat protein *in vivo* produces behavioral changes such as slowed cognitive movement, and neuropathologies such as increased cytokine production, neuronal apoptosis, and dendritic degeneration, pathologies similar to those seen in HAND patients (Kim et al., 2003; Fitting et al., 2010).

Tat's neurotoxic properties are dependent on various domains in its protein structure. Tat is an 86 to 101 amino acid protein, composed of 2 exons. The first exon comprises the first 72 amino acids and is divided into five functional domains (Kuppuswamy et al., 1989; Jeang et al., 1999). The first three domains comprise the activation domain: the N-terminal domain (amino acids 1-21), the cysteine-rich domain that forms intramolecular disulphide bonds (aa 22-37), and the core domain (aa 38-47). The fourth domain is basic (aa 47-72), containing a RKKRRQRR motif and guiding nuclear localization of Tat protein. The fifth domain is the glutamine-rich C-terminal domain, which is central to Tat's transactivation activity. The second exon of Tat (aa 72-86, 101) is less studied, but has been shown to enhance Tat uptake into neuronal cells (Ma and Nath, 1997) and contains two distinct motifs, the RGD sequence and the ESKKKVE motif (Brake et al., 1990). Various studies show that several regions within the first exon of Tat are required for its neurotoxic effects, for example the cysteine-rich domain (Aksenov et al., 2009), aa 31-61 (Nath et al., 1996), aa 46-60 (Sabatier et al., 1991), and aa 37-72 (Philippon et al., 1994) (Figure 1.2).

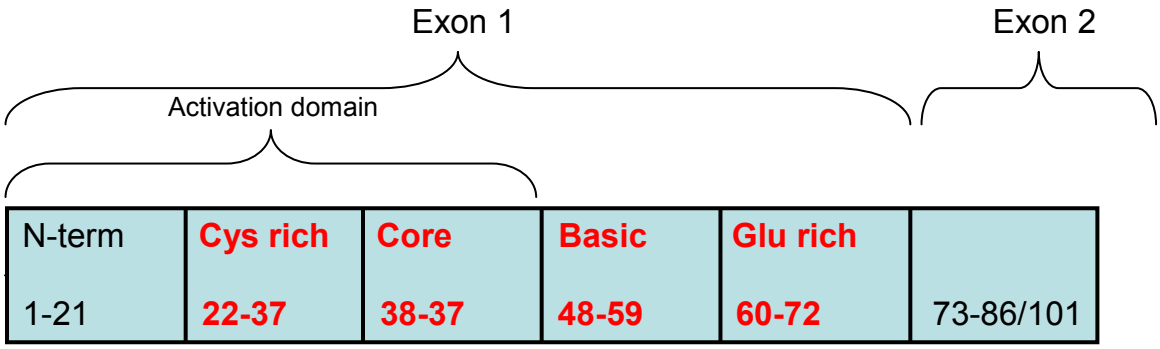

Figure 1.2**. Structure and functional domains of HIV Tat protein.** Regions of Tat that have been implicated in its neurotoxic effects are highlighted in red.

Together, these studies show that HIV Tat is a neurotoxic viral protein that is released into the CNS of patients infected with HIV, and contributes to the symptoms of HAND. Therefore, it is essential to determine the mechanisms by which Tat induces neurotoxicity, so that effective treatments may be developed.

VI. HIV Tat induces synapse loss

Changes in synapses that occur in response to CNS penetration of HIV can be correlated to cognitive decline seen in HAND. In order to track synaptic changes, our laboratory developed a novel, live cell confocal imaging assay that allows us to track synapse number in a single neuron over a specified time interval (Waataja et al., 2008). Hippocampal neurons are transfected with plasmid expression vectors for two contrasting fluorophores (Figure 1.3). The first is DsRed, a red fluorescent protein that expresses ubiquitously and allows us to visualize the morphology of the neuron (Figure 1.3, DsRed). The second is postsynaptic density protein 95 (PSD95) a scaffolding protein highly expressed at excitatory postsynaptic densities, fused to green fluorescent protein (PSD95-GFP), which expresses in a discrete punctate pattern (Figure 1.3, PSD95-GFP). Previous work showed that these PSD95-GFP puncta represent

functional excitatory postsynaptic sites (Waataja et al., 2008). This process allows us to quantify the number of synapses present in a live neuron at a given time point (Figure 1.3, Processed). Repeated imaging of the same neuron tracks changes in synapse number over a given time interval, in order to quantify the changes that ensue after treatment with drugs or toxic viral proteins such as HIV Tat.

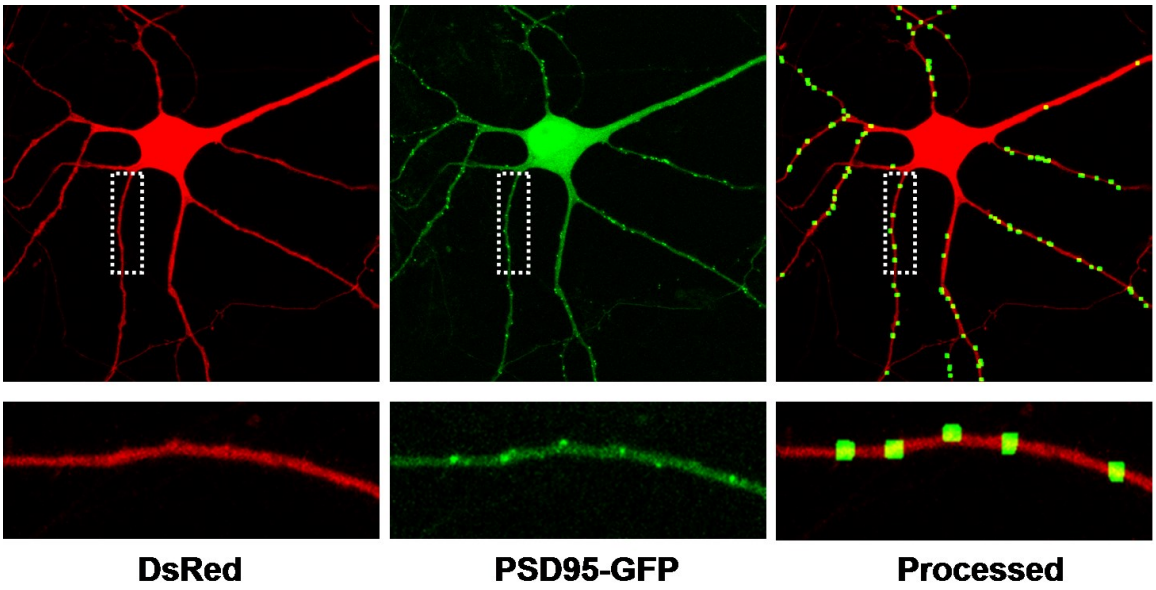

Figure 1.3. Live cell confocal imaging of fluorescently labeled synapses. Primary rat hippocampal neurons in culture are transfected with expression vectors for DsRed (left) and PSD95-GFP (center). DsRed fluorescence indicates neuronal morphology and serves as a mask for PSD95 puncta. PSD95-GFP expresses in a punctate pattern; PSD95 puncta represent functional excitatory postsynaptic sites. Neurons are imaged over an 8 µm z-stack, and a maximum projection for each fluorophore is created. PSD95-GFP puncta that fit the appropriate size and intensity criteria are quantified, dilated, and overlaid on the DsRed mask to produce a processed data image (right).

Using the method described above, previous work from our laboratory showed that exogenous application of the HIV protein Tat induced a significant decrease in the number of PSD95-GFP puncta over 24 hours (Kim et al., 2008), indicating a loss of excitatory synapses. This loss of synapses occurred prior to overt neuronal death, which was significant at 48 hrs, and was concentration-dependent. An exciting discovery during the course of this study was the result that Tat-induced synapse loss was reversible; treatment with a protein known as receptor-associated protein (RAP) induced a recovery of synapse number back to basal levels after Tat-induced synapse loss.

VII. Mechanisms of HIV Tat-induced synapse loss and recovery (Kim et al., 2008)

Tat induces synapse loss by binding to the low-density lipoprotein receptor-related protein (LRP). LRP is a multiligand receptor whose primary function is endocytic clearance of ligands from the extracellular space (May et al., 2007). Tat binds to and is taken up into the neuron by LRP (Liu et al., 2000), and induces synapse loss by 24 hours post-exposure. RAP is a competitive LRP antagonist (Bu and Rennke, 1996) that inhibited Tat-induced synapse loss when applied prior to Tat. Tat binding and uptake induces activation of the N-methyl-D-aspartate (NMDA) receptor, an ionotropic glutamate receptor. Pretreatment with the uncompetitive NMDA receptor antagonist MK801 (dizocilpine) also inhibited Tat-induced synapse loss.

The NMDA receptor is a neuron-specific tetrameric ion channel composed of two GluN1 subunits and two GluN2 subunits (Furukawa et al., 2005). GluN2 subunits can be further categorized into four isoforms: 2A, 2B, 2C, and 2D, the two dominant isoforms in the hippocampus being GluN2A and GluN2B (Monyer et al., 1994; Cull-Candy et al., 2001). NMDA receptor activation results in opening of the channel pore and Ca^{2+} influx

into the cell. Tat exposure induces Ca^{2+} influx into the postsynaptic density via LRP and the NMDA receptor to cause synapse loss; pre-treatment with the cell permeable Ca^{2+} chelator BAPTA-AM prevented Tat-induced synapse loss. In Chapter Two I describe the importance of NMDA receptor subunit composition to mechanisms of Tat-induced synapse loss and subsequent recovery. Selective antagonism of GluN2A-containing or GluN2B-containing NMDA receptors uncovered distinct and opposing roles of these subunits in mediating the neurotoxic effects of Tat.

NMDA receptor-mediated Ca^{2+} influx that is induced by Tat triggers two distinct pathways. Ca^{2+} activates neuronal nitric oxide synthase (nNOS). nNOS activation and subsequent nitric oxide (NO) production induces overt neuronal death by 48 hours post-Tat exposure; pretreatment with the nNOS antagonist L-NAME was able to protect against Tat-induced neuronal death. However, L-NAME pretreatment did not inhibit Tat-induced synapse loss, suggesting that synapse loss was mediated through a separate pathway. Moreover, Tat-induced neuronal death was not observed at 24 h, indicating that synapse loss occurred prior to overt cell death.

NMDA receptor-mediated Ca^{2+} influx also induces ubiquitination of PSD95, mediated by the E3 ligase MDM2 (Colledge et al., 2003). Inhibition of MDM2 activity with the antagonist nutlin-3, or by co-expression of the MDM2 inhibitor Arf, prevented Tat-induced synapse loss. MDM2 polyubiquitinates PSD95; mutation of PSD95-GFP to truncate the PEST sequence required for ubiquitination (Colledge et al., 2003) also prevented Tat-induced synapse loss. Ubiquitination and subsequent proteasomal degradation of PSD95-GFP results in the synapse loss we visualize using our imaging assay.

Surprisingly, when neurons were pretreated with nutlin-3, there was no protective effect seen against neuronal death. On the contrary, there was a sensitization effect; in

the presence of nutlin-3, neuronal death was seen using lower concentrations of Tat than with Tat alone. This suggests that synapse loss may be a coping mechanism; neurons may downregulate excitatory synapses in the presence of an excitotoxic stimulus such as Tat in order to protect against neuronal death.

An exciting discovery of this study was that if neurons were treated with RAP after 16 hours in the continued presence of Tat, after Tat-induced synapse loss had already occurred, this treatment induced a recovery of synapse number back to basal levels by 24 hours. RAP was unique in its ability to induce recovery; treatments at 16 hrs with reagents that prevented synapse loss, such as MK801, were unable to induce synapse recovery. Additionally, merely washing out Tat protein at 16 hours did not induce recovery, and no spontaneous recovery was seen in the absence of treatment.

Thus, HIV Tat induces excitotoxic synapse loss in hippocampal neurons. This synapse loss occurs prior to Tat-induced neuronal death, is dependent on Tat binding to LRP and potentiating NMDAR activity, and is reversible by the LRP antagonist RAP (Figure 1.4). We hypothesize that the phenomenon of synapse loss is a protective mechanism initiated by neurons in an attempt to decrease excitatory input. The recovery of synapse number induced by RAP is a robust phenomenon, yet the mechanisms of this recovery are as yet unknown. RAP is a competitive antagonist at LRP, preventing Tat from binding to or being taken up by LRP. However, this mechanism of action is insufficient to explain how RAP could induce recovery after 16 h of Tat exposure, when Tat has presumably already been bound and taken up into the neuron. In Chapter Four I describe a PKG-dependent pathway downstream of NMDA receptor signaling that suppresses synapse recovery after chronic (16 h) Tat exposure. Inhibition of this pathway induced synapse recovery.

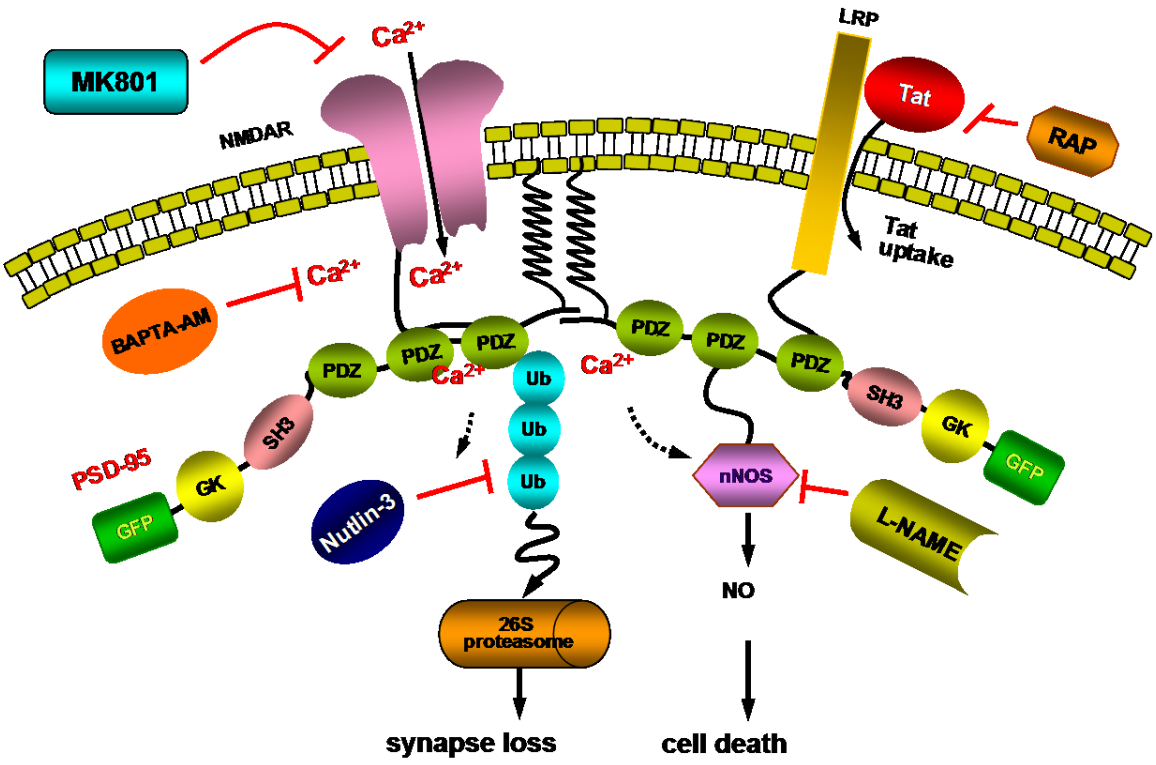

Figure 1.4. Mechanism of Tat-induced synapse loss and recovery. HIV Tat binds to LRP and is taken up by neurons. Tat uptake induces the formation of a complex with LRP, PSD95 and the NMDA receptor (NMDAR), inducing NMDAR-mediated Ca^{2+} influx. The rise in intracellular Ca2+ activates two separate pathways: synapse loss induced by polyubiquitination of PSD95 and subsequent proteasomal degradation, and cell death induced by NO production. The LRP antagonist RAP, the NMDAR antagonist MK801, the calcium chelator BAPTA-AM, and the MDM2 antagonist nutlin-3 can all prevent synapse loss. The nNOS inhibitor L-NAME can prevent cell death, but not synapse loss. Application of RAP after 16 h Tat exposure, and in the continued presence of Tat, induces recovery of synapse number by 24 h. Adapted from (Kim et al., 2008).

VIII. Summary of introduction and current studies

In summary, HIV infection is a worldwide pandemic. Adjunct to its detrimental effects on the immune system, HIV infection can penetrate the CNS and lead to a spectrum of cognitive symptoms. These symptoms, known as HAND, are poorly treated by mainline HIV therapies, creating a need for insight into the mechanisms of cognitive dysfunction mediated by HIV and its viral products so that improved therapies may be developed. The subject of this dissertation is the mechanisms of neurotoxicity produced by one such viral product, the HIV protein transactivator of transcription (Tat). Tat is a viral protein that is released in the CNS by infected cells, and has a variety of immune effects.

Tat is neurotoxic in a variety of *in vitro* and *in vivo* models. Tat induces overt neuronal death, and synapse loss, a neuropathology that correlates with cognitive decline. Our laboratory has developed a novel, fluorescence-based live cell confocal imaging assay that allows us to track the dynamic changes in synapse number for a single neuron over multiple time points. Previous work in our lab utilizing this assay showed that Tat induced synapse loss by 16 h that is sustained through 48 h. This loss was dependent on NMDA receptor activation and subsequent Ca^{2+} influx. Synapse loss occurred earlier than overt neuronal death and via a separate signaling pathway dependent on ubiquitination of PSD95 and subsequent proteasomal degradation. Synapse loss was reversible; treatment at 16 h with the LRP antagonist RAP induced a recovery of synapse number back to basal levels by 24 h. However, the mechanisms of RAP-induced synapse recovery are as yet unknown.

The work to date has laid the foundation for the studies outlined in this dissertation. I determined the role of NMDA receptor activity in Tat-induced neurotoxicity, and the importance of subunit composition in modulating the downstream effects of

Tat exposure. Selective inhibition of GluN2A-containing or GluN2B-containing NMDA receptors had distinct effects on Tat-induced cell death, as well as Tat-induced synapse loss and subsequent synapse recovery. Surprisingly, inhibition of GluN2B-containing NMDA receptors induced synapse recovery in the absence of RAP, indicating a role for GluN2B-containing receptors in suppression of synapse recovery.

I also determined the dynamics of presynaptic terminals in response to Tat exposure. Tat exposure induced loss of presynaptic terminals concurrent with loss of postsynaptic densities. Tat-induced loss of presynaptic terminals required postsynaptic LRP and NMDA receptor activity, as well as E3 ligase-mediated degradation of postsynaptic proteins. Again, inhibition of GluN2B-containing NMDA receptors induced recovery of presynaptic terminals after Tat exposure.

Finally, I elucidated the signaling pathway downstream of GluN2B-containing NMDA receptors that mediated suppression of synapse recovery after Tat-induced synapse loss. After 16 h Tat exposure, GluN2B-containing NMDA receptors were persistently activated, stimulating nNOS activation and NO production. This triggered production of cGMP and PKG activation, which phosphorylated VASP, an actin-associated protein. Pharmacological or genetic inhibition of any step in this pathway induced synapse recovery.

These studies highlight the mechanisms of Tat's neurotoxic effects, which can contribute to the pathology of HAND. Determining the means by which Tat induces neuronal injuries such as synapse loss is crucial to developing improved therapies for HAND patients.

Chapter Two:

Subtype selective NMDA receptor antagonists induce recovery of synapses lost following exposure to HIV Tat

Angela H. Shin, Hee Jung Kim, and Stanley A. Thayer

Content adapted from published article: **Shin A.H.,** Kim H.J., and Thayer S.A. (2012) Subtype selective NMDA receptor antagonists induce recovery of synapses lost following exposure to HIV-1 Tat. Br J Pharmacol, Jun; 166(3):1002-17.

Contributions: AHS collected and analyzed data, and contributed heavily to writing of manuscript.

I. Introduction

AIDS affects over 30 million people worldwide. Approximately 20% of HIV-infected patients suffer from neurological symptoms ranging from mild cognitive and motor impairment to dementia, known collectively as HIV-associated neurocognitive disorders (HAND) (Ellis *et al.*, 2007). HAND is an important complication of HIV infection of the brain because cognitive decline in some individuals progresses to where they are unable to perform basic functions of daily living (Kaul and Lipton, 2006; Hult et al., 2008; Minagar et al., 2008), and HIV patients showing neurocognitive impairment have shorter lifespans (Tozzi et al., 2005b). Despite the reduced incidence of severe dementia with widespread use of combined anti-retroviral therapies, increased diagnosis and prolonged life span of HIV patients increases the need for improved therapies to cope with the rising prevalence of HAND.

Cognitive decline in HAND patients correlates with dendritic pruning and loss of synaptic spines (Wiley et al., 1999; Sa et al., 2004). The mechanism by which HIV infection leads to neurocognitive dysfunction is largely indirect because the virus infects macrophages and microglia in the central nervous system, but not neurons. Infected cells within the brain secrete inflammatory cytokines and shed viral proteins which in turn exert toxic effects on neurons (Genis *et al.*, 1992; Speth *et al.*, 2001). The HIV protein Transactivator of transcription (Tat) is shed by infected cells and induces neuronal injuries that include dendritic pruning, loss of spine density, synapse loss, and overt neuronal death (Liu et al., 2000; Eugenin et al., 2007; Kim et al., 2008; Fitting et al., 2010). Moreover, introducing Tat into the brain produces neuropathological symptoms *in vivo* (Kim *et al.*, 2003; Maragos *et al.*, 2003), and Tat mRNA is found in the brains of HAND patients (Wiley et al., 1996; Hudson et al., 2000).

Tat induces synapse loss via a pathway distinct from that leading to neuronal

death (Kim *et al.*, 2008). Both processes are initiated by NMDA receptor activity, but synapse loss is mediated by the ubiquitin proteasome pathway and cell death is mediated by activation of nitric oxide synthase (NOS). Synapses lost following treatment with Tat can be recovered by treating with an antagonist to the lipoprotein receptor (Kim *et al.*, 2008). We hypothesize that synapse loss is a reversible mechanism that protects the neuron from excitotoxic stimuli such as Tat. Indeed, preventing synapse loss actually sensitizes neurons to Tat-induced cell death (Kim *et al.*, 2008). AIDS patients with HAND symptoms display cognitive improvement after starting treatment with antiretroviral therapy, suggesting that impairment is initially reversible (McArthur, 2004). Furthermore, lithium treatment increases the number of synapses *in vitro* (Kim and Thayer, 2009), and can improve neurological symptoms of HIV infection *in vivo* (Dou *et al.*, 2005; Letendre *et al.*, 2006). Perhaps inducing recovery of synapses can improve cognition in HAND patients.

The location and subunit composition of NMDA receptors determines the survival versus death promoting effects of glutamate. Activation of GluN2A-containing NMDA receptors, which are preferentially localized to synapses, exerts pro-survival effects. In contrast, NMDA receptors that contain GluN2B subunits are predominantly extrasynaptic and their activation initiates cell death (Hardingham et al., 2002; Liu et al., 2004a; Liu et al., 2007). The activity of NMDA receptors at synaptic relative to extrasynaptic sites may be vital to initiating synapse loss, or alternatively, inducing recovery of synapses. However, the role of NMDA receptor subunit composition in the mechanism of Tat-induced synapse loss, and subsequent recovery, has not been studied.

Dizocilpine (MK801) is a potent and efficacious NMDA receptor antagonist that affords short term protection from acute excitotoxicity, but is poorly tolerated *in vivo* due to psychotomimetic effects (Muir and Lees, 1995; Manahan-Vaughan et al., 2008).

Memantine blocks NMDA receptors with rapid binding kinetics that enable it to preferentially block extrasynaptic NMDA receptors (Xia *et al.*, 2010). It is well tolerated in humans and is clinically approved to improve cognition in Alzheimer's patients (Reisberg *et al.*, 2003). GluN2B-selective NMDA receptor antagonists such as ifenprodil (Williams, 1993; Tovar and Westbrook, 1999) can selectively target receptors that participate in the toxic effects of NMDA receptor stimulation while sparing survival promoting GluN2A containing receptors (Hardingham et al., 2002; Liu et al., 2004a; Liu et al., 2007). In contrast, GluN2A-selective NMDA receptor antagonists such as TCN201 (Bettini *et al.*, 2010) might reduce survival.

Here we examined the effects of dizocilpine, memantine, ifenprodil and TCN201 on death and synapse loss and recovery following HIV Tat. With the exception of TCN201, all the NMDA receptor antagonists protected from Tat-induced cell death. Memantine and ifenprodil failed to affect synapse loss, while dizocilpine and TCN201 were protective. Surprisingly, memantine and ifenprodil, but not dizocilpine or TCN201, induced recovery of synapses following exposure to Tat.

II. Methods

Materials. Materials were obtained from the following sources: the PSD95-GFP expression vector (pGW1-CMV-PSD95-EGFP) was kindly provided by Donald B. Arnold (Arnold and Clapham, 1999); the expression vector for DsRed2 (pDsRed2-N1) from Clontech (Mountain View, CA); HIV Tat (Clade B, recombinant) from Prospec Tany TechnoGene Ltd. (Rehovot, Israel); recombinant rat receptor associated protein (RAP) from Fitzgerald Industries International (Concord, MA); Dulbecco's modified Eagle medium (DMEM), fetal bovine serum, horse serum and propidium iodide (PI) from Invitrogen (Carlsbad, CA); memantine HCl, ifenprodil hemitartrate, and TCN201 from

Tocris (Ellsville, MO); penicillin/streptomycin, dizocilpine (MK801) and all other reagents from Sigma (St. Louis, MO).

Cell culture. Rat hippocampal neurons were grown in primary culture as described previously (Shen and Thayer, 1998) with minor modifications. Fetuses were removed on embryonic day 17 from maternal rats, anesthetized with CO_2, and sacrificed by decapitation. Hippocampi were dissected and placed in Ca^{2+} and Mg^{2+}-free HEPES-buffered Hanks salt solution (HHSS), pH 7.45. HHSS was composed of the following (in mM): HEPES 20, NaCl 137, $CaCl_2$ 1.3, $MgSO_4$ 0.4, $MgCl_2$ 0.5, KCl 5.0, KH_2PO_4 0.4, Na_2HPO_4 0.6, $NaHCO_3$ 3.0, and glucose 5.6. Cells were dissociated by trituration through a 5 ml pipette and a flame-narrowed Pasteur pipette, pelleted and resuspended in DMEM without glutamine, supplemented with 10% fetal bovine serum and penicillin/streptomycin (100 U/mL and 100 µg/mL, respectively). Dissociated cells were then plated at a density of 80,000-120,000 cells per dish onto a 25-mm-round cover glass (#1) glued to cover a 19 mm diameter opening drilled through the bottom of a 35 mm Petri dish. The cover glass was precoated with Matrigel (200 µL, 0.2mg/mL) (BD Biosciences, Billerica, MA). Neurons were grown in a humidified atmosphere of 10% CO_2 and 90% air (pH 7.4) at 37 ^{o}C, and fed at days 1 and 6 by exchange of 75% of the media with DMEM, supplemented with 10% horse serum and penicillin/streptomycin. Cells used in these experiments were cultured without mitotic inhibitors for at least 12 days, resulting in a mixed glial-neuronal culture. Immunocytochemistry experiments demonstrated that these cultures were composed of 18 $\pm$ 2 % neurons, 70 $\pm$ 3 % astrocytes and 9 $\pm$ 3 % microglia (Kim *et al.*, 2011).

Transfection. Rat hippocampal neurons were transfected between 10 and 12 days *in*

vitro using a modification of a protocol described previously (Kim *et al.*, 2008). Briefly, hippocampal cultures were incubated for at least 20 minutes in DMEM supplemented with 1 mM kynurenic acid, 10 mM $MgCl_2$, and 5 mM HEPES, to reduce neurotoxicity. A DNA/calcium phosphate precipitate containing 1 µg total plasmid DNA per well was prepared, allowed to form for 30 min at room temperature, and added to the culture. After a 90 minute incubation period, cells were washed once with DMEM supplemented with $MgCl_2$ and HEPES and then returned to conditioned media, saved at the beginning of the procedure. Transfected neurons were imaged 48-96 hours post-transfection. Transfection efficiency ranged from 1-5%.

Confocal imaging. Petri dishes containing transfected neurons were sealed with Parafilm, transferred to the stage of an inverted confocal microscope (Olympus Fluoview 300, Melville, NY) and viewed through a 60X oil-immersion objective (NA=1.4). To enable repeated imaging of the same cell over a 24 h period, the location of the cell was recorded using micrometers attached to the stage of the microscope. Multiple optical sections spanning 8 µm in the z-dimension were collected (1 µm steps), and these optical sections were combined through the z-axis into a compressed z stack. GFP was excited at 488 nm with an argon ion laser and emission collected at 530 nm (10 nm band pass). DsRed2 was excited at 543 nm with a green HeNe laser and emission collected at >605 nm. The cell culture dish was returned to the CO_2 incubator between image collections. Experiments studying synapse recovery were performed for 24 hours in the continuous presence of Tat, with or without the specified drugs added at 16 hours.

Image processing. To count and label PSD95-GFP puncta an automated algorithm was created using MetaMorph 6.2 image processing software described previously

(Waataja *et al.*, 2008). Briefly, maximum z-projection images were created from the DsRed2 and GFP image stacks. Next, a threshold set 1 s.d. above the image mean was applied to the DsRed2 image. This created a 1-bit image that was used as a mask via a logical AND function with the GFP maximum z-projection. A top-hat filter (80 pixels) was applied to the masked PSD95-GFP image. A threshold set 1.5 s.d. above the mean intensity inside the mask was then applied to the contrast enhanced image. Structures between 8 and 80 pixels (approximately 0.37 to 3.12 μm in diameter) were counted as PSDs. The structures were then dilated and superimposed on the DsRed2 maximum z-projection for visualization.

Toxicity. Cell death was quantified using propidium iodide (PI) fluorescence as previously described (Kim *et al.*, 2008). Cell culture was performed as described above except that 50,000 to 60,000 cells per well were plated in 96-well plates and grown for 12-14 days *in vitro*. The experiment was started at 12 days *in vitro* by replacing 100 μL (approximately 2/3 volume) of the cell culture medium with fresh DMEM containing 10% horse serum, penicillin/streptomycin, 70 μM PI and either Tat (50 ng/mL) or vehicle. The plate was placed in a FluoStar Galaxy multiwell fluorescent plate scanner (BMG Technologies GmbH, Offenburg, Germany) and maintained at 37 ^{o}C. PI fluorescence intensity measurements (excitation 544 nm ± 15 nm, emission 620 nm ± 15 nm) were taken at time 0 and 48 h. Between measurements, cells were returned to the incubator and kept at 37°C in 10% CO_2. Drugs, when present, were applied 15 min before application of Tat and included in the media exchange. Each treatment was performed in triplicate; a set of 3 wells from a single plating of cells was defined as an individual experiment (n=1).

Immunocytochemistry. Hippocampal cultures prepared as described earlier were transfected with pGW1-CMV-PSD95-EGFP on day 12 in culture. Forty-eight hours after transfection, cover slips with cells were washed with tris-buffered saline (TBS) and fixed with Lana's fixative (8% paraformaldehyde, 14% picrate, 0.16 M phosphate) for 10 min. The cells were washed with TBS, then permeabilized in TBS + 0.2% Triton X100 (Sigma) for 10 min at room temperature. After permeabilization, the cells were incubated with mouse anti-GluN2A (1:200, Chemicon/Millipore, Billerica, MA, USA) or mouse anti-GluN2B (1:200, BD Transduction Laboratories, San Jose, CA, USA) in TBS + 0.2% Tween-20 (Sigma) for 1 h at room temperature. Cells were washed with TBS and labelled proteins visualized with tetramethyl rhodamine isothiocyanate (TRITC)-conjugated goat anti-mouse antibody (Millipore, Billerica, MA, USA, 1:400) in TBS + 0.2% Tween-20. Cover slips were mounted with Fluoromount (Southern Biotech, Birmingham, AL, USA) and imaged on an inverted confocal microscope (Olympus Fluoview 300, Melville, NY, USA) using a 60X oil-immersion objective (NA = 1.4). TRITC was excited at 543 nm, and emission collected at >605 nm.

Statistics. For synapse loss and recovery studies, an individual experiment (n=1) was defined as the change in the number of PSDs from a single cell from a single coverslip. PSD counts were presented as mean ± SEM. Each experiment was replicated over at least 3 separate cultures. For cell survival studies, each treatment was performed in triplicate; thus, a set of 3 wells from a single plating of cells was defined as an individual experiment (n=1). In all statistical analyses we used Student's t-test for single or ANOVA with Tukey's post-hoc test for multiple statistical comparisons (OriginPro v8.5, Northampton, MA).

III. Results

Changes in the number of synapses between rat hippocampal neurons in culture were monitored by imaging neurons expressing PSD95-GFP and DsRed2, as previously described (Waataja *et al.*, 2008). The PSD95-GFP fusion construct expressed in a punctate pattern. Processing of PSD95-GFP images identified PSDs as fluorescent puncta meeting intensity and size criteria (average puncta size=0.52 μm^2) and in contact with a mask derived from the DsRed2 image (Figure 2.1, A). We have previously shown that fluorescent puncta co-localized with synaptically evoked local Ca^{2+} increases, functional neurotransmitter release sites and NMDA receptor immunoreactivity, indicating that they represent functional post-synaptic sites (Waataja *et al.*, 2008). The number of PSD95-GFP puncta was calculated for a single neuron over multiple time points to assess changes in synapse number (Figure 2.1, B). In untreated neurons the number of synaptic sites increased by 24 ± 5% (n = 66) over 24 h. Treatment with 50 ng mL^{-1} Tat for 24 h evoked a 24 ± 4% (n = 37) decrease in the number of postsynaptic sites (Figure 2.1, B).

Dizocilpine blocks Tat-induced changes in synapses and survival

Synapse loss induced by Tat is mediated by the NMDA receptor (Kim *et al.*, 2008). In Figure 2.1 B we show that treatment with dizocilpine prevented synapse loss evoked by 24 hour treatment with 50 ng/mL Tat. This protection was concentration dependent with an EC_{50} of 9.6 nM (Figure 2.1, C)

NMDA receptor activity is also required for Tat-induced cell death (Eugenin *et al.*, 2007). Treatment with Tat induced neuronal death by 48 hours which we quantified by uptake of PI. 50 ng/mL Tat increased PI fluorescence to 52 ± 15% (n = 13) of that evoked by 1 mM glutamate. Treatment with dizocilpine 15 minutes prior to and during

48 hour exposure to Tat afforded a concentration-dependent protection with an EC_{50} of 10.4 nM (Figure 2.1, D). Figure 2.1 E shows representative images of PI fluorescence superimposed on differential interference contrast images of the hippocampal culture under control conditions and following 48 h treatment with Tat. Treatment with Tat for 24 h, the time at which synapse loss was determined (Figure 2.1, B-C), did not significantly affect viability as determined by retention of the DsRed2 protein (Figure 2.1, B) and failure to take up PI (Kim *et al.*, 2008). Thus, synapse loss precedes neuronal death and both synapse loss and death are reduced by similar concentrations of dizocilpine.

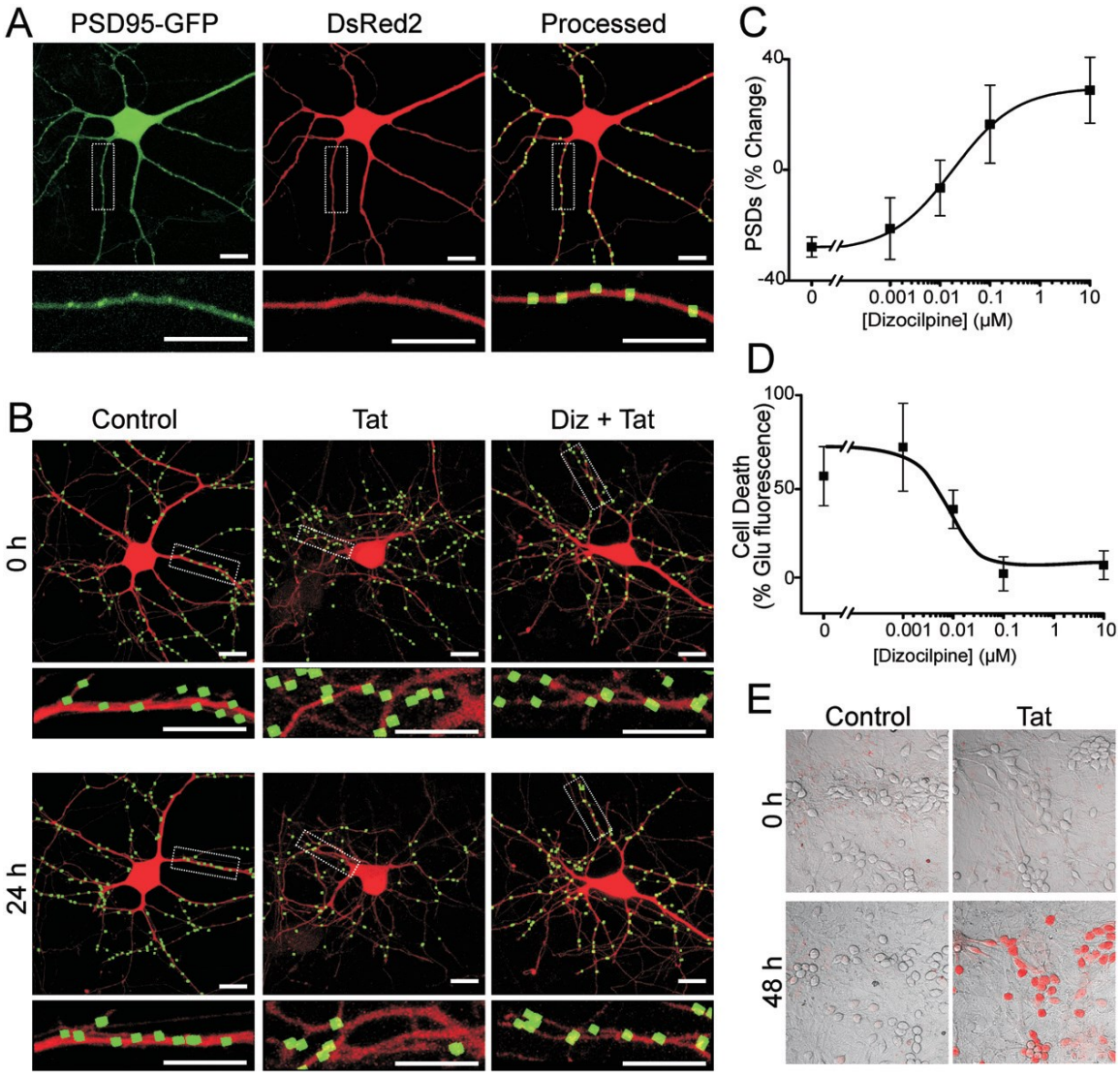

Figure 2.1. NMDA receptor activity is required for Tat-mediated neuronal death and synapse loss. Representative confocal images of neurons were collected and processed as described in Methods. Maximum projection images show a neuron expressing PSD95-GFP and DsRed2. PSD95-GFP puncta were identified by filtering compressed *z*-stacks (8 μm) of confocal images for fluorescent intensity and size and counted when in contact with a mask derived from the DsRed2 image. Labeled PSDs were dilated and overlaid on the DsRed2 image for visualization purposes (processed). The insets are enlarged images of the boxed region. Scale bars represent 10 μm. B, Processed images show neurons before (0 h) and after (24 h) no treatment (control), treatment with 50 ng/mL Tat (Tat), or treatment with 10 μM dizocilpine 15 min before and during treatment with Tat (Diz + Tat). The insets are enlarged images of the boxed regions. Scale bars represent 10 μm. C, Graph shows the % change in the number of PSD95-GFP puncta (mean ± SEM) for cells treated with 50 ng/mL Tat for 24 h in the presence of the indicated concentrations of dizocilpine ($n \geq 7$ for each data point). The curve was fit with a logistic equation of the form %PSD change = A2 + (A1 - A2)/(1 + (X/EC50)p) where X = dizocilpine concentration, A1 = -28 ± 2% PSD change without dizocilpine, A2 = 17 ± 4% PSD change at a maximally effective dizocilpine concentration and p = slope factor. EC50 was calculated using a nonlinear, least squares curve-fitting program. EC50 and p were 9.6 nM and 0.5, respectively. D, Graph shows cell death in cultures treated with 50 ng/mL Tat for 48 h in the presence of the indicated concentrations of dizocilpine ($n \geq 5$ for each data point). Cell death was quantified by PI fluorescence as described in Methods. PI fluorescence was normalized to that induced by treatment with 1 mM glutamate for 48 h, which kills virtually all neurons in this culture. The mean ± SEM % change in PI fluorescence is plotted against increasing concentrations of dizocilpine. The curve was fit with a logistic equation of the form % change in PI fluorescence = A1 + (A2 - A1)/(1 + (X/EC50)p) where X = dizocilpine concentration, A1 = -1 ± 5% PI fluorescence change at a maximally effective dizocilpine concentration, A2 = 54 ± 9% PI fluorescence change without dizocilpine, and p = slope factor. EC50 was calculated using a nonlinear, least squares curve-fitting program. EC50 and p were 10.4 nM and – 0.7, respectively. E, Representative images show differential-interference contrast micrographs of hippocampal neurons in culture with PI fluorescence (red) superimposed. Images from control and Tat-treated (50 ng/mL) cultures are shown before (0 h) and after (48 h) treatment.

Tat-induced loss of PSD95-GFP puncta is mediated by the low density lipoprotein receptor related protein (LRP) (Kim *et al.*, 2008). The loss of postsynaptic sites was reversed by treatment with RAP, a competitive antagonist of LRP. Treating neurons for 16 h with 50 ng/mL Tat induced significant synapse loss (Figure 2.2, A) that was sustained for 24 h (Figure 2.2, B). Addition of dizocilpine (10 μM) at 16 h to cells treated with Tat did not affect the sustained loss (Kim *et al.*, 2008). In contrast, adding RAP to Tat-treated cells at 16 h in the continuous presence of Tat produced a marked recovery of synaptic sites (n = 52) (Figure 2.2, A-B). Interestingly, the recovery of PSD95-GFP puncta induced by RAP was inhibited by adding 10 μM dizocilpine 15 minutes prior to the addition of RAP at 16 h (n = 29) (Figure 2.2, A-B), indicating that NMDA receptor activity was necessary for the recovery process. We next determined the concentration-dependence for dizocilpine's inhibition of synapse recovery. As shown in Figure 2.2 C, dizocilpine impaired synapse recovery with an EC_{50} of 24 nM. Taken together, these results show that NMDA receptor activity is not only required for Tat-induced synapse loss and neuronal death, it is also required for recovery of synapses following Tat-induced loss. Moreover, dizocilpine attenuated Tat-induced synapse loss, Tat-induced cell death and RAP-induced synapse recovery with comparable potencies.

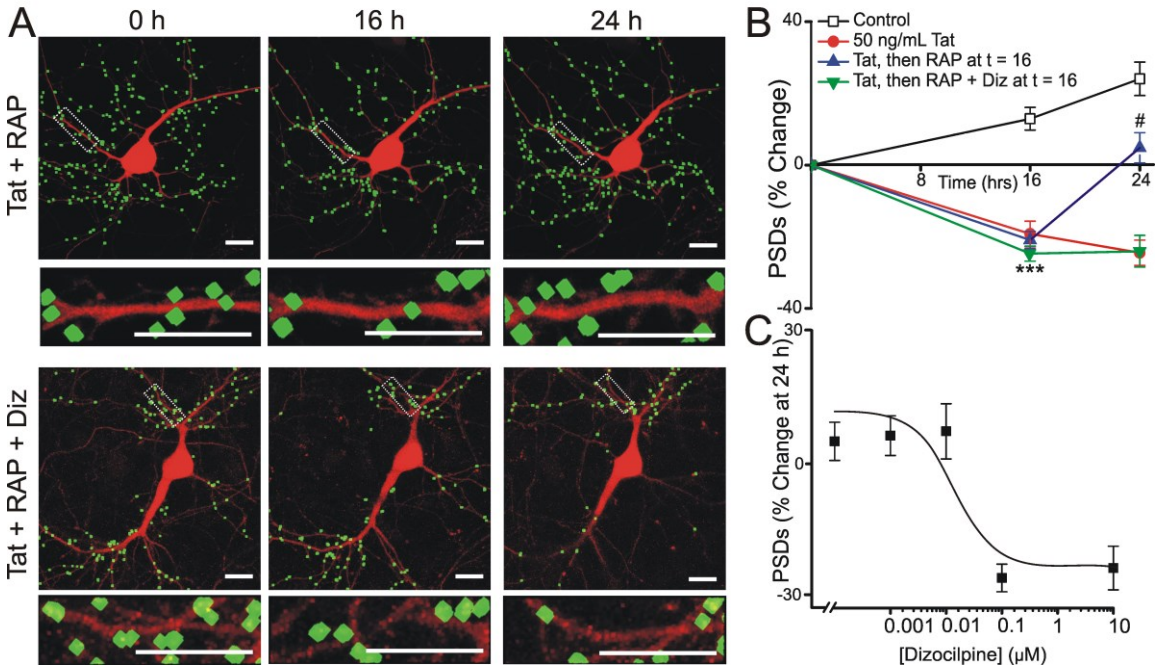

Figure 2.2. NMDA receptor activity is required for RAP-induced synapse recovery. A, Representative processed images of neurons before (0 h) and 16 and 24 h after treatment with 50 ng/mL Tat. After 16 h exposure to Tat the cells were treated with 50 nM RAP alone (Tat + RAP) or RAP + 10 μM dizocilpine (Tat + RAP + Diz) (dizocilpine was applied 15 min before adding RAP). The insets are enlarged images of the boxed region. Scale bars represent 10 μm. B, Graph summarizes % change in number of PSDs in the absence (control) or presence of 50 ng/mL Tat for 24 h. After 16 h exposure to Tat cells were then left untreated or treated with 50 nM RAP alone or RAP + 10 μM dizocilpine. Data are expressed as mean ± SEM. ***, $p < 0.001$ relative to control at 16 h; #, $p < 0.05$ relative to 50 ng/mL Tat at 24 h (ANOVA with Tukey's post-test). C, Graph shows the % change in the number of PSD95-GFP puncta (mean ± SEM) for cells treated with 50 ng/mL Tat for 24 h. 50 nM RAP was applied at 16 h in the presence of the indicated concentrations of dizocilpine ($n \geq 5$ for each data point). The curve was fit with a logistic equation of the form % PSD change = A1 + (A2 - A1)/[1 + (X/EC50)p] where X = dizocilpine concentration, A1 = -26 ± 3% PSD change at a maximally effective dizocilpine concentration, A2 = 5 ± 1% PSD change without dizocilpine and p = slope factor. EC50 was calculated using a nonlinear, least squares curve-fitting program. EC50 and p were 24.3 nM and – 0.9, respectively.

Memantine differentially affects survival and synapse loss

Dizocilpine is a high affinity uncompetitive NMDA receptor antagonist developed as a neuroprotective agent, but not used clinically due to psychotomimetic side effects (Muir and Lees, 1995). Memantine is an uncompetitive NMDA receptor antagonist that in contrast to dizocilpine, is well tolerated and used clinically to improve cognition in patients with Alzheimer's disease (Reisberg *et al.*, 2003). Therefore, we decided to test the effects of memantine on Tat-induced cell death and synapse loss. Memantine (10 μM) prevented Tat-induced neuronal death (Figure 2.3, A), similar to dizocilpine (n = 9). However, in contrast to dizocilpine, 10 μM memantine did not inhibit synapse loss induced by Tat (n = 13) (Figure 2.3, B-C). Even at 100 μM, a concentration 10-fold higher than that needed to prevent Tat-induced cell death, memantine had no effect on Tat-induced synapse loss (n = 5) (Figure 2.3, C).

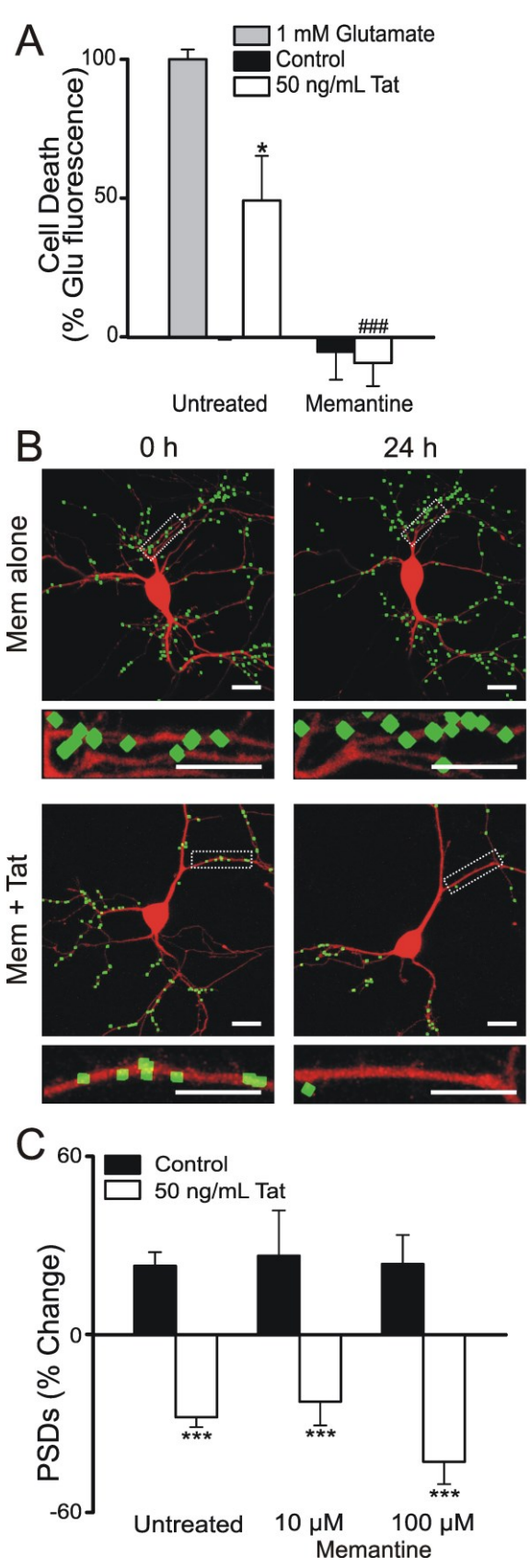

Figure 2.3. Memantine prevents Tat-induced cell death without affecting synapse loss. A, Cell death was measured with the PI fluorescence assay described in Methods. Bar graph summarizes PI uptake in neurons 48 h after no treatment (control), treatment with 1 mM glutamate, or treatment with 50 ng/mL Tat in the absence (untreated) or presence of 10 µM memantine as indicated. PI fluorescence was normalized to 1 mM glutamate treatment. Data are expressed as mean ± SEM. *, $p < 0.05$ relative to control, ###, $p < 0.001$ relative to Tat treatment alone (ANOVA with Tukey's post-test). B, Representative processed images of neurons incubated with 10 µM memantine before (0 h) and after (24 h) no treatment (Mem alone) or treatment with 50 ng/mL Tat (Mem + Tat). The insets are enlarged images of the boxed region. Scale bars represent 10 µm. C, Bar graph summarizes changes in PSD-GFP puncta (PSDs) after 24 h treatment under control conditions (solid bars) or following treatment with 50 ng/mL Tat in the absence or presence of the indicated concentration of memantine. Data are expressed as mean ± SEM. ***, $p < 0.001$ relative to control (Student's *t*-test).

Memantine induces recovery of synapses

We next examined the effect of memantine on the recovery of synaptic sites following Tat-induced loss. In contrast to dizocilpine, memantine significantly increased the number of synapses in Tat-treated cells. As shown in Figure 2.4 A and B, addition of 10 μM memantine to cells treated with 50 ng/mL Tat for 16 hours evoked a recovery in the number of PSD95-GFP puncta (n = 13). Furthermore, memantine did not inhibit recovery of synapses induced by RAP. When memantine was applied 15 minutes prior to the addition of RAP at 16 h, the number of synapses still increased similar to cells treated with RAP alone at 16 h (n = 14) (Figure 2.4, C). Memantine induced synapse recovery following Tat-induced synapse loss and did not interfere with synapse recovery in the presence of RAP. One mechanism by which memantine might selectively inhibit NMDA receptor-mediated cell death while sparing NMDA receptor-induced synapse loss would be if these two processes were mediated by different subsets of NMDA receptors. Immunocytochemistry experiments found these hippocampal neurons in culture to express both GluN2A and GluN2B immunoreactivity (Figure 2.5).

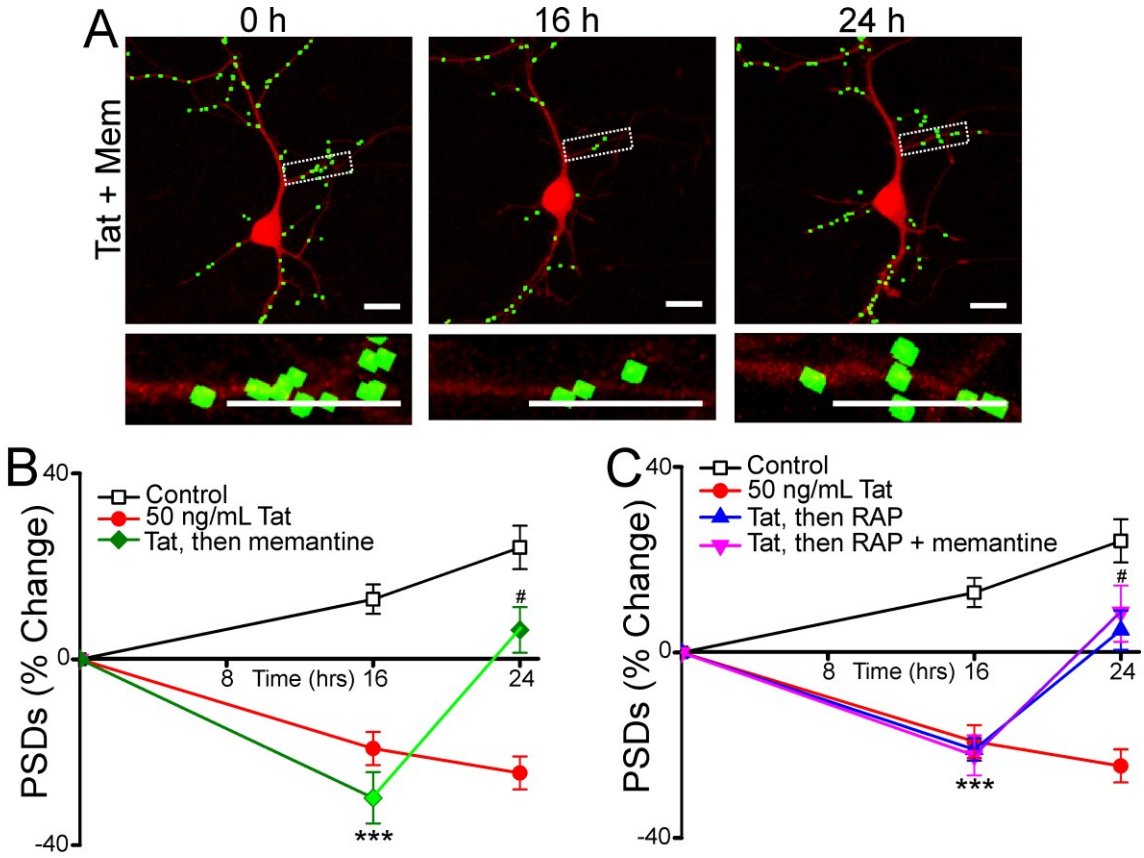

Figure 2.4. Memantine evokes synapse recovery after Tat-induced loss. A, Representative processed images of a neuron before (0 h) and 16 or 24 h after treatment with 50 ng/mL Tat. 10 μM memantine was applied after 16 h in the presence of Tat. The insets are enlarged images of the boxed region. Scale bars represent 10 μm. B–C, Graphs summarize % change in number of PSDs in the absence (control) or presence of 50 ng/mL Tat for 24 h. B, After 16 h exposure to Tat, cells were then left untreated or treated with 10 μM memantine. C, After 16 h exposure to Tat, cells were then left untreated, treated with 50 nM RAP alone or treated with RAP + 10 μM memantine. Memantine was added to neurons 15 min before 50 nM RAP. Data are expressed as mean ± SEM. ***, $p < 0.001$ relative to control at 16 h, #, $p < 0.05$ relative to 50 ng/mL Tat at 24 h (ANOVA with Tukey's post-test).

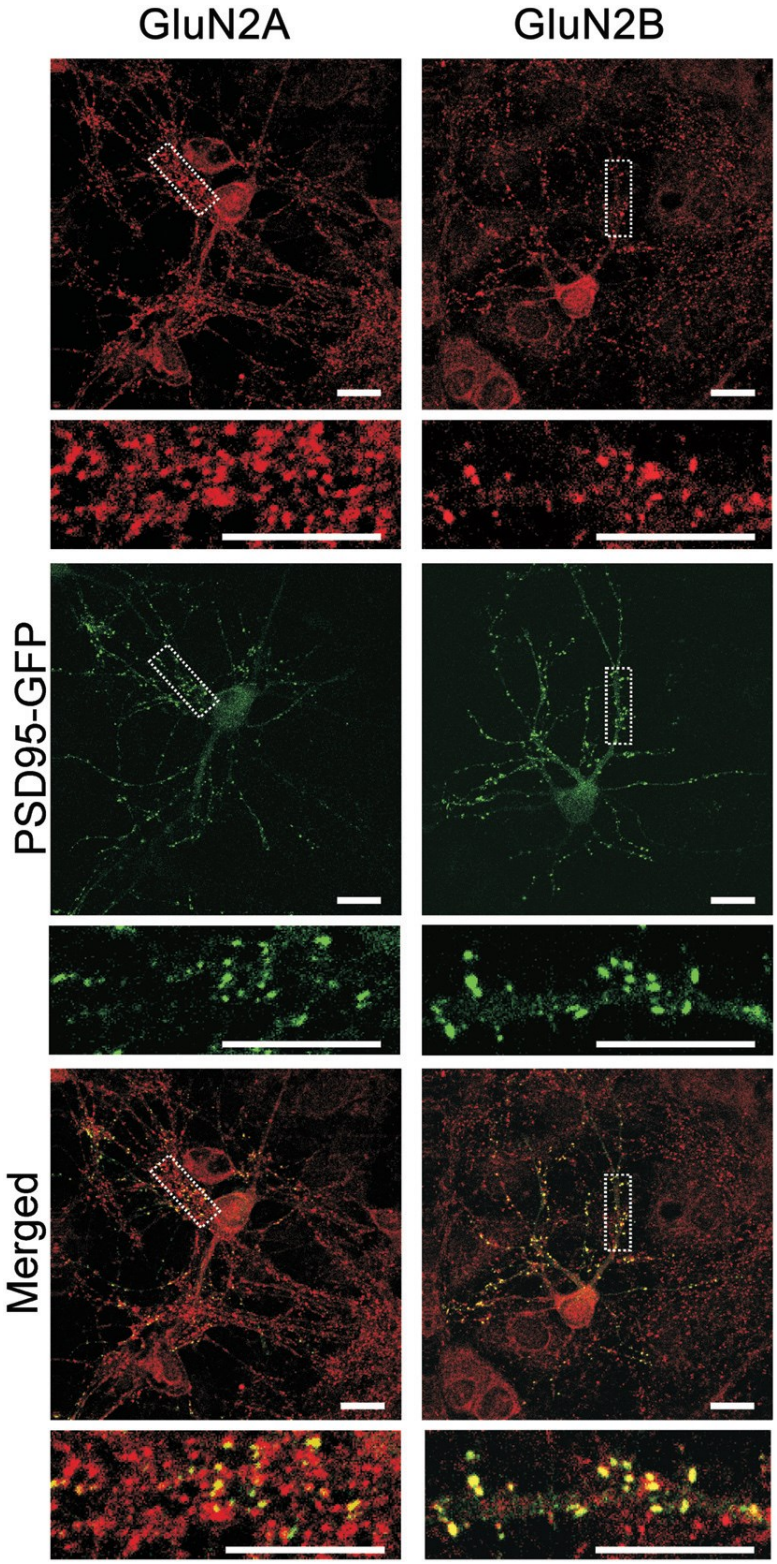

Figure 2.5. Hippocampal neurons in culture exhibit GluN2A and GluN2B immunoreactivity. Forty-eight hours after transfection with the PSD95-GFP expression vector, hippocampal cultures were fixed and labelled with GluN2A and GluN2B-selective antibodies (red) as described in Methods. PSD95-GFP puncta (green) co-localized with GluN2A and GluN2B immunoreactive puncta (merged, yellow). Note that non-transfected cells were also present in the field and thus not all immunoreactive puncta (red) co-localize with a PSD95-GFP puncta. Scale bars represent 10 μm.

Ifenprodil differentially affects survival and synapse loss

Memantine differs from dizocilpine in that it preferentially inhibits NMDA receptor activity at extrasynaptic sites (Xia *et al.*, 2010). Because GluN2B subunits are predominantly localized to extrasynaptic sites and their activation triggers cell death (Liu *et al.*, 2007), we hypothesized that memantine protected from Tat-induced neuronal death by preferentially inhibiting GluN2B-containing NMDA receptors while sparing synaptic plasticity induced by GluN2A-containing NMDA receptor activity. We tested this hypothesis with the use of the NMDA receptor antagonist ifenprodil.

Ifenprodil is an uncompetitive antagonist that is selective for GluN2B-containing NMDA receptors at a concentration of 10 μM (Williams, 1993; Avenet et al., 1996). Ifenprodil (10 μM) prevented Tat-induced neuronal death (n = 13) (Figure 2.6, A). However, this concentration of ifenprodil did not inhibit synapse loss induced by Tat (n = 9) (Figure 2.6, B-C). This result is similar to that seen with memantine, indicating that GluN2B-containing, or extrasynaptic NMDA receptors were not required for Tat-induced synapse loss.

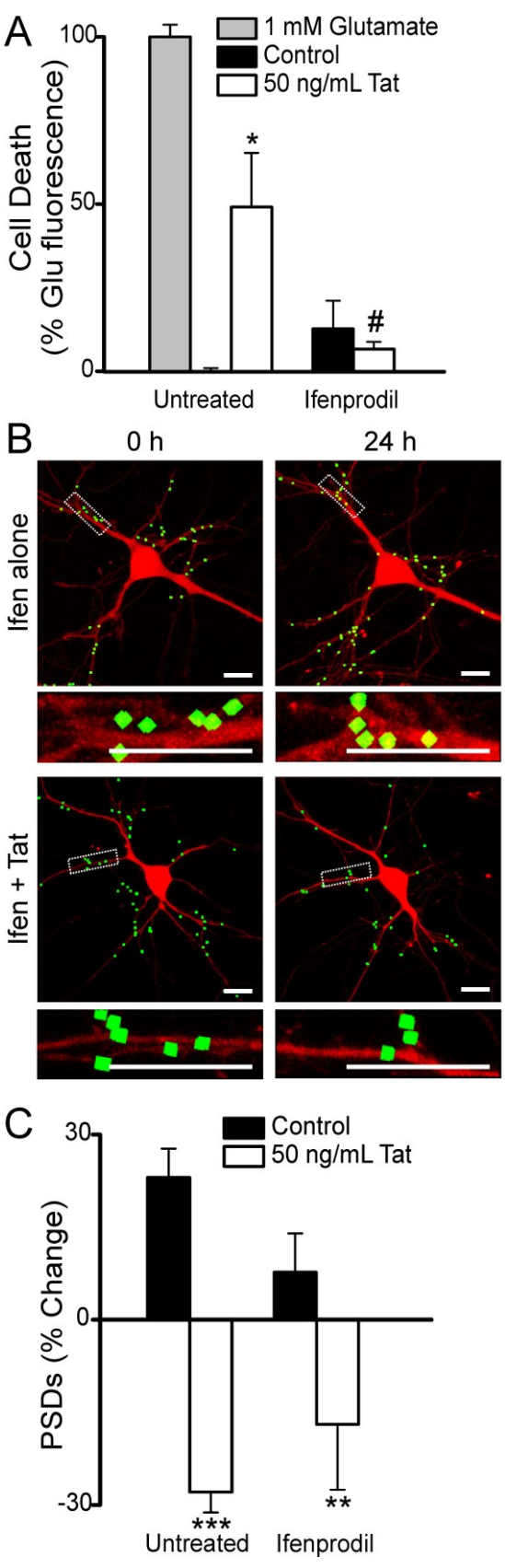

Figure 2.6. Ifenprodil improves survival without inhibiting Tat-induced synapse loss. A, Cell death was measured with the PI fluorescence assay described in Methods. Bar graph summarizes PI uptake in neurons 48 h after no treatment (control), treatment with 1 mM glutamate or treatment with 50 ng/mL Tat in the absence (untreated) or presence of 10 μM ifenprodil as indicated. PI fluorescence was normalized to 1 mM glutamate treatment. Data are expressed as mean ± SEM. *, $p < 0.05$ relative to control, #, $p < 0.05$ relative to Tat treatment alone (ANOVA with Tukey's post-test). B, Representative processed images of neurons incubated with 10 μM ifenprodil before (0 h) and after (24 h) no treatment (Ifen alone) or treatment with 50 ng/mL Tat (Ifen + Tat). The insets are enlarged images of the boxed region. Scale bars represent 10 μm. C, Bar graph summarizes changes in PSD-GFP puncta (PSDs) after 24 h treatment under control conditions or following treatment with 50 ng/mL Tat in the absence (untreated) or presence of 10 μM ifenprodil. Data are expressed as mean ± SEM. **, $p < 0.01$ relative to control; ***, $p < 0.001$ relative to control (Student's t test).

Ifenprodil induces synapse recovery

We next examined the effect of ifenprodil on the recovery of synaptic sites following Tat-induced loss. Similar to memantine, 10 μM ifenprodil significantly increased the number of synapses in Tat-treated cells (Figure 2.7, A-B). As shown in Figure 2.7 A, addition of 10 μM ifenprodil after a 16 hour treatment with 50 ng/mL Tat evoked recovery in the number of PSD95-GFP puncta (n = 11). Furthermore, 10 μM ifenprodil did not inhibit recovery of synapses when applied 15 min prior to the addition of RAP at 16 hours (n = 9) (Figure 2.7, C). This result is similar to that seen with memantine. Ifenprodil has non-selective effects at high concentrations (Williams, 1993). However, we were unable to study the effects of ifenprodil at concentrations greater than 10 μM because 24 hour exposure to a high concentration of ifenprodil (100 μM) was directly toxic to the neuronal culture.

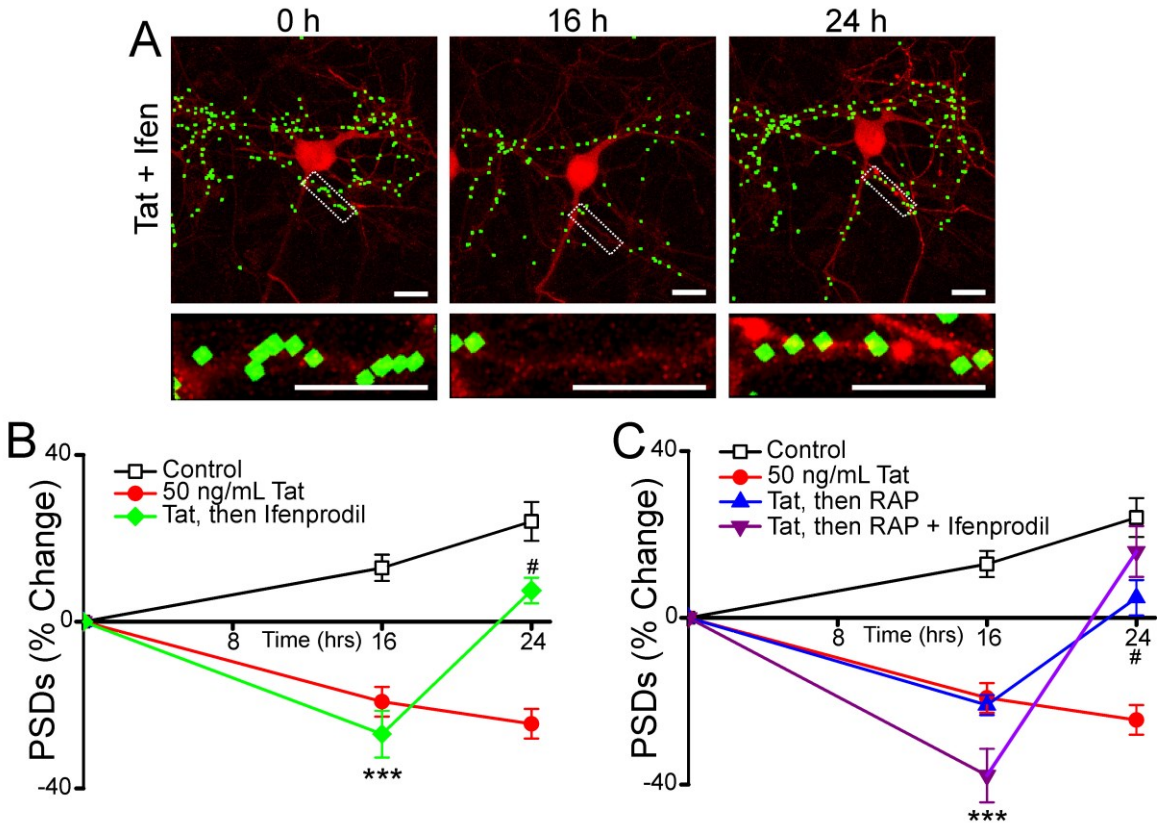

Figure 2.7. Ifenprodil evokes synapse recovery after Tat-induced loss. A, Representative processed images of a neuron before (0 h) and 16 or 24 h after treatment with 50 ng/mL Tat; 10 µM ifenprodil was applied after 16 h in the presence of Tat. The insets are enlarged images of the boxed region. Scale bars represent 10 µm. B–C , Graphs summarize % change in number of PSDs in the absence (control) or presence of 50 ng/mL Tat for 24 h. B, After 16 h exposure to Tat cells were then left untreated or treated with 10 µM ifenprodil. C, After 16 h exposure to Tat cells were then left untreated, treated with 50 nM RAP alone or treated with RAP + 10 µM ifenprodil. Ifenprodil was added to neurons 15 min before 50 nM RAP. Data are expressed as mean ± SEM. ***, $p < 0.001$ relative to control at 16 h; #, $p < 0.05$ relative to 50 ng/mL Tat at 24 h (ANOVA with Tukey's post-test).

TCN201 differentially affects survival and synapse loss

If the effects of memantine and ifenprodil on synapse loss and recovery differed from dizocilpine due to their GluN2B-selective actions, then a GluN2A-selective antagonist should produce opposite effects. TCN201 is selective for GluN2A-containing NMDA receptors at concentrations less than 50 μM (Bettini *et al.*, 2010). TCN201 at a concentration of 10 μM did not protect against Tat-induced cell death (n = 11) (Figure 2.8, A), in contrast to ifenprodil and memantine. However, this same concentration of TCN201 prevented Tat-induced synapse loss (n = 10) (Figure 2.8, B-C). These results suggest that activation of GluN2A-containing NMDA receptors are required for Tat-induced synapse loss, but do not participate in Tat-induced cell death.

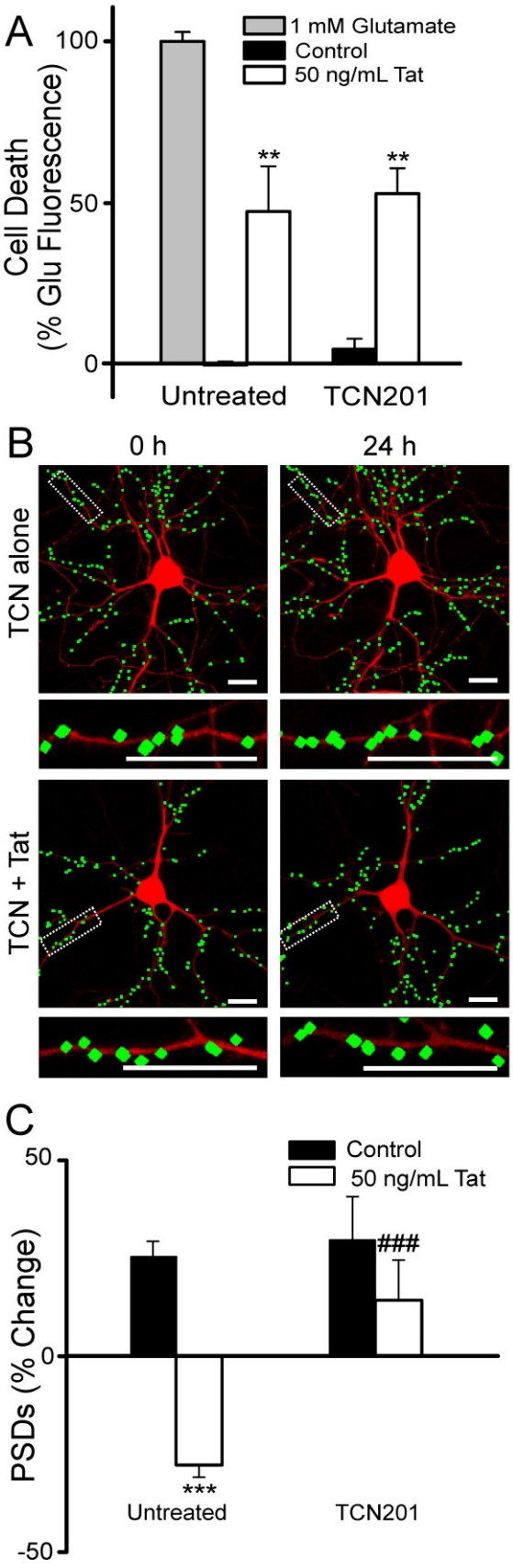

Figure 2.8. TCN201 inhibits Tat-induced synapse loss without affecting survival. A, Cell death was measured with the PI fluorescence assay described in Methods. Bar graph summarizes PI uptake in neurons 48 h after no treatment (control), treatment with 1 mM glutamate, or treatment with 50 ng/mL Tat in the absence (untreated) or presence of 10 μM TCN201 as indicated. PI fluorescence was normalized to 1 mM glutamate treatment. Data are expressed as mean ± SEM. **, $p < 0.01$ relative to control (ANOVA with Tukey's post-test). B, Representative processed images of neurons incubated with 10 μM TCN201 before (0 h) and after (24 h) no treatment (TCN alone) or treatment with 50 ng/mL Tat (TCN + Tat). The insets are enlarged images of the boxed region. Scale bars represent 10 μm. C, Bar graph summarizes changes in PSD-GFP puncta (PSDs) after 24 h treatment under control conditions or following treatment with 50 ng/mL Tat in the absence or presence of 10 μM TCN201. Data are expressed as mean ± SEM. ***, $p < 0.001$ relative to control; ###, $p < 0.001$ relative to 50 ng/mL Tat alone (ANOVA with Tukey's post-test).

TCN201 does not induce synapse recovery

We next examined the effects of TCN201 on synapse recovery. When applied 16 h after the application of 50 ng/mL Tat, 10 μM TCN201 showed no effect (n = 13) (Figure 2.9, A-B). The significant reduction in the number of synapses observed at the time of TCN201 application (t=16 h) was sustained in the presence of drug, in contrast to the effects of ifenprodil and memantine which induced synapse recovery. Furthermore, when 10 μM TCN201 was applied 15 min prior to RAP, it prevented RAP-induced recovery of synapses (n = 10) (Figure 2.9, C), similar to the effects of dizocilpine.

Taken together, these results indicate that memantine, as well as GluN2B-selective concentrations of ifenprodil protect from Tat-induced cell death, fail to affect Tat-induced synapse loss and will precipitate a recovery of synapses lost following Tat treatment. In contrast, GluN2A-selective concentrations of TCN201 do not protect from Tat-induced cell death, yet inhibit Tat-induced synapse loss. TCN201 inhibited RAP-induced synapse recovery. The NMDA receptor antagonist dizocilpine, which lacks subunit selectivity, inhibited all aspects of Tat-induced toxicity, synapse loss, and subsequent recovery.

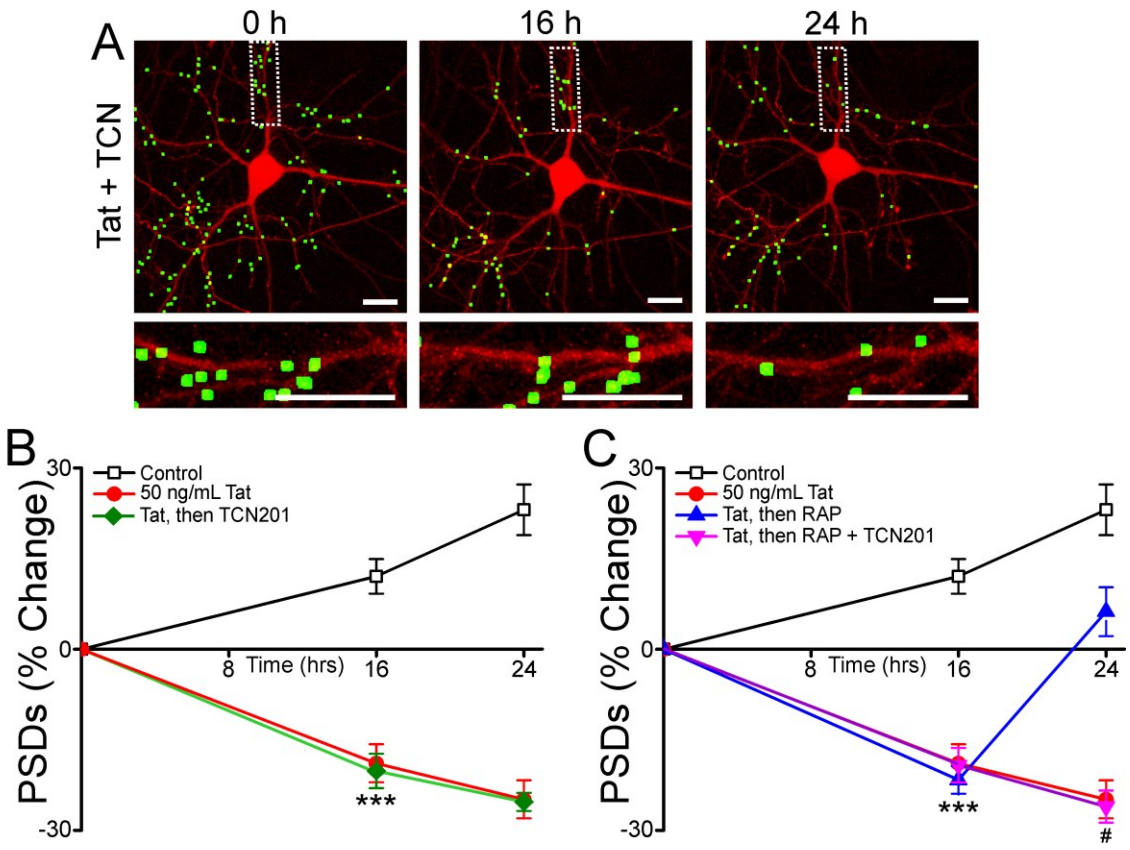

Figure 2.9. TCN201 inhibits synapse recovery after Tat-induced loss. A, Representative processed images of a neuron before (0 h) and 16 or 24 h after treatment with 50 ng/mL Tat. 10 µM TCN201 was applied after 16 h in the presence of Tat. The insets are enlarged images of the boxed region. Scale bars represent 10 µm. B–C, Graphs summarize % change in number of PSDs in the absence (control) or presence of 50 ng/mL Tat for 24 h. B, After 16 h exposure to Tat cells were then left untreated or treated with 10 µM TCN201. C, After 16 h exposure to Tat cells were then left untreated, treated with 50 nM RAP alone or treated with RAP + 10 µM TCN201. TCN201 was added to neurons 15 min before 50 nM RAP. Data are expressed as mean ± SEM. ***, $p < 0.001$ relative to control at 16 h; #, $p < 0.05$ relative to 50 ng/mL Tat, then RAP at 24 h (ANOVA with Tukey's post-test).

IV. Discussion and conclusions

Dendritic pruning and loss of synaptic spines correlates with cognitive decline in patients with HIV associated dementia (Masliah et al., 1997; Everall et al., 1999). HIV neurotoxicity is mediated in part by viral proteins, such as Tat, shed by infected non-neuronal cells (King *et al.*, 2006). In this study we used a live cell, confocal imaging assay to track dynamic changes in synapse number in neurons exposed to the HIV protein Tat. Tat induced a marked loss of synapses by 24 h. Synapse loss following 16 exposure to Tat was reversible, although prolonged exposure led to cell death by 48 h. All three events—death, synapse loss and synapse recovery—required NMDA receptor activity (Figure 2.10). We examined the effects of four NMDA receptor antagonists with distinct mechanisms of action on these processes. Dizocilpine blocked all three processes. Memantine and ifenprodil prevented Tat-induced cell death. These drugs failed to affect Tat-induced synapse loss but, if applied late after significant synapse loss was evident, memantine and ifenprodil induced a recovery of synapse number. In contrast, TCN201 inhibited Tat-induced synapse loss as well as RAP-induced synapse recovery, but could not induce recovery, nor protect against Tat-induced cell death. These results suggest specific roles for NMDA receptor subtypes in these processes. Furthermore, the pharmacology of synapse loss and recovery changed during the course of the neurodegenerative process.

Figure 2.10. Modulation of HIV Tat-induced changes in synapses and survival by subtype specific NMDA receptor antagonists. Summary scheme links effects of pharmacological agents to hypothesized functions mediated by GluN2A- and GluN2B-containing NMDA receptors.

Considerable evidence implicates HIV Tat as a significant contributing factor in HAND. It is present in the serum of HAND patients, and Tat protein and mRNA levels in the parenchyma correlate with the severity of neurological symptoms (Wiley et al., 1996; Hudson et al., 2000). Intracerebroventricular injection of Tat induced behavioral alterations, impaired long-term potentiation and produced neuronal and glial toxicity (Bruce-Keller *et al.*, 2003; Li *et al.*, 2004). *In vitro* and *in vivo* studies have demonstrated that Tat induces dendritic pruning (Fitting *et al.*, 2010), synapse loss (Kim *et al.*, 2008) and cell death (Eugenin *et al.*, 2007). The imaging-based assay employed for this study is well suited for evaluating synaptic changes induced by neurotoxins such as Tat. Because the assay tracks the number of synapses on the same cell before and during the course of toxin exposure, it is especially useful for studying the recovery of synapses. Thus, this cell culture model is suitable for studying the effects of neuroprotective agents on cell survival and synapse loss and recovery.

The uncompetitive NMDA receptor antagonist dizocilpine inhibited Tat-induced neuronal death, Tat-induced synapse loss and RAP-induced synapse recovery in a concentration-dependent manner. The EC_{50} values for all three effects were in the 10-25 nM range, consistent with those reported previously for dizocilpine inhibition of synaptic transmission (Wong *et al.*, 1986), and NMDA-induced cell death (Gill *et al.*, 1987). Dizocilpine does not distinguish among NMDA receptor subtypes and while it is use-dependent (Foster and Wong, 1987; Huettner and Bean, 1988), the prolonged exposures employed in this study would effectively block all receptors in the spontaneously active network that forms in culture. Thus, we conclude from the dizocilpine experiments that NMDA receptor activity is necessary for Tat-induced cell death, and for synapse loss and recovery. Tat-induced cell death was previously shown to require NMDA receptor mediated Ca^{2+} entry (Bonavia *et al.*, 2001; Eugenin *et al.*, 2007). Tat-induced synapse loss was also previously shown to be triggered by NMDA receptor activity (Kim *et al.*, 2008). NMDA receptor activity is required to remodel synapses (Shi and Ethell, 2006), and can promote synaptogenesis and stabilize synapses during development in a subunit-specific manner (Gambrill and Barria, 2011). Here we showed that NMDA receptor activity was required for the recovery of synapses lost during a neurodegenerative process. That synapse recovery might follow some of the same processes responsible for synapse formation during development is plausible. Dizocilpine is highly efficacious in acute neurotoxicity models (Gill *et al.*, 1987). However, it is poorly tolerated in humans because of psychotomimetic side effects (Muir and Lees, 1995; Manahan-Vaughan et al., 2008) consistent with inhibition of synaptic plasticity. Dizocilpine blocks long-term potentiation, (Coan *et al.*, 1987), long-term depression (Massey *et al.*, 2004) and, as shown here, synapse loss and recovery. Thus, dizocilpine inhibits the homeostatic regulation of synapses after toxic environmental changes.

Memantine, like dizocilpine, is an uncompetitive NMDA receptor antagonist. However, it is of lower potency and displays higher binding off-rate kinetics (Parsons et al., 1993; Chen and Lipton, 1997). The binding kinetics in particular are thought to confer selectivity to extrasynaptic NMDA receptors (Xia *et al.*, 2010). The rapid kinetics spare transiently activated receptors involved in synaptic transmission while inhibiting extrasynaptic receptors preferentially activated following sustained elevation of glutamate. Extrasynaptic NMDA receptors that are thought to preferentially activate cell death processes can be activated by excess synaptic activity that produces glutamate spillover (Rusakov and Kullmann, 1998), or the tonic increase in extracellular glutamate produced by enhanced release or impaired uptake by astrocytes (Pasti *et al.*, 2001). Sparing of synaptic NMDA receptors by memantine is consistent with our observation that it does not affect Tat-induced synapse loss but does prevent Tat-induced cell death. Reported EC_{50} values for memantine inhibition of NMDA-induced responses are in the low micro molar range (Chen and Lipton, 1997). However, the lower potency of memantine relative to dizocilpine cannot explain the failure of memantine of prevent Tat-induced synapse loss because even at 100 μM, a concentration 10 times higher than that needed to prevent Tat-induced cell death, memantine failed to affect synapse loss. Memantine is approved for use in patients with Alzheimer's disease to improve cognition. The drug is well-tolerated, presumably because it spares synaptic plasticity, but is of modest efficacy. Perhaps analogs with altered binding kinetics can be developed that spare synaptic activation of NMDA receptors, but display greater neuroprotective efficacy. Our observation that memantine reversed synapse loss induced by Tat is intriguing. Clearly the pharmacology of synapse loss and recovery has changed during the course of exposure to Tat. It is possible that the pattern of NMDA receptor activation changes following exposure to Tat such that it favors memantine binding. Alternatively,

excessive activation of extrasynaptic NMDA receptors might lead to receptor internalization (Roche et al., 2001; Nong et al., 2003) changing the relative balance of extrasynaptic to synaptic NMDA receptors.

Ifenprodil exerts its selective effects via a mechanism different from that of memantine, although the functional outcome in our assays was comparable. Ifenprodil is an GluN2B-selective NMDA receptor antagonist; its affinity for GluN2B-containing NMDA receptors is 10 times higher than for GluN2A-containing NMDA receptors (Williams, 1993). Ifenprodil and dizocilpine have similar binding kinetics (Black *et al.*, 1996). Thus, subunit selectivity is responsible for its profile of antagonism, one that is distinct from dizocilpine and similar to memantine. The preferential localization of GluN2B subunits to NMDA receptors at extrasynaptic sites (Liu *et al.*, 2007) is consistent with the similar effects observed with memantine. Activation of GluN2B-containing NMDA receptors triggers cell death processes possibly because binding sites for death-inducing signaling molecules such as NOS are present on the carboxyl tail of GluN2B subunits (Christopherson *et al.*, 1999). GluN2A-containing NMDA receptors are highly localized to synapses, and their activation has been shown to promote survival (Liu *et al.*, 2007). Sparing GluN2A-containing NMDA receptors might account for the failure of ifenprodil to prevent Tat-induced synapse loss if the pro-survival GluN2A subtype of receptor mediated loss of synapses as a protective mechanism. However, the ifenprodil-evoked increase in synapses following Tat-induced loss suggests that the abundance of GluN2B- relative to GluN2A-containing NMDA receptors changes over the course of exposure to Tat. A changing pharmacological profile over the course of disease has important implications for when to administer and how to design neuroprotective drugs.

TCN201 exerted effects opposite to those elicited by the GluN2B preferring antagonists, memantine and ifenprodil. This observation is consistent with the

selectivity of TCN201 for GluN2A-containing NMDA receptors (Bettini *et al.*, 2010). Previous reports demonstrated differential effects of GluN2A- versus GluN2B-prefering antagonists on synaptic plasticity (Ge *et al.*, 2010) and a prominent role for NMDA receptors containing GluN2B, but not GluN2A, subunits in initiating cell death (Hardingham et al., 2002; Liu et al., 2004a; Liu et al., 2007). GluN2A-containing NMDA receptors participate in anxiety- and depression-like behaviors (Boyce-Rustay and Holmes, 2006) suggesting that they may be useful pharmacological targets. Our results caution that drugs targeting GluN2A-containing NMDA receptors may interfere with the synaptic changes that enable neurons to adapt to synaptically driven excitotoxicity.

We hypothesize that synapse loss is a protective mechanism that enables the cell to cope with excitotoxic stimuli such as Tat by down regulating excitatory input. Synapse loss is triggered by Ca^{2+} influx via NMDA receptors with subsequent activation of an ubiquitin ligase (Colledge *et al.*, 2003; Kim *et al.*, 2008). This pathway is separate from the one driving cell death, which also requires NMDA receptor activation but is mediated by Ca^{2+} dependent nNOS activation (Kim *et al.*, 2008). Tat-induced, NO-mediated neuronal death is an apoptotic process (Kruman *et al.*, 1998). Using the same hippocampal cultures and synapse and survival assays described here, we previously reported that inhibiting the ubiquitin-proteasome pathway with nutlin-3 prevented Tat-induced synapse loss, but not Tat-induced neuronal death. Conversely, L-NAME, an nNOS inhibitor, did not inhibit synapse loss, but prevented neuronal death induced by Tat. In the presence of nutlin-3 the EC_{50} for Tat induced neuronal death was shifted to the left. Thus, the inhibition of PSD95 degradation by the ubiquitin proteasome pathway increases the sensitivity to Tat-induced death. The coupling of nNOS to GluN2B subunits is consistent with the ability of dizocilpine, memantine and ifenprodil, but not TCN201, to prevent Tat-induced cell death (Christopherson *et al.*, 1999). The pro-

survival role previously attributed to GluN2A-containing NMDA receptors is consistent with the idea that synaptic activity drives synapse loss by activation of GluN2A-containing NMDA receptors and that this loss improves survival. We speculate that Tat and NMDA receptor antagonists shift the delicate balance between survival and full integration into synaptic circuits.

Linking GluN2B subunits to NOS mediated death and GluN2A to the ubiquitin-proteasome pathways and synapse loss does not adequately explain the recovery of synapses induced by application of memantine or ifenprodil after Tat-induced synapse loss. The recovery of synapses induced by block of GluN2B-containing NMDA receptors suggests that activation of these receptors suppress new synapse formation. The failure of these drugs to affect Tat-induced synapse loss when given before Tat and the induced recovery produced by their late application, suggest that the composition of functional NMDA receptors changes during exposure to Tat. NMDA receptors internalize following sustained activation (Roche et al., 2001; Nong et al., 2003) and synapse loss clearly reduces NMDA receptor levels. The mechanism by which these drugs can induce recovery has yet to be elucidated. Indeed, the mechanism by which RAP can induce synapse recovery is not yet known; RAP is classified as a competitive antagonist for LRP, but this mechanism alone cannot explain how synapse recovery occurs at a time point when Tat is presumably already internalized.

We propose that memantine and ifenprodil, by inhibiting a select subset of NMDA receptors as compared to the broad actions of dizocilpine, display several properties desirable for neuroprotective drugs. They improve survival by preventing Tat-induced activation of cell death pathways. Memantine and ifenprodil did not interfere with Tat-induced synapse loss which allows a potentially beneficial reduction in excitatory input. Surprisingly, these drugs induced the recovery of synapses lost during exposure to Tat.

These findings may be broadly applicable to other neurodegenerative processes with an excitotoxic component.

Chapter Three:

HIV Tat induces excitotoxic loss of presynaptic terminals in hippocampal cultures

Angela H. Shin and Stanley A. Thayer

Content adapted from published article: **Shin A.H.,** and Thayer S.A. (2013) HIV-1 Tat induces excitotoxic loss of presynaptic terminals in hippocampal cultures. Mol Cell Neuroscience, Jan; 54: 22-29.

Contributions: AHS collected and analyzed data, and contributed heavily to writing of manuscript.

I. Introduction

Human immunodeficiency virus (HIV) infection is a worldwide epidemic that affects approximately 30 million people (Kaul et al., 2001). Neurocognitive deficits are a significant consequence of HIV infection and affect approximately 30-50% of HIV-infected patients (Cysique et al., 2004; Tozzi et al., 2005a). Neurological symptoms range in severity from mild cognitive impairment to severe HIV-associated dementia, and are collectively known as HIV-associated neurocognitive disorders (HAND) (Ellis et al., 2007). HAND is a major consequence of HIV infection; progression of these neurological symptoms often renders patients incapable of functioning without daily assistance (Kaul and Lipton, 2006; Hult et al., 2008; Minagar et al., 2008). Additionally, while the advent of combined anti-retroviral therapies has reduced the incidence of HIV-associated dementia, the increased lifespan of HIV-infected patients has increased the prevalence of HAND diagnoses, providing a compelling need to develop improved therapies to combat the rising incidence of HAND.

HIV induces neurotoxicity and subsequent neurocognitive deficits by an indirect mechanism. The virus infects macrophages and microglia, not neurons in the CNS, and these infected cells in turn secrete inflammatory cytokines and shed viral proteins that are toxic to neurons (Genis et al., 1992; Speth et al., 2001). One such toxic protein is the HIV Transactivator of transcription (Tat), which is shed by infected cells. Tat mRNA and protein are found in the CNS of HAND patients (Hofman et al., 1994; Wiley et al., 1996; Del Valle et al., 2000; Hudson et al., 2000) and Tat protein induces HAND neuropathologies *in vivo* (Kim et al., 2003; Fitting et al., 2010). *In vitro* effects of Tat include dendritic pruning, decreased spine density, and synapse loss (Liu et al., 2000; Eugenin et al., 2007; Kim et al., 2008). Clinical studies have shown that the extent of cognitive decline in HAND patients correlates closely with dendritic damage and

synapse loss, rather than overt neuronal death (Wiley et al., 1999; Sa et al., 2004).

Tat induces the loss of excitatory synapses via a mechanism that is distinct from that by which it elicits cell death (Kim et al., 2008). Tat binds to the low density lipoprotein receptor-related protein (LRP), and activates NMDA receptors. The subsequent postsynaptic calcium influx triggers two independent pathways. Loss of the postsynaptic density results from calcium-induced activation of an ubiquitin ligase. Cell death results from calcium-dependent activation of neuronal nitric oxide synthase (nNOS) (Kim et al., 2008). Interestingly, Tat-induced loss of postsynaptic densities is reversible. What is not known, however, is how loss and recovery of postsynaptic densities relates to the dynamics of presynaptic terminals during exposure to HIV Tat.

Synaptophysin is an abundant membrane glycoprotein found on synaptic vesicles at the presynaptic terminal (Wiedenmann and Franke, 1985; Rehm et al., 1986; Johnston and Sudhof, 1990). Synaptophysin is a calcium-binding protein that is nonessential for vesicle release (McMahon et al., 1996), and is a major component of small synaptic vesicles. It is recruited to presynaptic active zones during synaptogenesis, albeit later than precursor proteins such as Bassoon or Piccolo (Fletcher et al., 1991; Friedman et al., 2000; Ziv and Garner, 2004), and is thus a good marker for presynaptic terminals.

In this study, we examined the effects of HIV Tat on presynaptic terminals by tracking the expression of a synaptophysin-GFP fusion protein. HIV Tat decreased the number of presynaptic terminals on hippocampal neurons in culture. Moreover, this loss was triggered by NMDA receptor activity, indicating that loss of presynaptic terminals was initiated by postsynaptic mechanisms. Tat-induced loss of presynaptic terminals was reversible, and this recovery was initiated by modulating NMDA receptor activity. These results suggest that Tat-induced synapse loss and recovery are driven by

postsynaptic mechanisms.

II. Methods

Materials. Materials were obtained from the following sources: the Syn-GFP expression vector (pSynaptophysin-GFP-C1) was kindly provided by Jane Sullivan (University of Washington, Seattle, WA); the expression vector for DsRed2 (pDsRed2-N1) from Clontech (Mountain View, CA); HIV Tat (Clade B, full length, recombinant) from Prospec Tany TechnoGene Ltd. (Rehovot, Israel) and through the NIH AIDS Research and Reference Reagent Program (HIV Tat protein (full length, Clade B) from Dr. John Brady and DAIDS, NIAID); recombinant rat receptor associated protein (RAP) from Fitzgerald Industries International (Concord, MA); Dulbecco's modified Eagle medium (DMEM), fetal bovine serum, and horse serum from Invitrogen (Carlsbad, CA); ifenprodil hemitartrate from Tocris (Ellsville, MO); penicillin/streptomycin, MK801, and all other reagents from Sigma (St. Louis, MO). For control experiments, Tat was heat-inactivated by incubation at 85°C for 30 min.

Cell culture. Rat hippocampal neurons were grown in primary culture as described previously (Shen and Thayer, 1998). Fetuses were removed on embryonic day 17 from maternal rats euthanized by CO_2 inhalation. Hippocampi were dissected and placed in Ca^{2+} and Mg^{2+}-free HEPES-buffered Hanks salt solution (HHSS), pH 7.45. HHSS was composed of the following (in mM): HEPES 20, NaCl 137, $CaCl_2$ 1.3, $MgSO_4$ 0.4, $MgCl_2$ 0.5, KCl 5.0, KH_2PO_4 0.4, Na_2HPO_4 0.6, $NaHCO_3$ 3.0, and glucose 5.6. Cells were dissociated by trituration through a 5 mL pipette and a flame-narrowed Pasteur pipette and resuspended in DMEM without glutamine, supplemented with 10% fetal bovine serum and penicillin/streptomycin (100 U/mL and 100 µg/mL, respectively).

Dissociated cells were then plated at a density of 100,000-120,000 cells per dish onto a 25-mm-round cover glass (#1) glued to cover a 19 mm diameter opening drilled through the bottom of a 35 mm Petri dish. The cover glass was precoated with Matrigel (200 µL, 0.2mg/mL) (BD Biosciences, Billerica, MA). Neurons were grown in a humidified atmosphere of 10% CO_2 and 90% air (pH 7.4) at 37 ^{o}C, and fed on days 1 and 6 by exchange of 75% of the media with DMEM, supplemented with 10% horse serum and penicillin/streptomycin. Cells used in these experiments were cultured without mitotic inhibitors for at least 12 days, resulting in a mixed glial-neuronal culture. Immunocytochemistry experiments demonstrated that these cultures were composed of 18 $\pm$ 2 % neurons, 70 $\pm$ 3 % astrocytes and 9 $\pm$ 3 % microglia (Kim et al., 2011).

Transfection. Rat hippocampal neurons were transfected between 10 and 12 days *in vitro* using a modification of a protocol described previously (Kim et al., 2008). Briefly, hippocampal cultures were incubated for at least 20 minutes in DMEM supplemented with 1 mM kynurenic acid, 10 mM $MgCl_2$, and 5 mM HEPES, to reduce neurotoxicity. A DNA/calcium phosphate precipitate containing 1 µg total plasmid DNA per well was prepared, allowed to form for 30 min at room temperature, and added to the culture. After a 90 minute incubation period, cells were washed once with DMEM supplemented with $MgCl_2$ and HEPES and then returned to conditioned media, saved at the beginning of the procedure. Transfected neurons were imaged 48-72 hours post-transfection. Transfection efficiency ranged from 1-5%.

Confocal imaging. Petri dishes containing transfected neurons were sealed with Parafilm, transferred to the stage of an inverted confocal microscope (Olympus Fluoview 300, Melville, NY) and viewed through a 60X oil-immersion objective (NA=1.4). To

enable repeated imaging of the same cell over a 24 h period, the location of the cell was recorded using micrometers attached to the stage of the microscope. Optical sections spanning 8 μm in the z-dimension were collected (1 μm steps), and were combined through the z-axis into a compressed z stack. GFP was excited at 488 nm with an argon ion laser and emission collected at 530 nm (10 nm band pass). DsRed2 was excited at 543 nm with a green HeNe laser and emission collected at >605 nm. The cell culture dish was returned to the CO_2 incubator between image collections. Experiments studying synapse recovery were performed for 24 hours in the continuous presence of Tat, with or without the specified drugs added at 16 hours.

Image processing. To count and label Syn-GFP puncta an automated algorithm was created using MetaMorph 6.2 image processing software described previously (Waataja et al., 2008). Briefly, maximum z-projection images were created from the DsRed2 and GFP image stacks. Next, a threshold set 1 s.d. above the image mean was applied to the DsRed2 image. This created a 1-bit image that was used as a mask via a logical AND function with the GFP maximum z-projection. A top-hat filter (80 pixels) was applied to the masked Syn-GFP image. A threshold set 1.5 s.d. above the mean intensity inside the mask was then applied to the contrast enhanced image. Structures between 8 and 80 pixels (approximately 0.66 to 6.64 μm in diameter) and in contact with the DsRed2 mask were counted as presynaptic terminals. The structures were then dilated and superimposed on the DsRed2 maximum z-projection for visualization. All Syn-GFP puncta in the representative processed images displayed in the figures were included in the quantitative analysis.

Immunocytochemistry. Hippocampal cultures were prepared as described above

and maintained for at least 12 days in culture. Cells on coverslips were transfected with an expression plasmid for Syn-GFP as described above. After 48 hrs, cells were washed with tris-buffered saline (TBS), and then fixed with Lana's fixative (8% paraformaldehyde, 14% picrate, 0.16 M PO_4) for 10 min. The cells were washed with TBS, then permeablized in TBS + 0.2% Triton X100 (Sigma) for 10 min at room temperature. After permeablization, cells were incubated with mouse anti-Bassoon monoclonal antibody (1:200, Enzo Life Sciences, Farmingdale, NY) in TBS + 0.2% Tween-20 (Sigma) for 1 h at room temperature. Cells were washed with TBS and labeled with tetramethyl rhodamine isothiocyanate (TRITC)-conjugated goat anti-mouse antibody (Millipore, Billerica, MA, 1:400) in TBS + 0.2% Tween-20. Coverslips were mounted with DPX mountant (Sigma) and visualized on an inverted confocal microscope (Olympus Fluoview 300, Melville, NY) using a 60X oil-immersion objective (NA=1.4). TRITC was excited at 543 nm, and emission collected at >605 nm.

Statistics. For synapse loss and recovery studies, an individual experiment (n=1) was defined as the change in the number of Syn-GFP puncta from a single cell from a single coverslip. Puncta counts were presented as mean ± SEM. Each experiment was replicated over at least 3 separate cultures. In all statistical analyses we used Student's t-test for single or ANOVA with Tukey's post-hoc test for multiple statistical comparisons (OriginPro v8.5, Northampton, MA).

III. Results

Synaptophysin-GFP labels pre-synaptic terminals

The number of presynaptic terminals in rat hippocampal cultures was measured by confocal imaging of neurons transfected with an expression construct for the

presynaptic protein synaptophysin fused to GFP (Syn-GFP). Synaptophysin is part of the neurotransmitter release machinery and is an established marker for presynaptic terminals. The neurons were co-transfected with an expression construct for DsRed2, a red fluorescent protein that filled the neuron and enabled visualization of cell morphology (Figure 3.1, A, DsRed). Syn-GFP expressed in a distinct punctate pattern (Figure 3.1, A, Syn-GFP). Neurons were imaged on a laser scanning confocal microscope as described in Methods. Image processing identifed Syn-GFP puncta meeting size and intensity criteria in contact with DsRed2 fluorescence, using a previously described algorithm (Shin et al., 2012). These puncta were dilated and overlaid on the DsRed2 maximum projection for visualization purposes (Figure 3.1, A, Processed). The same neuron was repeatedly imaged over time and the number of Syn-GFP puncta counted at each time point to determine changes in number of presynaptic terminals impinging on a single cell.

Syn-GFP puncta represented presynaptic terminals because they co-localized with Bassoon immunoreactivity (Figure 3.1, B). Bassoon is a scaffolding protein concentrated at presynaptic terminals (tom Dieck et al., 1998). 78 ± 4% of Syn-GFP puncta co-localized with Bassoon immunoreactivity, confirming that Syn-GFP expression in our culture accurately labels presynaptic terminals. The presynaptic terminals seen are a mixture of autapses resulting from an axon extending from the DsRed filled soma displayed in the field as well as boutons from axons emanating from cells outside the field of view.

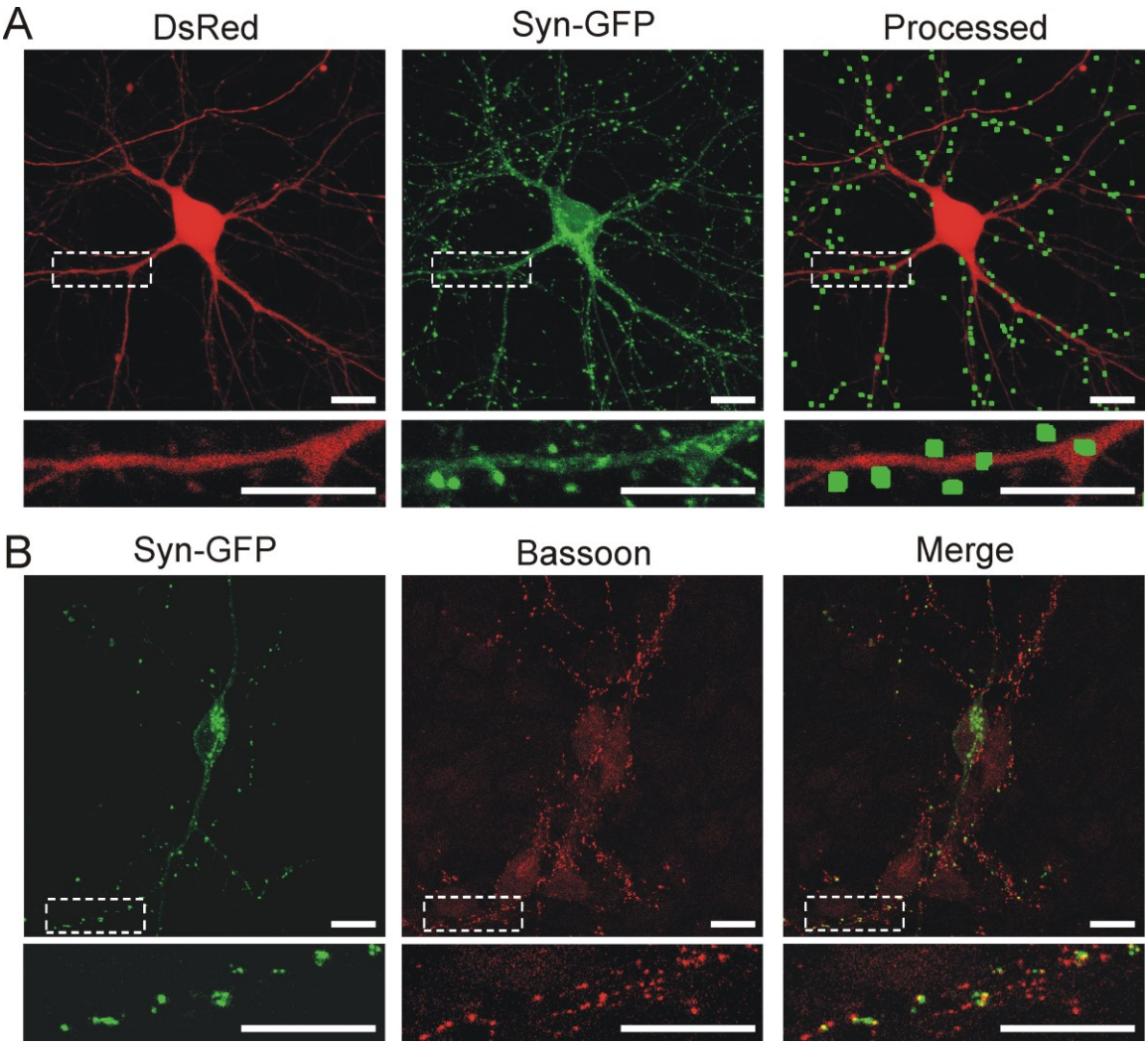

Figure 3.1. Synaptophysin-GFP puncta represent presynaptic terminals. A, representative confocal images were collected and processed as described in Methods. Maximum z-projections show a neuron expressing DsRed2 (DsRed) and Syn-GFP. Syn-GFP puncta were identified from compressed z-stacks of confocal images by filtering for puncta size and fluorescence intensity. Puncta were dilated and overlaid on the DsRed maximum projection (Processed). Heavy intracellular labeling in the soma was not counted by the algorithm. Insets are enlarged images of the boxed regions. Scale bars represent 10 µm. B, representative confocal images of neurons expressing Syn-GFP and immunolabeled for Bassoon. Syn-GFP puncta co-localized with Bassoon immunoreactivity (Merge). Note that non-transfected cells were also present in the field, and thus not all Bassoon-immunoreactive puncta (red) co-localize (yellow) with a Syn-GFP puncta (green). Insets are enlarged images of the boxed regions. Scale bars represent 10 µm.

HIV Tat induces loss of Syn-GFP puncta

We previously found that 24 hr exposure to the HIV Tat protein decreased the number of postsynaptic densities in hippocampal neurons in culture (Kim et al., 2008). Here, we studied the effects of Tat on presynaptic terminals. As shown in Figure 3.2 A, 24 hr treatment with Tat produced a marked decrease in the number of Syn-GFP puncta. Treatments of this duration did not produce cell death (Kim et al., 2008), nor did Tat significantly alter cell morphology (Figure 3.2, A). Figure 3.2 B shows the time course for changes in the number of Syn-GFP puncta during exposure to 50 ng/mL Tat. HIV Tat induced an 8 ± 4% loss in the number of Syn-GFP puncta by 8 h, 8 ± 4% loss by 16 h, and 13 ± 4% loss by 24 h. This loss was significant relative to control values by 16 h, and sustained over a 48 h interval. This time course is similar to that seen for Tat-induced changes in postsynaptic densities (Kim et al., 2008). In contrast to Tat-treated cells, control cells exhibited a 25 ± 12% increase in the number of Syn-GFP puncta over 48 h. Heat-inactivated Tat did not induce a loss in the number of Syn-GFP puncta (26 ± 8% increase, n = 6), confirming that Syn-GFP loss was due to functional HIV Tat protein.

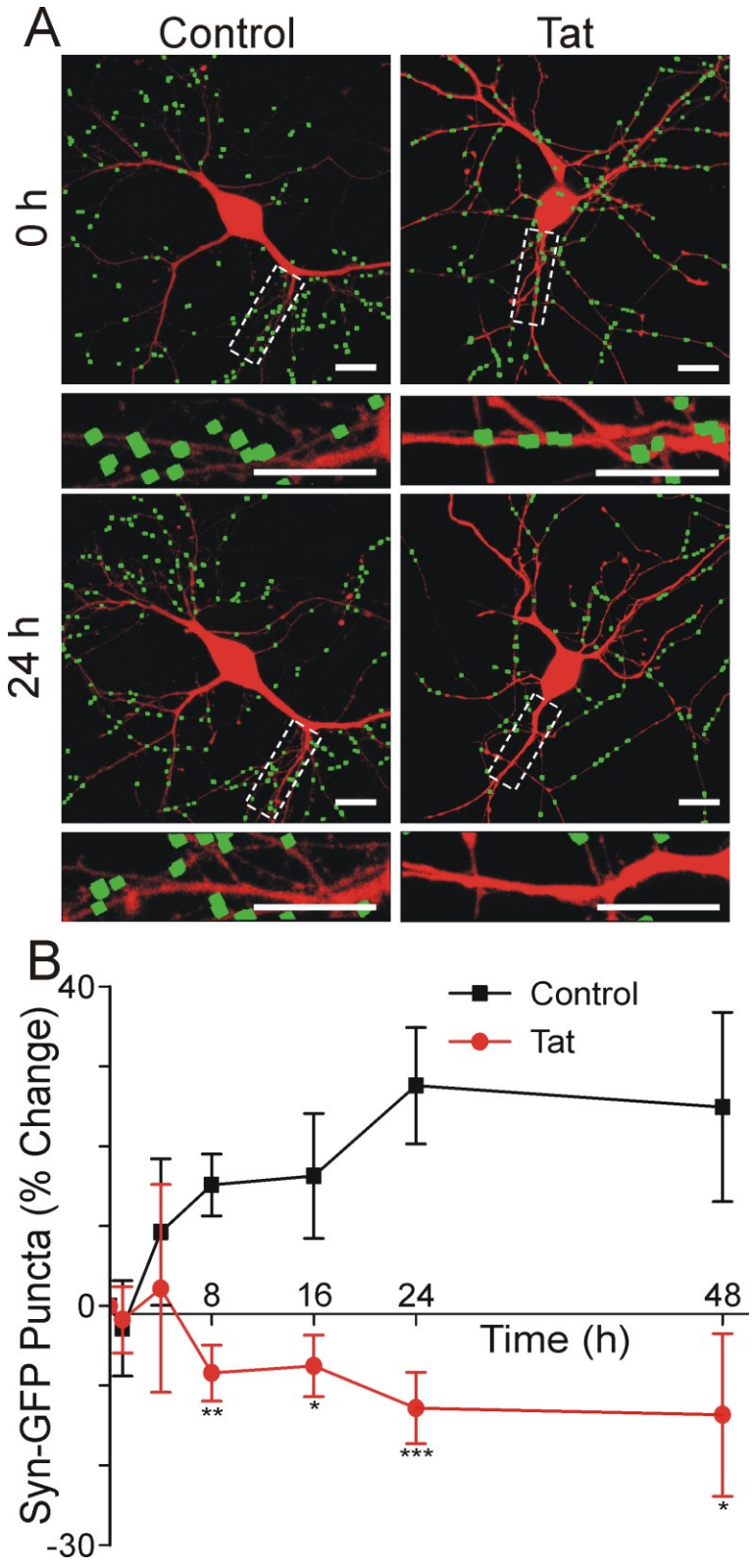

Figure 3.2. HIV Tat induces loss of presynaptic terminals. A, representative processed images show neurons before (0 h) and after (24 h) no treatment (Control) or treatment with 50 ng/mL Tat (Tat). Insets are enlarged images of the boxed regions. Scale bars represent 10 µm. B, Graph shows % change in number of Syn-GFP puncta over a 48 h interval ($n \geq 6$ for each time point). Neurons were either untreated (Control, black squares) or treated with 50 ng/mL Tat (Tat, red circles) after the initial time point (t = 0 h). *, $p<0.05$, **, $p<0.01$, ***, $p<0.001$ vs. Control values at corresponding time point (ANOVA with Tukey's post-test). All data are expressed as mean ± SEM.

Tat-induced Syn-GFP loss is dependent on post-synaptic activity

Loss of postsynaptic densities is initiated by Tat binding to the low density lipoprotein receptor-related protein (LRP), and over-activating NMDA receptors. We sought to determine whether the same mechanisms were involved in Tat-induced Syn-GFP loss. Tat (50 ng/mL) induced a 15 $\pm$ 3 % loss of Syn-GFP puncta (Figure 3.3, A). Pre-treating neurons with the LRP antagonist receptor-associated protein (RAP, 50 nM) prior to Tat exposure, inhibited Tat-induced Syn-GFP loss (Figure 3.3, A-B). Additionally, pre-treating neurons with the NMDA receptor antagonist dizocilpine (MK801) (10 μM) prior to Tat exposure inhibited Tat-induced Syn-GFP loss. We previously showed that both RAP and MK801 inhibited Tat-induced loss of post-synaptic densities (Kim et al., 2008). These data are consistent with the idea that loss of presynaptic terminals induced by Tat is driven by its activity on postsynaptic sites.

Tat-induced loss of postsynaptic densities required ubiquitination of PSD95 and proteasomal degradation; inhibition of the E3 ligase MDM2 with the antagonist nutlin-3 prevented Tat-induced loss of postsynaptic densities (Kim et al., 2008). Pretreating neurons with 1 μM nutlin-3 prior to Tat exposure inhibited Tat-induced Syn-GFP loss (Figure 3.4, A-B). These data indicate that ubiquitination of postsynaptic proteins is required for loss of presynaptic terminals during Tat exposure.

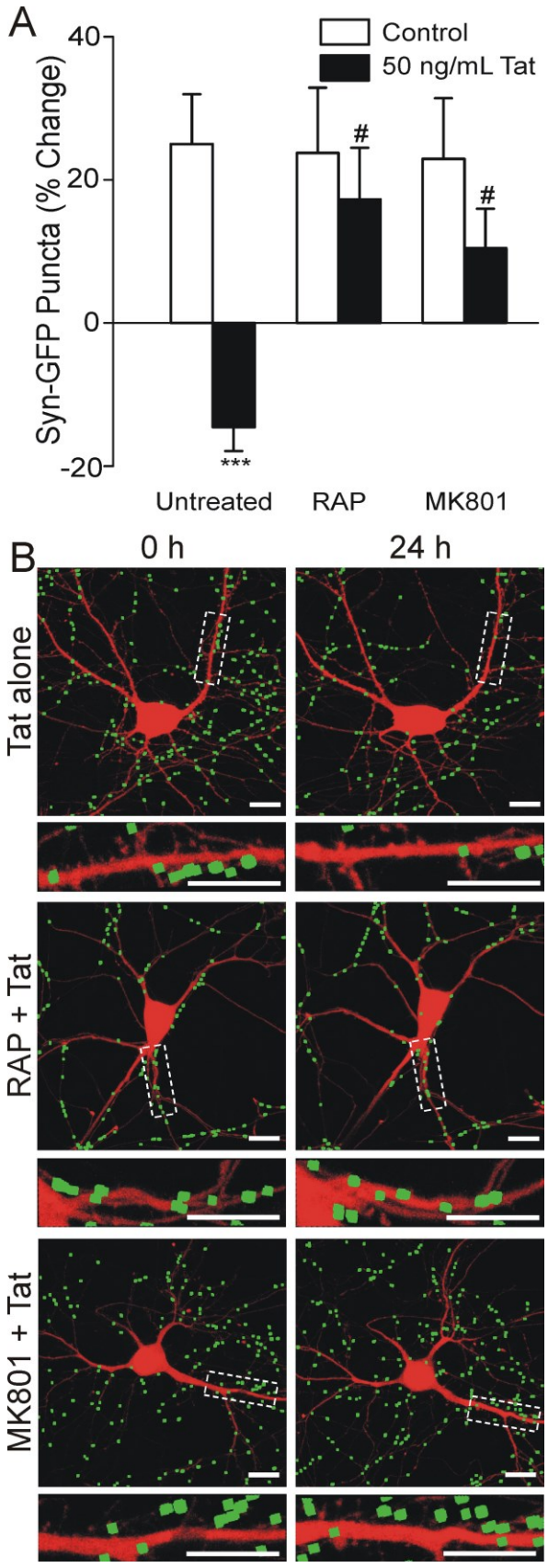

Figure 3.3. Tat-induced Syn-GFP loss requires postsynaptic activity. A, Bar graph summarizes % change in number of Syn-GFP puncta over 24 h under control conditions (open bars) or in the presence of 50 ng/mL Tat (solid bars) ($n \geq 9$ for all groups). Neurons were imaged in the absence (Untreated) or the presence of 50 nM RAP or 10 μM MK801 as indicated. ***, $p < 0.001$ vs. Control; #, $p<0.05$ vs. Tat alone (ANOVA with Tukey's post-test). All data are expressed as mean ± SEM. B, representative processed images of neurons before (0 h) or after (24 h) treatment with 50 ng/mL Tat. Neurons were either untreated (Tat alone), or pretreated with 50 nM RAP (RAP + Tat) or 10 μM MK801 (MK801 + Tat). Insets are enlarged images of the boxed regions. Scale bars represent 10 μm.

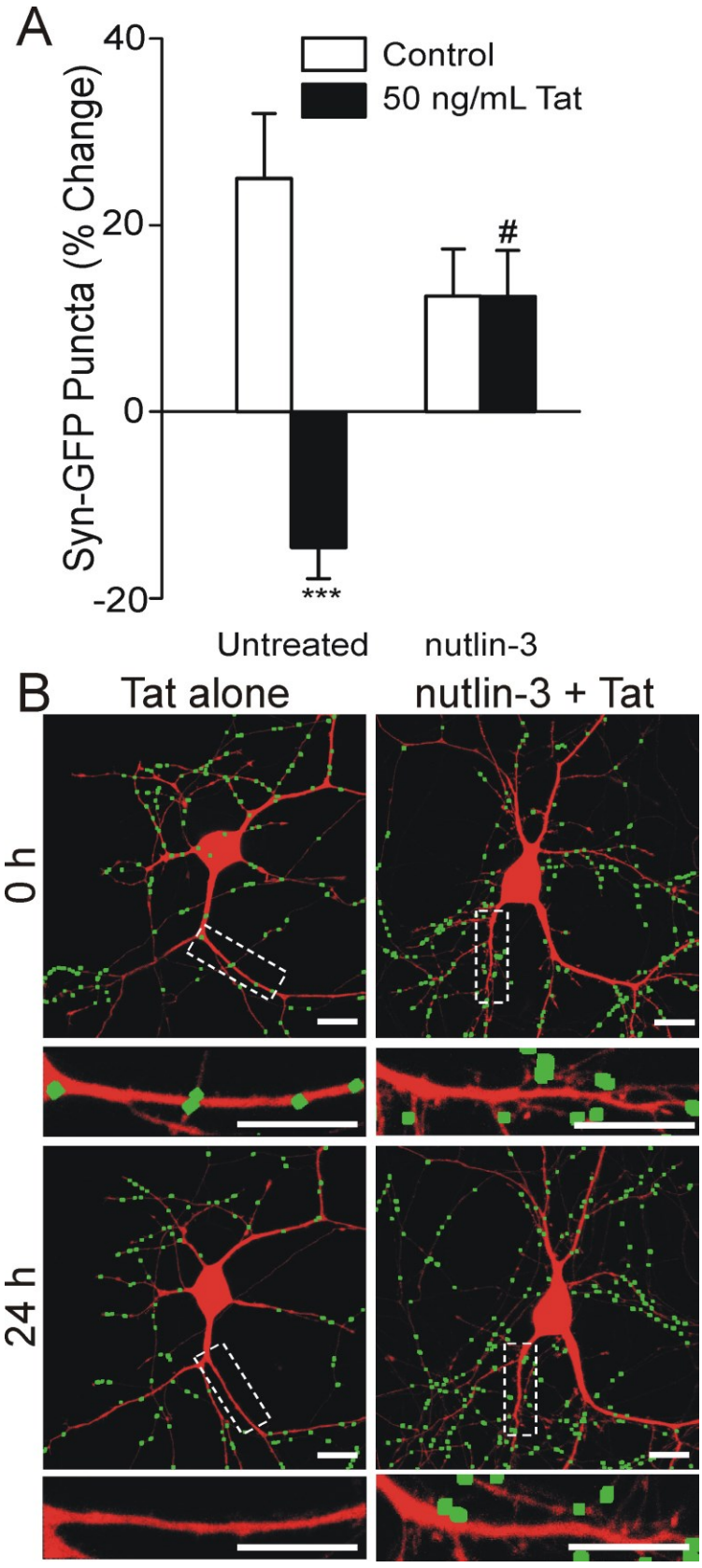

Figure 3.4. Tat-induced Syn-GFP loss requires E3 ligase activity. A, Bar graph summarizes % change in number of Syn-GFP puncta over 24 h under control conditions (open bars) or in the presence of 50 ng/mL Tat (solid bars) ($n \geq 9$ for all groups). Neurons were imaged in the absence (Untreated) or the presence of 1 μM nutlin-3. ***, $p < 0.001$ vs. Control; #, $p<0.05$ vs. Tat (ANOVA with Tukey's post-test). All data are expressed as mean ± SEM. B, representative processed images of neurons before (0 h) or after (24 h) treatment with 50 ng/mL Tat. Neurons were either untreated (Tat alone), or pretreated with 1 μM nutlin-3 (nutlin-3 + Tat). Insets are enlarged images of the boxed regions. Scale bars represent 10 μm.

Tat-induced Syn-GFP loss is reversible

Tat-induced loss of postsynaptic densities is reversible (Kim et al., 2008). Treating neurons with ifenprodil, an GluN2B subunit-selective NMDA receptor antagonist, during Tat exposure induced recovery of postsynaptic densities, whereas no spontaneous recovery was seen in the absence of drug (Shin et al., 2012). We sought to determine whether presynaptic terminals could also be recovered after Tat-induced loss. Neurons were treated with 50 ng/mL Tat for 16 hrs, and then treated with 10 μM ifenprodil. Application of ifenprodil induced a recovery in the number of Syn-GFP puncta, whereas no recovery was seen without ifenprodil treatment (33 ± 8% with ifenprodil; -16 ± 5% with Tat alone at 24 h) (Figure 3.5, A-B). These data indicate that Tat-induced loss of presynaptic terminals is reversible. Furthermore, because ifenprodil acts on postsynaptic NMDA receptors, this recovery was initiated by altered postsynaptic activity.

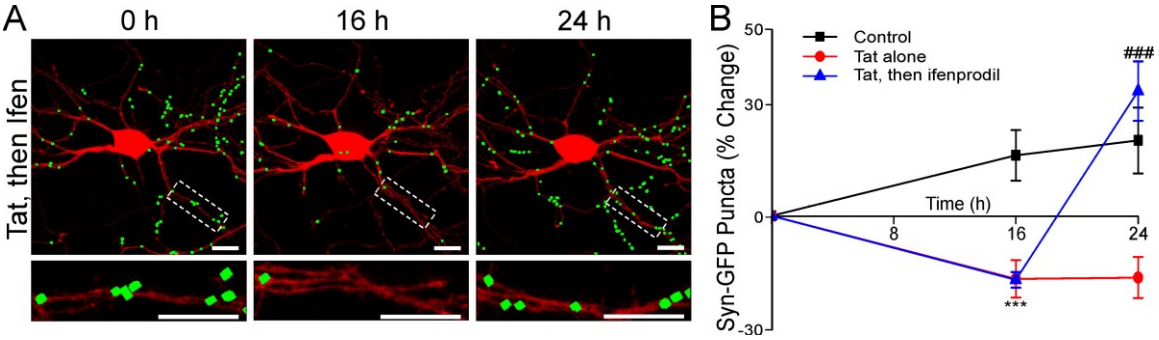

Figure 3.5. Tat-induced Syn-GFP loss is reversible. A, representative processed images of a neuron before (0h) and 16 h or 24 h after treatment with 50 ng/mL Tat. 10 μM ifenprodil was applied immediately after acquisition of the image at t = 16 h. Tat was present throughout the experiment. Insets are enlarged images of the boxed regions. Scale bars represent 10 μm. B, Graph summarizes % changes in number of Syn-GFP puncta in the absence (Control), or presence of 50 ng/mL Tat ($n \geq 6$ for all groups). After 16 h exposure to Tat, neurons were then left untreated (Tat alone) or treated with 10 μM ifenprodil (Tat, then ifenprodil). All data are expressed as mean ± SEM. ***, $p < 0.001$ vs. Control at 16 h, ###, $p < 0.001$ vs. Tat alone at 24 h (ANOVA with Tukey's post-test).

IV. Discussion and conclusions

Dendritic pruning and synapse loss are hallmarks of HAND pathology (Masliah et al., 1997; Everall et al., 1999). The HIV protein Tat is shed by infected cells in the central nervous system and *in vitro*, it binds LRP to activate NMDA receptors, resulting in the loss of postsynaptic densities (Kim et al., 2008; Shin et al., 2012). Here, we examined the effects of Tat on presynaptic terminals. Tat induced loss of presynaptic terminals that mirrored loss of postsynaptic densities with respect to time course and pharmacology. Loss of presynaptic terminals was dependent on postsynaptic activity, suggesting that Tat acts directly on the postsynaptic density, and that loss of presynaptic terminals is a consequence of this action. Tat-induced loss of presynaptic terminals was reversible, and recovery of the number of presynaptic terminals was evoked by inhibition of GluN2B-containing NMDA receptors. Thus, the mechanism of recovery of presynaptic terminals after Tat-induced loss is also dependent upon postsynaptic activity.

We imaged Syn-GFP to visualize presynaptic terminals on individual neurons. Syn-GFP expressed as distinct puncta that co-localized with immunoreactivity for the presynaptic marker protein Bassoon, indicating that Syn-GFP fluorescence was appropriately localized to presynaptic terminals. Furthermore, we have previously shown that Syn-GFP puncta responded to other stimuli such as IL-1β or lithium, treatments that induce decreases and increases in the number of postsynaptic densities, respectively (Kim and Thayer, 2009; Mishra et al., 2012). Therefore, Syn-GFP is a valid and responsive marker for presynaptic terminals and suitable for live cell imaging.

Tat mRNA was detected in brain extracts from patients with HIV encephalitis but not in samples from HIV patients without dementia (Hudson et al., 2000). Tat protein levels in the serum of HIV patients are in the low ng/mL range (Westendorp et al., 1995; Xiao et al., 2000). The Tat protein detected in the brains of patients with HIV

encephalitis using immunohistochemistry indicated that Tat was taken up by cells (Del Valle et al., 2000), consistent with the LRP mediated mechanism that underlies the synapse loss we describe *in vitro*. Soluble Tat has not been measured in the CNS of HAND patients, an observation thought to result from LRP-mediated uptake *in vivo* and rapid proteolysis in post mortem tissue (Li et al., 2009). Previous work from our lab found the EC_{50} for Tat in this assay to be approximately 6 ng/mL, which is well within the concentration range used *in vitro* (Eugenin et al., 2007; Aksenova et al., 2008; Li et al., 2008). We used a maximally effective concentration of Tat (50 ng/mL) in the present study.

HIV Tat induced a 15 ± 3% decrease in the number of Syn-GFP puncta over 24 hours. RAP, an LRP antagonist, and MK801, an NMDA receptor antagonist, both inhibited Tat-induced loss of Syn-GFP puncta, indicating that Tat binding to LRP and subsequent activation of NMDA receptors were required for Tat-induced loss of presynaptic terminals. NMDA receptor activation and subsequent loss of presynaptic terminals are also seen in other neurotoxic processes. For example, treatment with the inflammatory cytokine IL-1β induced loss of Syn-GFP puncta that was also prevented by MK801 (Mishra et al., 2012). LRP and NMDA receptors are highly expressed at postsynaptic densities and Tat forms a macromolecular complex with LRP, the NMDA receptor and PSD95 (Eugenin et al., 2007). Tat has been shown to alter the expression and activity of presynaptic neurotransmitter transporters in other brain regions, such as the dopamine transporter in the striatum and midbrain (Perry et al., 2010; Midde et al., 2012) and the vesicular monoamine transporter-2 in the striatum (Theodore et al., 2012). However, there is no evidence suggesting that Tat binds to presynaptic targets or exerts any direct presynaptic effects in the hippocampus. Thus, we suggest that Tat-induced synapse loss described here is initiated by postsynaptic processes. However, the

temporal resolution of our experiments could not resolve a clear chronological sequence for the loss of the PSD versus the presynaptic terminal. In summary, Tat clearly initiates the loss of both pre- and post-synaptic structures by binding to postsynaptic LRP but, we did not determine whether the PSD or presynaptic terminal was lost first.

Treatment with nutlin-3, an inhibitor of the E3 ligase MDM2, prevented Tat-induced loss of presynaptic terminals. MDM2 ubiquitinates PSD95 (Colledge et al., 2003; Bianchetta et al., 2011), but no evidence suggests MDM2-mediated ubiquitination of presynaptic proteins, suggesting that postsynaptic E3 ligase activity was required for loss of Syn-GFP puncta. Treatment with nutlin-3 prevents Tat-induced degradation of PSD95 (Kim et al., 2008), consistent with the idea that inhibition of MDM2 prevents degradation of postsynaptic proteins that are required for synapse maturation and maintenance. Other than PSD95, we have not identified specific postsynaptic proteins responsible for the presynaptic loss described here. However, there is precedent for postsynaptic proteins coordinating presynaptic stability by direct interactions such as those mediated by cadherins, integrins, and neuroligin (Scheiffele et al., 2000; Chavis and Westbrook, 2001; Togashi et al., 2002). It is possible that postsynaptic proteins are ubiquitinated concurrently with PSD95 in the presence of Tat; alternatively, loss of PSD95 might affect the function of proteins that interact with it (Meyer et al., 2004). The mechanism by which synaptophysin is eliminated from the presynaptic terminal has yet to be elucidated; our assay cannot distinguish diffusion of Syn-GFP out of the presynaptic terminal from degradation.

Finding that Tat-induced loss of presynaptic terminals was reversible is particularly interesting. We had previously shown that Tat-induced loss of postsynaptic densities could be reversed by ifenprodil, an antagonist for GluN2B-containing NMDA receptors. In the current study we show that ifenprodil induced recovery of presynaptic

terminals as well. No spontaneous recovery was seen; Tat-induced loss of presynaptic terminals was only reversed in the presence of ifenprodil. This observation further supports our contention that the postsynaptic side of the synapse drives loss and recovery. These data indicate that the GluN2B-containing NMDA receptors inhibit recovery of synapses after Tat exposure. The mechanism by which GluN2B-containing NMDA receptors regulate synapse recovery is unclear. Immunocytochemistry experiments indicate that the hippocampal cultures used here express both GluN2A-containing and GluN2B-containing NMDA receptors (Shin et al., 2012). Many studies have shown that GluN2A versus GluN2B-containing NMDA receptors have distinct roles in maintaining neuronal survival, and couple to different downstream effectors (Christopherson et al., 1999; Liu et al., 2004a; Liu et al., 2007). GluN2A and GluN2B-containing NMDA receptors differentially affect Tat-induced postsynaptic changes and neuronal death induced by Tat (Shin et al., 2012). Furthermore, NMDA receptor activity has been shown to inhibit maturation of nascent synapses during synaptogenesis (Gray et al., 2011), and the pathway by which this inhibition occurred is distinct for GluN2A-containing receptors versus GluN2B-containing receptors. In contrast, inhibition of GluN2B-containing NMDA receptors at mature synapses seemed to have little effect. This is consistent with our previous study, which showed that inhibiting GluN2B-containing NMDA receptors failed to prevent Tat-induced loss of synapses, but did induce recovery of synapses after the initial loss (Shin et al., 2012).

Tat-induced loss of presynaptic terminals was moderate (-15% change over 24 h), in contrast to the effect seen with the same concentration of Tat at postsynaptic densities (-24% change over 24 h, (Shin et al., 2012)). One possible explanation for this observation is that synaptophysin is expressed at excitatory as well as inhibitory presynaptic terminals (Fykse et al., 1993). Even though the majority of synapses in the

hippocampus are glutamatergic, the more moderate effect seen on Syn-GFP puncta may result from an increase in the number of inhibitory synapses as a compensatory measure in response to increased excitation. Indeed, preliminary results from our laboratory indicate that inhibitory synapses increase in number after exposure to HIV Tat (Hargus and Thayer, unpublished observations).

Our results indicate that GluN2B-containing receptors play a pivotal role in recovery of presynaptic terminals, and that inhibition of postsynaptic GluN2B-containing NMDA receptors is required to initiate synapse recovery after an excitotoxic insult such as HIV Tat. Postsynaptic initiation of the recovery of presynaptic terminals is in contrast to studies observing synaptogenesis, wherein presynaptic molecule recruitment and differentiation precedes postsynaptic development (Friedman et al., 2000; Ziv, 2001). Direct study of the chronology of synapse loss and recovery is limited by the resolution of our assay. However, the pharmacology of presynaptic loss and recovery strongly suggests that postsynaptic signaling initiates both synapse loss and synapse recovery. Therefore, synapse recovery may occur via a novel pathway that requires block of GluN2B-containing NMDA receptor activity. Further work is required to eludicate the mechanisms of synapse recovery after Tat-induced loss, and the pathway by which GluN2B-containing receptors can inhibit recovery.

In conclusion, our study has shown that HIV Tat exposure can induce a reversible loss of presynaptic terminals in hippocampal neurons in culture. This loss and recovery mirrors the effects of Tat on postsynaptic densities and was inhibited by pharmacological agents that act on postsynaptic targets. Thus, the mechanisms initiating both processes are located postsynaptically, in contrast to the mechanisms of synaptogenesis. Eludicating the pathways by which Tat affects the loss and recovery of hippocampal synapses may be crucial to developing targeted therapies for treating

HAND. Moreover, the role of NMDA receptor subtypes is crucial to these processes. Common pathways may underlie the synapse loss and recovery associated with many neurodegenerative processes. Determining the signaling pathways activated by NMDA receptor subtypes and how they regulate the loss and recovery of synapses may advance the development of therapeutic approaches to treating neurological disorders of multiple etiologies.

Chapter Four:

Recovery of synapses lost during exposure to HIV Tat protein is induced by inhibition of a protein kinase G signaling pathway downstream of GluN2B-containing NMDA receptors

Angela H. Shin and Stanley A. Thayer

Content adapted from manuscript submitted to The Journal of Neuroscience, April 2013.

Contributions: AHS collected and analyzed data, and contributed heavily to writing of manuscript.

I. Introduction

HIV infects over 30 million people worldwide. HIV-associated neurocognitive disorders (HAND) are a significant consequence of HIV infection (Antinori et al., 2007). HAND ranges from mild cognitive impairment to a dementia that renders patients incapable of independent daily living (Heaton et al., 2004). With highly active antiretroviral therapy (HAART), the severity of HAND symptoms has decreased. However, the prevalence of HAND is increasing, primarily due to the increased lifespan of HIV patients (Suarez et al., 2001; Robertson et al., 2004). This, coupled with the lack of effective treatment for HAND, creates a need for improved therapies.

HIV-induced neurotoxicity is indirect; the virus does not infect neurons, but productively infects macrophages and microglia in the CNS (Pulliam et al., 1991; Minagar et al., 2002). Infected cells release inflammatory cytokines and toxic viral proteins, such as HIV transactivator of transcription (Tat) (Genis et al., 1992; Nath et al., 1999; Speth et al., 2001). Tat protein and mRNA are found in the CNS of HAND patients (Hofman et al., 1994; Wiley et al., 1996; Del Valle et al., 2000; Hudson et al., 2000). Tat is secreted into the extracellular space and taken up into uninfected cells (Liu et al., 2000; King et al., 2006). Tat induces neurotoxicity *in vitro* (Liu et al., 2000; Eugenin et al., 2007; Kim et al., 2008), and Tat expression produces pathologies similar to HAND *in vivo* (Kim et al., 2003; Fitting et al., 2010). Thus, Tat is a neurotoxic viral protein that is implicated in the pathology of HAND.

Cognitive decline in HAND patients correlate with synaptodendritic injury, such as dendritic pruning and altered synaptic networks, rather than overt neuronal death (Masliah et al., 1997; Adle-Biassette et al., 1999; Everall et al., 1999; Wiley et al., 1999; Sa et al., 2004). Tat induces loss of excitatory synapses between hippocampal neurons *in vitro*, via binding the low-density lipoprotein receptor-related protein (LRP), and

subsequent NMDA receptor (NMDAR) overactivation (Kim et al., 2008). Importantly, Tat-induced loss of excitatory synapses is reversible.

NMDAR kinetics and downstream signaling mechanisms are highly influenced by subunit composition. GluN2A- and GluN2B-containing NMDARs are strongly expressed in the hippocampus and have strikingly different roles. GluN2A-containing receptors are preferentially localized at excitatory synapses and mediate pro-survival signaling, whereas GluN2B-containing receptors are preferentially located extrasynaptically and mediate pro-death signaling (Hardingham et al., 2002; Liu et al., 2004a; Liu et al., 2007). We have previously shown that inhibiting GluN2A-containing NMDARs prevented Tat-induced excitatory synapse loss, but failed to induce synapse recovery. In contrast, inhibiting GluN2B-containing NMDARs did not prevent Tat-induced synapse loss initially, but induced synapse recovery following prolonged exposure to Tat (Shin et al., 2012). However, the mechanism by which GluN2B-containing NMDARs inhibit synapse recovery is unknown.

In this study, we determined the mechanisms downstream of GluN2B-containing NMDARs that suppress synapse recovery. We found that Tat induces NO and cGMP production and activation of protein kinase G (PKG), as indicated by phosphorylation of the actin-associated protein vasodilator-stimulated phosphoprotein (VASP). Inhibiting this pathway decreased VASP phosphorylation and induced synapse recovery.

II. Methods

Materials. Reagents were obtained from the following sources: the PSD95-GFP expression vector (pGW1-CMV-PSD95-EGFP) was kindly provided by Donald B. Arnold (Arnold and Clapham, 1999); the PSD95(L241K)-GFP mutant construct was generated from the pGW1-CMV-PSD95-EGFP expression vector by Mutagenex Inc., (Piscataway,

NJ); the expression vector for DsRed (pDsRed2-N1) from Clontech (Mountain View, CA); HIV-1 Tat (Clade B, recombinant) from Prospec Tany TechnoGene Ltd. (Rehovot, Israel); DMEM, fetal bovine serum (FBS), and horse serum (HS) from Invitrogen (Carlsbad, CA); ifenprodil hemitartrate, 1H-protein oxadiazolog13quinoxalin-1-one (ODQ), 2-(4-Carboxyphenyl)-4,4,5,5-tetramethylimidazoline-1-oxyl-3-oxide (c-PTIO), 8-Br-cGMP, and (9*S*,10*R*,12*R*)-2,3,9,10,11,12-Hexahydro-10-methoxy-2,9-dimethyl-1-oxo-9,12-epoxy-1*H*-diindolo[1,2,3-*fg*:3',2',1'-*kl*]pyrrolo[3,4-*i*][1,6]benzodiazocine-10-carboxylic acid, methyl ester (KT 5823) from Tocris (Bristol, UK); penicillin/streptomycin, L-NAME, and all other reagents from Sigma (St. Louis, MO).

Cell culture. Rat hippocampal neurons were grown in primary culture as described previously (Shen and Thayer, 1998) with minor modifications. Fetuses were removed on embryonic day 17 from maternal rats killed with CO_2, and decapitated to isolate brain matter. Hippocampi were dissected and placed in Ca^{2+} and Mg^{2+}-free HEPES-buffered Hanks salt solution (HHSS), pH 7.45. HHSS was composed of the following (in mM): HEPES 20, NaCl 137, $CaCl_2$ 1.3, $MgSO_4$ 0.4, $MgCl_2$ 0.5, KCl 5.0, KH_2PO_4 0.4, Na_2HPO_4 0.6, $NaHCO_3$ 3.0, and glucose 5.6. Tissue was suspended in DMEM without glutamine, supplemented with 10% FBS and penicillin/streptomycin (100 U/mL), and dissociated by triturating through a series of graduated flame-narrowed Pasteur pipettes. Dissociated cells were then plated at a density of 100,000-120,000 cells per dish onto a 25-mm-round cover glass (#1) glued to cover a 19 mm diameter opening drilled through the bottom of a 35 mm Petri dish. The cover glass was precoated with Matrigel (200 µL, 0.2mg/mL) (BD Biosciences, Billerica, MA). Neurons were grown in a humidified atmosphere of 10% CO_2 and 90% air (pH 7.4) at 37 ^oC, and fed at days 1 and 6 by exchange of 75% of the media with DMEM, supplemented with 10% HS and

penicillin/streptomycin. Cells used in these experiments were cultured without mitotic inhibitors for at least 12 days. Immunocytochemistry experiments demonstrated that these cultures were composed of 18 ± 2 % neurons, 70 ± 3 % astrocytes and 9 ± 3 % microglia (Kim et al., 2011).

Transfection. Rat hippocampal neurons were transfected between 10 and 12 days in vitro using a modification of a protocol described previously (Kim et al., 2008). Briefly, hippocampal cultures were incubated for at least 20 minutes in DMEM supplemented with 1 mM kynurenic acid, 10 mM $MgCl_2$, and 5 mM HEPES, to reduce neurotoxicity. A DNA/calcium phosphate precipitate containing 1 μg total plasmid DNA per well was prepared, allowed to form for 30 min at room temperature, and added to the culture. After a 90 minute incubation period, cells were washed once with DMEM supplemented with $MgCl_2$ and HEPES and then returned to conditioned media saved at the beginning of the procedure. Neurons were transfected with equal amounts of DsRed expression vector, and either PSD95-GFP vector or PSD95(L241K)-GFP vector. Transfected neurons were imaged 48-96 hours post-transfection. Transfection efficiency ranged from 1-5%.

Confocal imaging. Petri dishes containing transfected neurons were sealed with Parafilm, transferred to the stage of an inverted confocal microscope (Olympus Fluoview 1000, Center Valley, PA) and viewed through a 60X oil-immersion objective (NA=1.4). To enable repeated imaging of the same cell over a 24 h period, the coordinates of each cell were recorded using the Multi-Area Time Lapse function of Fluoview 1000. Multiple optical sections of 1 μm each, spanning 8 μm total in the z-dimension, were collected and combined into a compressed z stack. GFP was excited at 488 nm with an argon

ion laser and emission collected at 530 nm (10 nm band pass). DsRed2 was excited at 543 nm with a green HeNe laser and emission collected at >605 nm. The cell culture dish was returned to the CO_2 incubator between imaging sessions. Synapse recovery experiments were performed for 24 hours in the continuous presence of Tat, with or without the specified drugs added at 16 hours.

Image processing. To count and label PSD95-GFP puncta an automated algorithm was created using MetaMorph 6.2 image processing software described previously (Waataja et al., 2008). Briefly, maximum z-projection images were created from the DsRed2 and GFP image stacks. Next, a threshold set 1 s.d. above the image mean was applied to the DsRed2 image. This created a 1-bit image that was used as a mask via a logical AND function with the GFP maximum z-projection. A top-hat filter (80 pixels) was applied to the masked PSD95-GFP image. A threshold set 1.5 s.d. above the mean intensity inside the mask was then applied to the contrast enhanced image. Structures between 8 and 80 pixels (approximately 0.37 to 3.12 μm in diameter) were counted as PSDs. The structures were then dilated and superimposed on the DsRed2 maximum z-projection for visualization.

Western Blotting. To quantify levels of VASP phosphorylation, rat hippocampal neurons were grown in culture as described above, except plated at a density of 500,000-600,000 cells/well in 6-well plates. 24 h after treatments, cells were harvested with RIPA lysis buffer (Triton X-100 1.0%; deoxycholate 0.5%; SDS 2.0%, NaCl 150 mM; Na_2PO_4 10 mM) with protease (cOmplete ULTRA, Roche Applied Science) and phosphatase inhibitors (Cocktails 2 and 3, Sigma). Samples were incubated on ice for 20 min, sonicated briefly to shear DNA, and centrifuged (15,000 rpm, 4°C) for 15 min.

Supernatant was resuspended in Laemmli sample buffer (Bio-Rad) and heated for 5 min at 90°C, then resolved via SDS-PAGE on a 10% polyacrylamide gel. For immunodetection of VASP protein, equal amounts of sample were loaded per condition. Proteins were transferred to a nitrocellulose membrane (iBlot, Invitrogen) and blocked in 5% milk for 1h at room temperature. Membranes were incubated overnight at 4°C with the following primary antibodies: rabbit anti-VASP (H90) (1:100, Santa Cruz Biotechnology, Inc.); rabbit anti-phospho-VASP (Ser239) (1:100, Santa Cruz Biotechnology, Inc.); rabbit anti-phospho-VASP (Ser157) (1:100, Santa Cruz Biotechnology, Inc.); and mouse anti-β-tubulin (1:1000, Abcam), in 3% milk. Secondary detection occurred with the following antibodies: goat anti-rabbit IRDye 680RD (1:2000, Li-Cor Biosciences) and goat-anti-mouse IRDye 800CW (1:5000, Li-Cor Biosciences). Fluorescence was detected and quantified using the Odyssey Infrared imaging system (Li-Cor Biosciences).

Statistics. For imaging studies, an individual experiment (n=1) was defined as the percent change in the number of PSDs from a single cell from a single coverslip. Percent changes in PSD counts are presented as mean ± SEM. For Western Blot analyses, the fluorescence intensities of VASP-immunoreactive bands were divided by the fluorescence intensities of the corresponding β-tubulin-immunoreactive band in each lane to account for sample concentration. Intensities are presented as percent change normalized to Control conditions. For all analyses, each experiment was replicated over at least 3 separate cultures. In all statistical analyses Student's t-test for single or ANOVA with Tukey's post-hoc test for multiple statistical comparisons were used (OriginPro v8.5, Northampton, MA).

III. Results

Ifenprodil induces recovery of PSD95-GFP puncta lost during exposure to HIV Tat.

We used a live cell imaging assay to track the number of excitatory synapses between rat hippocampal neurons in culture, as previously described (Waataja et al., 2008). Neurons were transfected with expression vectors for DsRed2 and PSD95-GFP. 48 h after transfection, neurons were imaged on a confocal microscope. DsRed2 expression was ubiquitous, and PSD95-GFP expressed in a discrete punctate pattern (Figure 1A). Previous work from our laboratory showed that PSD95-GFP puncta co-localized with NMDA receptor immmunoreactivity, functional neurotransmitter release sites, and synaptically evoked local Ca^{2+} increases, indicating that these puncta represented functional excitatory synapses (Waataja et al., 2008). Images were processed to identify fluorescent puncta based on intensity and size (average puncta size = 0.52 μm^2) criteria, and in contact with the DsRed2 mask. Qualifying puncta were counted, dilated and overlaid on the mask (Processed, Figure 1A). The number of PSDs was measured at multiple time points to assess dynamic changes in synapse number for an individual neurons.

As shown previously and replicated here, exposure to 50 ng/mL HIV Tat significantly decreased the number of synapses by 16 h (-26 ± 3%, n = 23), and loss was sustained through 24 h (-34 ± 4%). In contrast, a 22 ± 4% increase (n = 28) in synapse number was seen over 24 h under control conditions ((Kim et al., 2008), Figure 1C). 10 μM ifenprodil, an antagonist of GluN2B-containing NMDARs, failed to inhibit Tat-induced synapse loss if applied prior to Tat exposure at 0 h (-25 ± 5% with Tat alone, n = 7; -27 ± 6% with ifenprodil, n = 8), consistent with our previous study (Figure 1B, (Shin et al., 2012)). Addition of this same concentration of ifenprodil 16 h after exposure to Tat induced a recovery in synapse number by 24 h in the continued presence of Tat (-32 ±

5% at 16 h; 12 ± 5% at 24 h) that was similar to control values ((Shin et al., 2012), Figure 1, C-E). Additionally, merely washing out Tat from the cultures did not induce synapse recovery, nor was any spontaneous recovery observed (Kim et al., 2008). These results suggest that following 16 h exposure to Tat, tonic activation of GluN2B-containing NMDARs is suppressing synapse recovery. We next sought to determine the downstream signaling mechanism by which antagonism of GluN2B-containing NMDARs could induce synapse recovery.

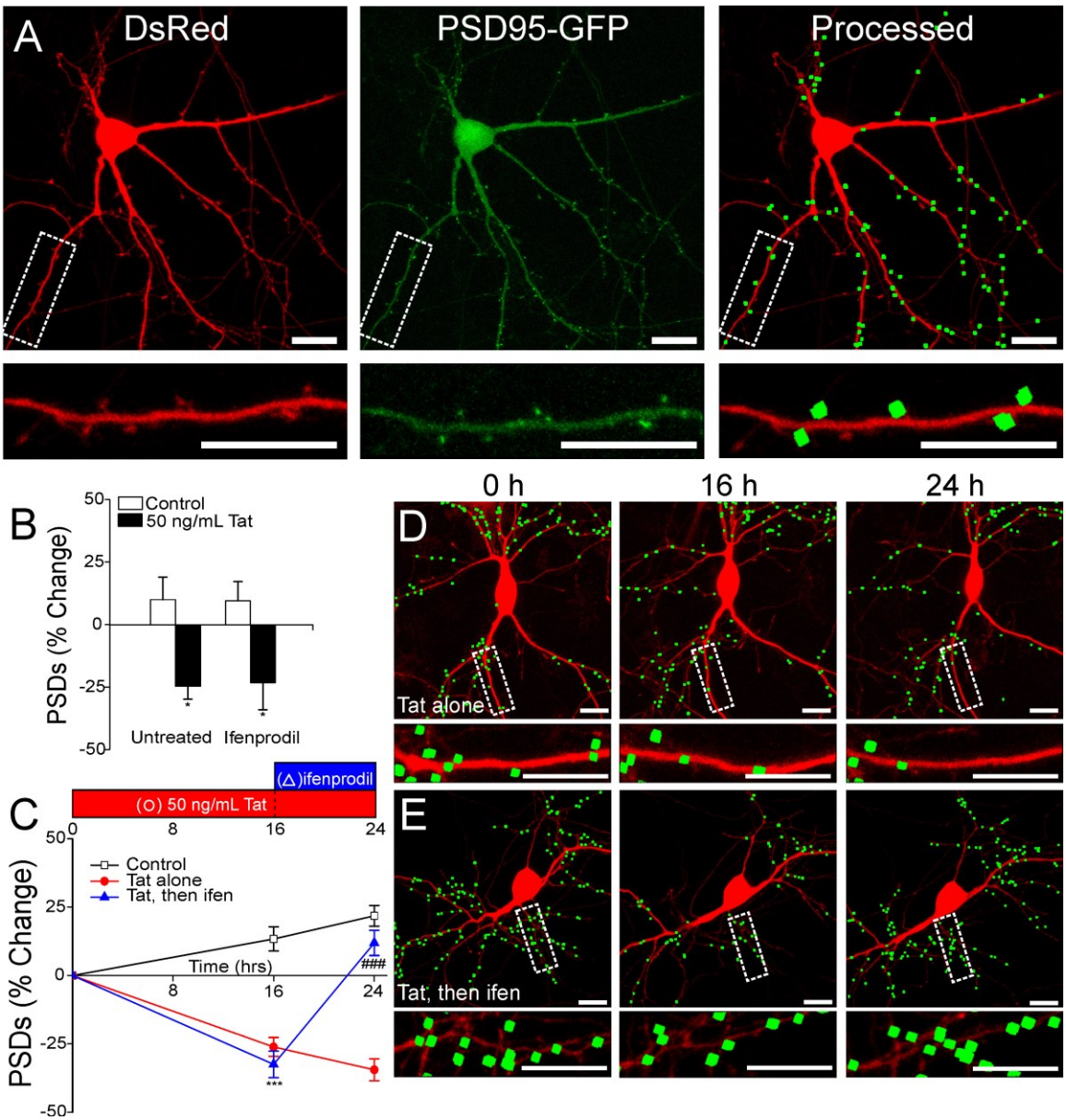

Figure 4.1. HIV Tat induces loss of excitatory synapses that is reversed by ifenprodil. A, Representative confocal images were collected and processed as described in Methods. PSD95-GFP puncta were identified by applying digital filters to compressed z-stacks of the confocal image (PSD95-GFP). PSDs were counted if they met a fluorescence intensity threshold, met size criteria, and were in contact with a mask derived from the DsRed image (DsRed). Qualifying PSD puncta were dilated and overlaid on the DsRed image for visualization purposes (Processed). The insets are enlarged images of the boxed region. Scale bars represent 10 μm. B, Bar graph summarizes percent change in PSD number in the absence (Control, open bars) or presence of Tat (50 ng/mL Tat, black bars) after 24 h. Neurons were either untreated or pretreated with 10 μM ifenprodil 15 min prior to Tat application. *, $p < 0.05$ relative to corresponding Control condition (ANOVA with Tukey's post-test), $n \geq 5$ for each condition. Data are represented as mean ± SEM. C, Line graph summarizes percent change in PSD number in the absence (Control, open symbols) or presence of 50 ng/mL Tat (closed symbols). Cells were either left untreated at 16 h (Tat alone, red circles) or treated with 10 μM ifenprodil (Tat, then ifen, blue triangles). Ifenprodil was applied at 16 h in the continued presence of Tat. ***, $p < 0.001$ at 16 h relative to control; ###, $p < 0.001$ at 24 h relative to Tat alone (ANOVA with Tukey's post-test); $n \geq 10$ for each condition. Data are represented as mean ± SEM. D-E, Representative processed images of neurons treated with Tat for 24 h. Neurons were imaged prior to Tat exposure (0 h), then imaged at 16 h and either untreated (D, Tat alone), or treated with 10 μM ifenprodil (E, Tat, then ifen). A final image of each neuron was collected at 24 h. The insets are enlarged images of the boxed region. Scale bars represent 10 μm.

Ifenprodil-induced recovery requires inhibition of postsynaptic nNOS

NMDAR activation and subsequent Ca^{2+} influx at the postsynaptic density induce activation of neuronal nitric oxide synthase (nNOS) (Ko and Kelly, 1999; Burette et al., 2002). We showed previously that inhibition of nNOS does not protect against Tat-induced synapse loss, but does prevent Tat-induced cell death (Kim et al., 2008). We sought to determine whether inhibition of nNOS downstream of NMDARs could induce recovery in a manner similar to that evoked by application of ifenprodil.

Treatment with the nNOS inhibitor L-NAME (100 μM) after 16 h Tat exposure induced a recovery in synapse number by 24 h in the continued presence of Tat (-29 ± 5% at 16 h; 13 ± 7% at 24 h, n = 16) (Figure 4.2, A-B). L-NAME alone did not produce a significant increase in synapse number in the absence of Tat (10 ± 9% at 24 h, n = 7). L-NAME failed to inhibit Tat-induced synapse loss when applied before Tat (0 h) (Kim et al., 2008), showing a profile of efficacy similar to that of ifenprodil.

NO is a gas, capable of diffusing through the cell membrane to act on sites distant from its site of production. For example, it can diffuse across the synaptic cleft to elicit presynaptic effects (Feil and Kleppisch, 2008). We used the membrane impermeable NO scavenger c-PTIO to eliminate extracellular NO, and examined its effect on synapse recovery. c-PTIO (30 μM) was previously shown to inhibit the retrograde actions of postsynaptically produced NO (Ko and Kelly, 1999). However, this concentration of c-PTIO failed to induce synapse recovery when applied after 16 h Tat exposure (-31 ± 5% at 16 h; -28 ± 6% at 24 h, n = 7) (Figure 4.2, A-B), indicating that preventing the diffusion of NO to the presynaptic terminal was not sufficient to induce synapse recovery. Taken together, these data suggest that nNOS produces NO, which in turn acts postsynaptically to inhibit synapse recovery.

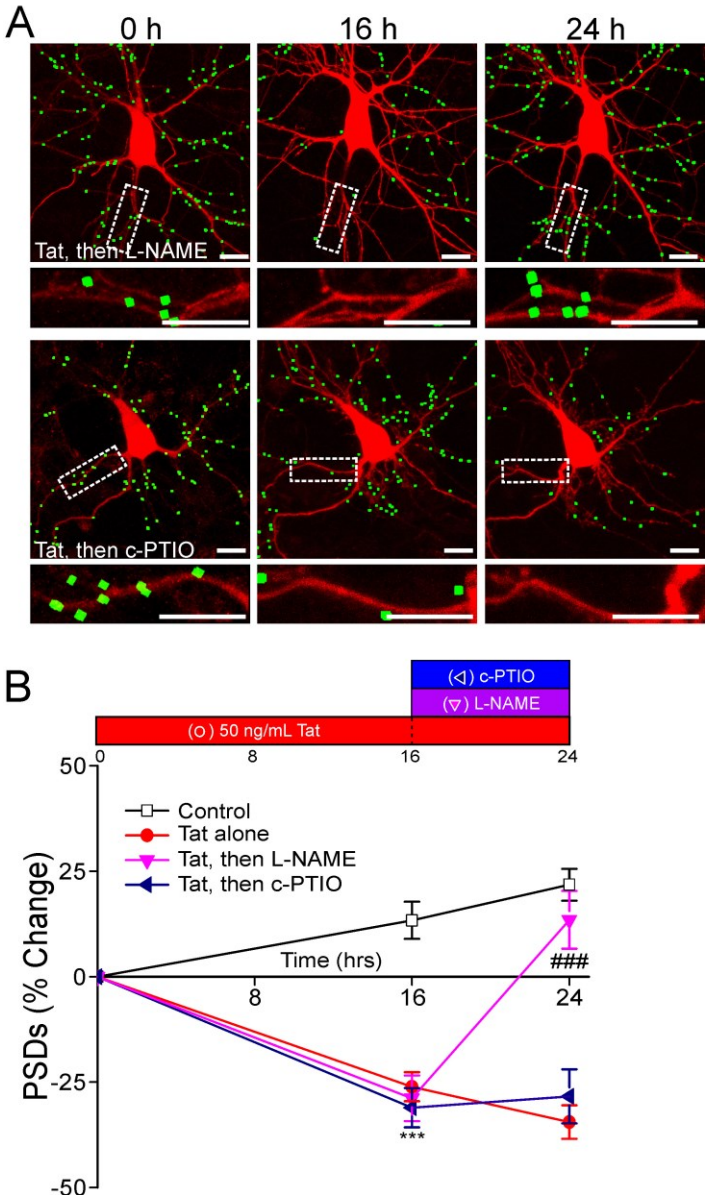

Figure 4.2. Inhibition of postsynaptic nNOS induces synapse recovery. A, Representative processed images of neurons before (0 h) and 16 h and 24 h after treatment with 50 ng/mL Tat. At 16 h, neurons were either treated with 100 µM L-NAME (Tat, then L-NAME) or 30 µM c-PTIO (Tat, then c-PTIO). The insets are enlarged images of the boxed region. Scale bars represent 10 µm. B, Line graph summarizes percent change in PSD number in the absence (Control, open symbols) or presence of 50 ng/mL Tat (closed symbols). Cells were either left untreated at 16 h (Tat alone, red circles), or treated with 100 µM L-NAME (Tat, then L-NAME, pink triangles) or 30 µM c-PTIO (Tat, then c-PTIO, blue triangles). All drugs were applied at 16 h in the continued presence of Tat. ***, $p < 0.001$ at 16 h relative to control; ###, $p < 0.001$ at 24 h relative to Tat alone (ANOVA with Tukey's post-test); $n \geq 7$ for each condition. Data are represented as mean ± SEM.

nNOS-mediated inhibition of synapse recovery requires interaction with PSD95

nNOS couples to NMDA receptors at the postsynaptic density by binding to PSD95 (Christopherson et al., 1999). We sought to determine whether nNOS interaction with PSD95 was required to suppress synapse recovery. nNOS binding to PSD95 is dependent on tertiary protein structure. Disruption of this structure by introducing an L241K mutation in the PDZ2 domain of PSD95 completely eliminates binding of nNOS to PSD95 (Christopherson et al., 1999). We introduced this L241K mutation in PSD95-GFP to determine whether nNOS binding to PSD95 was required for its effects on synapse recovery. PSD95(L241K)-GFP expressed in a punctate pattern and responded to Tat exposure similar to wild-type PSD95-GFP (Figure 3, A-B). In contrast to WT PSD95-GFP however, treatment with 10 μM ifenprodil after 16 h Tat exposure failed to induce synapse recovery in neurons expressing PSD95(L241K)-GFP (-28 ± 4% at 16 h; -38 ± 7% at 24 h, n = 10) (Figure 3, A-B). These data indicate that binding to PSD95 holds nNOS in close apposition to NMDARs to enable suppression of synapse recovery by GluN2B-containing NMDARs.

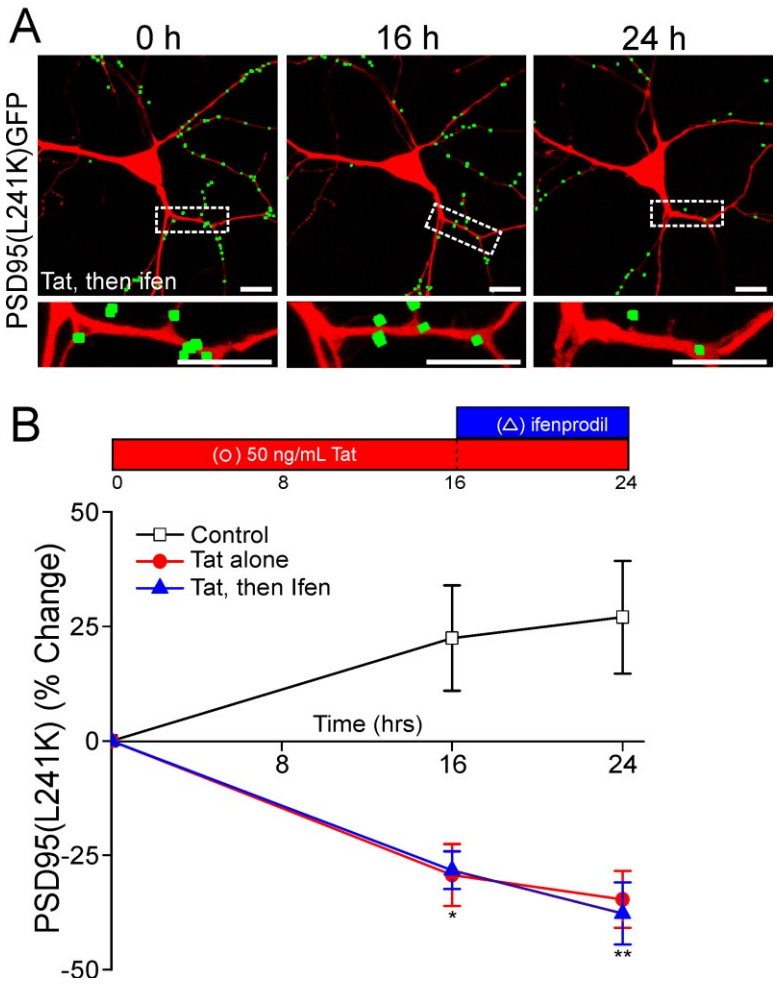

Figure 4.3. nNOS interaction with PSD95 is required for synapse recovery. A, Representative processed images of neurons before (0 h) and 16 h and 24 h after treatment with 50 ng/mL Tat. Neurons were transfected with expression vectors for DsRed and PSD95(L241K)-GFP 48-96 h prior to imaging as described in Materials and Methods. At 16 h, neurons were treated with 10 µM ifenprodil (Tat, then ifen). The insets are enlarged images of the boxed region. Scale bars represent 10 µm. B, Line graph summarizes percent change in PSD number (of PSD95(L241K)-GFP puncta) in the absence (Control, open symbols) or presence of 50 ng/mL Tat (closed symbols). Cells were either left untreated at 16 h (Tat alone, red circles), or treated with 10 µM ifenprodil (Tat, then ifen, blue triangles). Ifenprodil was applied at 16 h in the continued presence of Tat. *, $p < 0.05$ at 16 h relative to control; **, $p < 0.01$ at 24 h relative to control (ANOVA with Tukey's post-test); $n \geq 6$ for each condition. Data are represented as mean ± SEM.

Synapse recovery requires inhibition of NO-induced cGMP production

In the hippocampus, NO activates soluble guanylyl cyclase (sGC) to produce cGMP (Friebe and Koesling, 2003). We hypothesized that NO-induced cGMP production inhibits synapse recovery. This hypothesis was tested by using the selective sGC antagonist ODQ (Garthwaite et al., 1995). 1 μM ODQ applied after 16 h Tat exposure, induced recovery of synapse number by 24 h in the continuous presence of Tat (-24 ± 3% at 16 h; 5 ± 5% at 24 h, n = 18) (Figure 4.4, A-B). ODQ alone did not produce a significant increase in synapse number in the absence of Tat (23 ± 9% at 24 h, n = 5). To verify that ODQ's effects were due to inhibition of cGMP production, we applied the non-hydrolyzable, membrane permeable cGMP analog 8-Br-cGMP (100 μM) with ODQ at 16 h. In the presence of 8-Br-cGMP, ODQ failed to evoke synapse recovery, indicating that synapse recovery induced by ODQ is due to its inhibition of cGMP production (-22 ± 5% at 16 h; -28 ± 3% at 24 h, n = 8) (Figure 4.4, A-B).

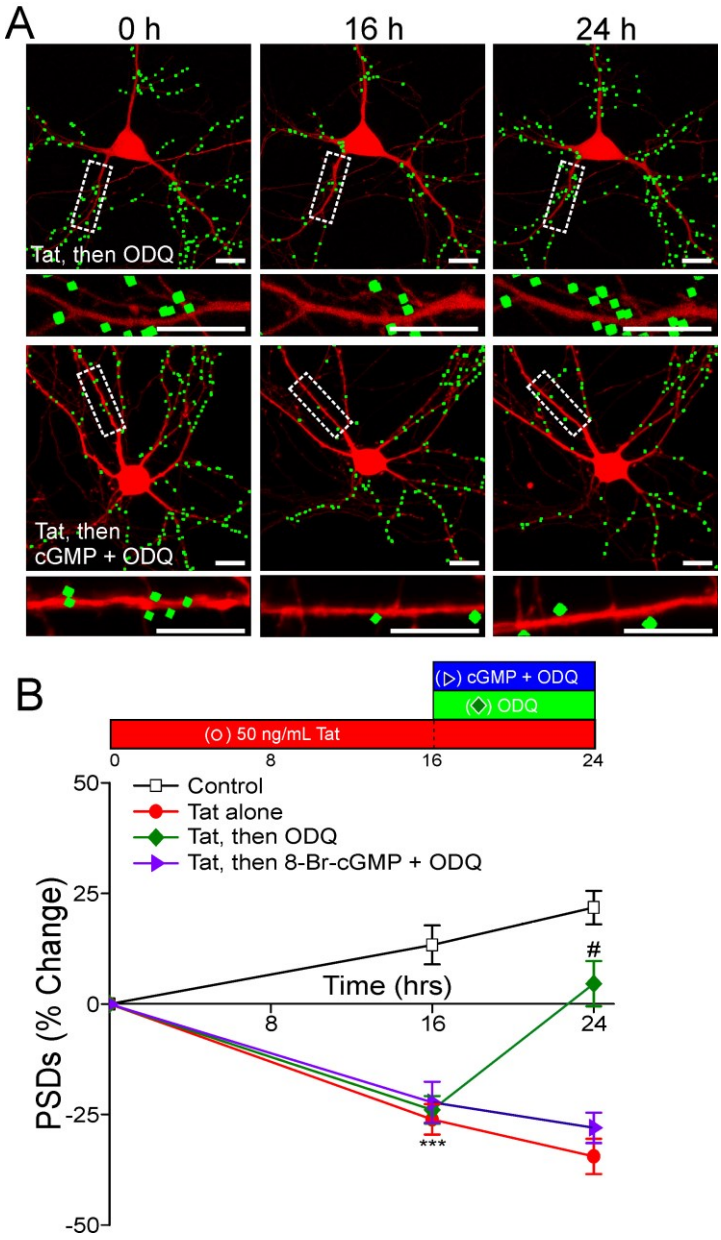

Figure 4.4. Inhibition of synapse recovery requires production of cGMP by sGC. A, Representative processed images of neurons before (0 h) and 16 h and 24 h after treatment with 50 ng/mL Tat. At 16 h, neurons were either treated with 1 µM ODQ (Tat, then ODQ) or 100 µM 8-Br-cGMP and 1 µM ODQ (Tat, then cGMP + ODQ). The insets are enlarged images of the boxed region. Scale bars represent 10 µm. B, Line graph summarizes percent change in PSD number in the absence (Control, open symbols) or presence of 50 ng/mL Tat (closed symbols). Cells were either left untreated at 16 h (Tat alone, red circles), or treated with 1 µM ODQ (Tat, then ODQ, green diamonds) or 100 µM 8-Br-cGMP and 1 µM ODQ (Tat, then 8-Br-cGMP + ODQ, blue triangles). All drugs were applied at 16 h in the continued presence of Tat. 8-Br-cGMP was applied 15 min prior to ODQ treatment. ***, $p < 0.001$ at 16 h relative to control; #, $p < 0.05$ at 24 h relative to Tat alone (ANOVA with Tukey's post-test); $n \geq 8$ for each condition. Data are represented as mean ± SEM.

Inhibition of PKG activity induces synapse recovery

cGMP activates protein kinase G (PKG) (Kleppisch and Feil, 2009). We examined whether cGMP-induced activation of PKG inhibited synapse recovery. Treatment with the PKG inhibitor KT 5823 (10 μM) after 16 h Tat exposure induced recovery of synapse number by 24 h, in the continuous presence of Tat (-34 ± 7% at 16 h; 0 ± 5% at 24 h, n = 8) (Figure 4.5, A-B). KT 5823 alone did not produce a significant increase in synapse number in the absence of Tat (13 ± 7% at 24 h, n = 8). These data indicate that PKG activity inhibits synapse recovery after Tat-induced synapse loss. PKG is known to phosphorylate the actin-associated protein VASP on Ser239 (Butt et al., 1994). Western blot analysis confirmed that 24 h exposure to Tat induced a 35 ± 8% increase in Ser239 phosphorylation of VASP (Figure 4.5, C-D). This increase in Ser239 phosphorylation was reversed by treatment with 10 μM ifenprodil after 16 h Tat exposure, mirroring the effects of ifenprodil on synapse recovery. Tat exposure did not change overall levels of VASP protein, or induce an increase in VASP phosphorylation at Ser157, a protein kinase A (PKA) phosphorylation site (Butt et al., 1994), indicating that the increase in VASP phosphorylation was not due to increased levels of protein, and was due to PKG activity. Taken together, these data indicate that persistent Tat exposure increases PKG activity downstream of GluN2B-containing NMDARs, increasing phosphorylation of VASP.

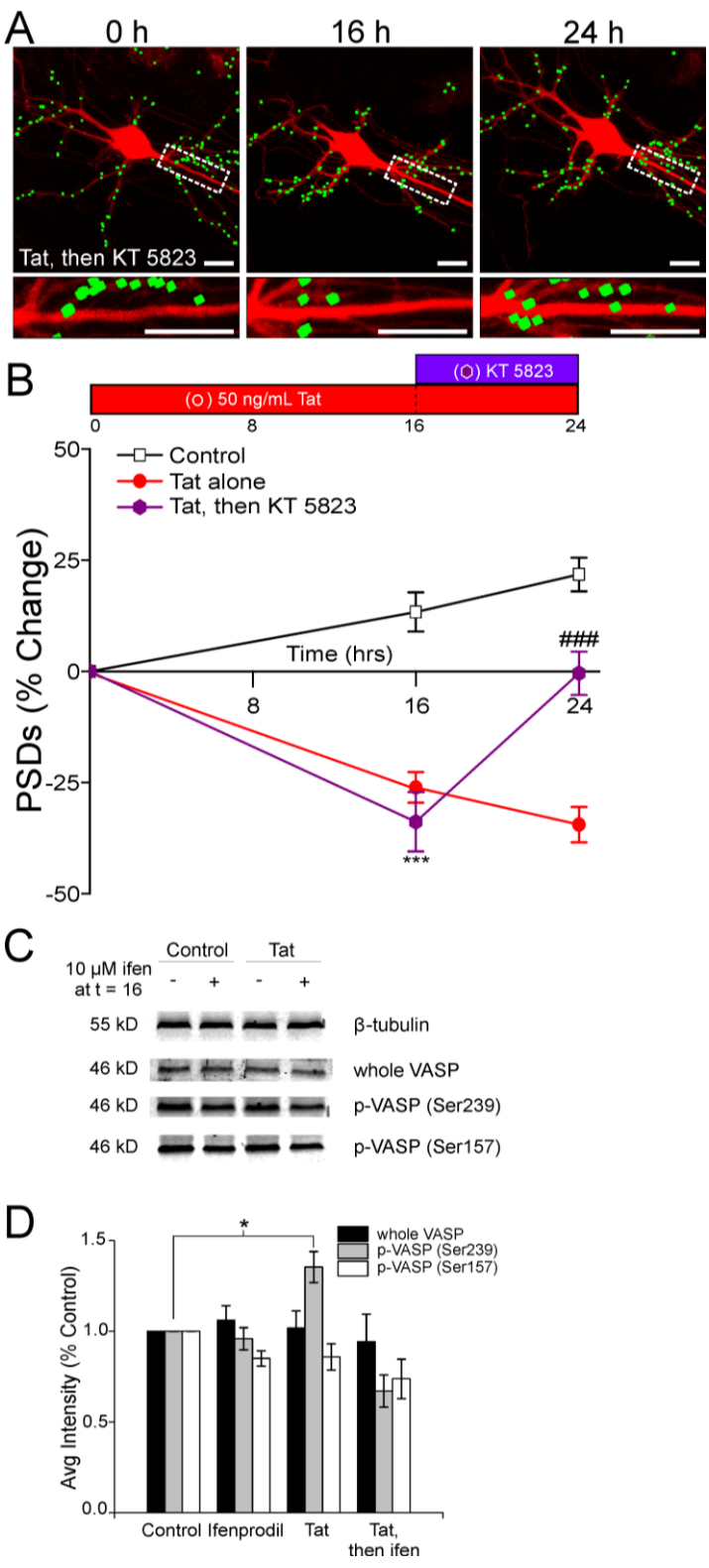

Figure 4.5. Inhibition of synapse recovery requires PKG activity. A, Representative processed images of neurons before (0 h) and 16 h and 24 h after treatment with 50 ng/mL Tat. At 16 h, neurons were treated with 10 μM KT 5823 (Tat, then KT 5823). The insets are enlarged images of the boxed region. Scale bars represent 10 μm. B, Line graph summarizes percent change in PSD number in the absence (Control, open symbols) or presence of 50 ng/mL Tat (closed symbols). Cells were either left untreated at 16 h (Tat alone, red circles), or treated with 10 μM KT 5823 (Tat, then KT 5823, pink hexagons). KT 5823 was applied at 16 h in the continued presence of Tat. ***, $p < 0.001$ at 16 h relative to control; ###, $p < 0.001$ at 24 h relative to Tat alone (ANOVA with Tukey's post-test); $n \geq 8$ for each condition. Data are represented as mean ± SEM. C, Representative Western Blots of neuronal cultures either untreated (Control) or treated with 50 ng/mL Tat (Tat) for 24 h. 10 μM ifenprodil was added after 16 h Tat exposure (t = 16) as indicated. D, Bar graph summarizes change in VASP phosphorylation as indicated by average fluorescence intensity changes. All data are normalized to Control conditions. *, $p < 0.05$ relative to control (Student's t-test). Data are represented as mean ± SEM.

IV. Discussion and conclusions

Synaptodendritic damage correlates with cognitive decline in HAND (Ellis et al., 2007). The HIV protein Tat is released from infected cells in the CNS (Liu et al., 2000), and elicits dendritic pruning, altered synaptic transmission, and synapse loss (Maragos et al., 2003; Li et al., 2004; Kim et al., 2008). We showed previously that Tat-induced synapse loss was reversed by selectively inhibiting GluN2B-containing NMDARs (Shin et al., 2012). In this study, we delineated the signaling pathway downstream from these receptors using an imaging assay to track changes in the number of excitatory synapses. In the presence of Tat, GluN2B-containing NMDARs activated a nNOS-sGC-PKG signaling cascade that suppressed the recovery of synapses. Inhibition of any step in this serial pathway induced recovery of excitatory synapse number (Figure 4.6).

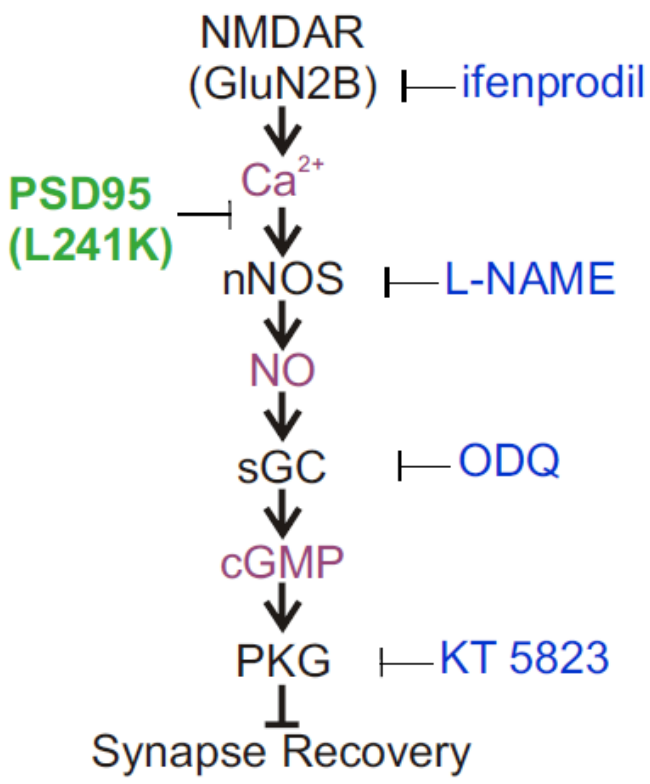

Figure 4.6. Pathway activated by GluN2B-containing NMDARs to suppress synapse recovery after Tat-induced synapse loss.

The downstream effects of NMDAR activation are dependent on the subunit composition and subcellular localization of the receptor (Hardingham et al., 2002; Liu et al., 2004a; Liu et al., 2007). For example, GluN2A-containing NMDARs induce pro-survival signals such as Akt kinase activation whereas GluN2B-containing NMDARs induce pro-death signaling by activating caspases (Liu et al., 2007). GluN2A-containing NMDARs are preferentially found at synapses whereas GluN2B-containing receptors are localized to extrasynaptic sites (Tovar and Westbrook, 1999, 2002; Massey et al., 2004). Tat-induced synapse loss was prevented by treatment with TCN201, an antagonist selective for GluN2A-containing NMDARs (Shin et al., 2012). Inhibiting synapse loss sensitized neurons to Tat-induced death (Kim et al., 2008). Thus, we hypothesize that synapse loss is a coping mechanism that attempts to reduce excess excitatory input. This idea is consistent with the generally pro-survival role of GluN2A-mediated signaling. In contrast, GluN2B-containing NMDARs do not play a major role during initial Tat-induced synapse loss, as evidenced by the fact that ifenprodil does not prevent synapse loss (Figure 4.1 B). Prolonged exposure to Tat produces neuronal death (Eugenin et al., 2007) which can be prevented by ifenprodil (Shin et al., 2012). The C-terminal domain of the GluN2B subunit couples to nNOS via PSD95, consistent with NO mediating Tat-induced neuronal death (Martel et al., 2012). Our study highlights a unique role for GluN2B-containing NMDARs in which they suppress synapse recovery following exposure to Tat (Shin et al., 2012). Thus, inhibiting GluN2B-containing NMDARs during Tat induced neurotoxicity provides the dual benefits of improving neuronal survival and inducing the recovery of synapses. The sustained activation of GluN2B-containing NMDARs following exposure to Tat may result from the formation of a complex containing NMDARs, PSD95, LRP and nNOS (Eugenin et al., 2007). Indeed, inhibiting LRP after 16 h exposure to Tat induced the recovery of excitatory synapses (Kim et al.,

2008). Therefore, in our system GluN2B-containing NMDARs are not actively suppressing the formation of synapses in the absence of Tat, which may explain why ifenprodil only increased synapse number after treatment with Tat. Activation of GluN2B-containing NMDARs suppresses synapse maturation in the developing hippocampus, and genetic deletion of GluN2B increases the number of functional synapses (Gray et al., 2011), suggesting that similar mechanisms may participate both in the regulation of synapse formation during development and in the recovery of synapses after injury.

Inhibition of nNOS did not affect synapse loss (Kim et al., 2008), yet, as shown here, it did induce synapse recovery, consistent with distinct pathways for GluN2A-mediated synapse loss and GluN2B-mediated suppression of synapse recovery. Furthermore, genetically uncoupling nNOS from PSD95 using the L241K mutation prevented the induction of synapse recovery by ifenprodil. Previous studies have shown that nNOS needs to be in close apposition to NMDARs to mediate NMDA-induced cell death (Cui et al., 2007; Eugenin et al., 2007). c-PTIO, which cannot cross membranes, did not induce synapse recovery, indicating that NO did not diffuse through the extracellular space to distant targets, such as the presynaptic terminal, to suppress synapse recovery. A postsynaptic role for NO here contrasts with its role in LTP, where diffusion to the presynaptic terminal and subsequent stimulation of cGMP production potentiates neurotransmitter release (Arancio et al., 1996). Postsynaptic action of NO is consistent with proposed mechanisms for NMDA-induced NO-mediated neuronal death in which NO reacts with reactive oxygen species (Lipton et al., 1993) and is consistent with previous studies showing that Tat-induced synapse loss and recovery are driven by postsynaptic mechanisms (Shin et al., 2012). Thus, prolonged exposure to Tat activates nNOS via a GluN2B-dependent mechanism; NO then can initiate apoptotic signaling through a redox-based mechanism and suppress synapse recovery by activating sGC.

Inhibition of sGC was sufficient to induce synapse recovery. Our results do not exclude effects on synaptic transmission mediated by cGMP-independent means, such as s-nitrosylation which has been shown to decrease NMDAR-mediated currents, inhibit production of the NMDAR co-agonist D-serine, and decrease synaptic delivery of PSD95 (Lipton et al., 1993; Mustafa et al., 2007; Ho et al., 2011). However, exogenous 8-Br-cGMP maintained the suppression of synapse recovery when sGC was inhibited, indicating an essential role for cGMP. cGMP can activate several targets in neurons including PKG, cyclic nucleotide-gated ion channels (Parent et al., 1998), and phosphodiesterases (PDEs) (Repaske et al., 1993; van Staveren et al., 2005). While PKG-independent actions of cGMP in response to Tat exposure cannot be absolutely excluded, inhibition of PKG with KT5823 induced recovery of synapses, indicating that PKG activation is the primary means by which cGMP suppresses synapse recovery.

The sustained activation of PKG by Tat could act on many downstream effectors; plausible targets in the hippocampus include CaMKII, the small GTPase RhoA, α-synuclein, and VASP (Liu et al., 2004b; Ninan and Arancio, 2004; Wang et al., 2005). We focused on VASP because PKG phosphorylation of VASP is well characterized and it phosphorylates a site distinct from PKA (Butt et al., 1994). Thus, VASP is widely used to detect PKG activation. Sustained exposure to Tat increased PKG-mediated phosphorylation of VASP. Ifenprodil reversed this increase, demonstrating that PKG activation is linked to GluN2B signaling at the cell surface. It is plausible that phosphorylation of VASP suppresses synapse recovery. VASP regulates neuritogenesis, axonal maintenance, spine assembly, and synaptic potentiation (Wang et al., 2005; Kwiatkowski et al., 2007; Franco et al., 2010; Lin et al., 2010). However, we did not explicitly test the role of VASP in synapse recovery.

Memantine is an uncompetitive NMDAR antagonist used clinically to improve

cognition in patients with Alzheimer's disease (Areosa et al., 2005; Mount and Downton, 2006). It preferentially inhibits extrasynaptic NMDARs (Xia et al., 2010) suggesting that inhibiting the GluN2B signaling pathway described here may contribute to its mechanism of action. In our studies memantine showed a profile similar to that of ifenprodil, inducing synapse recovery but not affecting the initial Tat-induced loss of synapses (Shin et al., 2012). These observations lend support towards establishing proof for the principle that drugs that facilitate synapse recovery have the potential to improve cognition. Clinically, most patients with neurodegenerative disease present with symptoms well after disease onset, so drugs that facilitate the recovery of function may have broader application than those designed to prevent the initial impairment.

We have described a unique role for a signaling pathway downstream from GluN2B-containing NMDARs. The HIV protein Tat induced the serial activation of nNOS, sGC and PKG postsynaptically, which suppressed the recovery of synapses lost following activation of a separate pathway. If sustained activation of nNOS, sGC and PKG provides some benefit to neuronal or network function it is not apparent. The results presented in this report suggest that Tat-induced activation of this pathway contributes to the neuropathology associated with HIV infection and that elements of the signaling cascade are potentially useful targets for drugs to improve cognitive function in HAND patients.

Chapter Five:

Concluding Remarks

I. Summary of current studies

In the previous chapters, I describe studies I performed that expanded upon current knowledge of HIV Tat's neurotoxicity in an *in vitro* system. Tat induces reversible loss of excitatory synapses, and the divergence between the mechanisms of Tat-induced neuronal death and Tat-induced synapse loss was previously described (Kim et al., 2008). In Chapter Two, I expanded upon these findings by performing a pharmacological study to show that NMDA receptor subunit composition dictates the downstream effects of Tat. GluN2A-containing receptors inhibit the processes of synapse loss and recovery, whereas GluN2B-containing receptors mediate Tat-induced cell death, and suppress synapse recovery (Shin et al., 2012). In Chapter Three, I identified the primary target of Tat-mediated synapse loss as the postsynaptic density. While Tat-induced loss of presynaptic terminals is concurrent with loss of postsynaptic densities, the essential mechanisms responsible for Tat's deleterious effects are located postsynaptically. Thus, postsynaptic mechanisms drive Tat-induced synapse loss as well as subsequent recovery. An intriguing discovery of this study was that, as with postsynaptic densities, recovery of presynaptic terminals following Tat-induced loss was also contingent upon inhibition of GluN2B-containing NMDA receptors (Shin and Thayer, 2013). These findings, along with those in Chapter Two, led me to the final chapter of my dissertation identifying the signaling pathway downstream of GluN2B-containing NMDA receptors that suppressed synapse recovery after Tat-induced synapse loss. In Chapter Four I showed that the canonical NO/cGMP/PKG signaling pathway was activated downstream of GluN2B-containing NMDA receptors following persistent Tat exposure, leading to suppression of synapse recovery. Inhibiting this pathway after Tat-induced synapse loss induced a recovery in synapse number.

II. Advantages and limitations of live cell imaging

A novel live cell imaging assay that was developed in our laboratory was used for these studies. The assay utilized primary hippocampal neuronal cultures that were transfected with expression vectors for our proteins of interest fused to a fluorescent marker. The resulting fluorescent expression of synaptic marker proteins allowed us to quantify dynamic changes in synapse number in a single neuron after exposure to HIV Tat and pharmacological agents. This assay allowed me to track the synaptic dynamics of live neurons over a time interval. Many studies of neuronal injury rely on immunolabeling of the relevant proteins. As such, the cells or tissue to be studied must be fixed prior to labeling, rather than studying a live neuronal network. In contrast, our assay observes changes in a living culture, allowing us to visualize exciting single cell effects of Tat in real-time.

Another advantage of our live cell imaging assay is the ability to visualize a particular synaptic protein. PSD95 is a scaffolding protein at excitatory postsynaptic densities (Cho et al., 1992; Hunt et al., 1996), and our previous work showed that the fusion protein PSD95-GFP utilized in our assay expressed in discrete puncta correlating with functional excitatory synaptic sites (Waataja et al., 2008). The ability to visualize a particular synaptic protein over time allowed us to further elucidate mechanistic details of Tat-induced synapse loss; genetic modification of PSD95-GFP showed that ubiquitination was required for Tat-induced synapse loss (Kim et al., 2008), and that interaction with nNOS was required for synapse recovery (A.H. Shin and S.A. Thayer, submitted work). These studies show that this assay is amenable to genetic manipulations that supplement the pharmacological approaches used in these studies. Thus, the live cell imaging assay employed throughout this dissertation is a good tool to better understand the signaling pathways that underlie the physiological manifestation

of synapse loss and recovery.

However, the assay is not without its limitations. One significant limitation of the use of fluorescent marker proteins is that it is impossible to correlate the dynamics of the fusion proteins to their endogenous counterparts within a single neuron. In order to visualize endogenous PSD95, it would be necessary to fix and probe the cultures, which then makes a live cell time-lapse assay impossible to execute. Thus, simultaneous quantification of endogenous protein is not possible alongside the exogenously expressed fusion proteins in studies utilizing this assay. PSD95 has been shown to be an essential protein at excitatory postsynaptic densities, required for spine development and increasing excitatory function at these sites (Cho et al., 1992; El-Husseini et al., 2000). The PSD95-GFP fusion protein expresses at excitatory postsynaptic sites, as evidenced by its co-localization with NMDAR immunoreactivity and synaptic Ca^{2+} release sites (Waataja et al., 2008). Additionally, PSD95-GFP puncta respond to treatments that modulate neuronal excitability, such as the GABA receptor antagonist bicuculline or the sodium channel blocker tetrodotoxin (N.J Hargus and S.A. Thayer, unpublished observations). Overexpression of exogenous PSD95-GFP results in an increase in the number of PSD95-GFP puncta over a 24 hour interval, consistent with the idea that PSD95 stimulates PSD formation but indicating that we have perturbed the endogenous system. Thus, the imaging assay utilized in these studies, while in good agreement with literature indicating the functional dynamics of synapses, is an artificial system created to model synaptic dynamics, and this caveat must be taken into consideration when assessing the significance of the work presented in this dissertation.

The other significant limitation of utilizing our live cell imaging assay lies in its innate simplicity. Experimental analysis is performed as a percent change over time in the total number of qualifying puncta in a single neuron. Therefore, within the studies

outlined here, I discuss changes in overall synapse number and not in the recovery of any one synaptic site after Tat-induced loss. The mechanisms surrounding the recovery of a synapse may be a simple recycling of dendritic proteins at the spine where it once was located; alternatively new synapses may form at sites distinct from those that had existed prior to Tat exposure. Within the scope of this assay, the synapses on a particular neuron are assessed as a population. Whether synapses return to their former sites during synapse recovery is an intriguing question, but cannot be ascertained solely using the imaging assay utilized here. Supplemental techniques to answer this question, as well as others, will be required to fully elucidate the mechanisms of synapse loss and recovery, especially the signaling pathways involved. I show an example of this in Chapter Four, where we confirm PKG activation by analyzing levels of VASP phosphorylation. Another possibility may be to use biotin labeling of intercellular contacts (BLINC), a method by which interaction between the transsynaptic partners neurexin and neuroligin stimulate biotinylation of a fused peptide (Thyagarajan and Ting, 2010). Fluorescent labeling of the biotinylated peptide allows visualization of a complete synapse, and could aid in a chronological study of Tat-induced loss of pre- and post-synaptic sites. In order to fully understand the mechanics of the synaptic dynamics seen in our assay, similar comprehensive and multi-technique approaches will be required.

III. Future directions

The discovery that GluN2B-containing NMDA receptors can be activated after exposure to Tat and tonically suppress recovery is intriguing, and poses a number of exciting questions for future projects. I delineated a signaling cascade downstream of GluN2B-containing NMDA receptors that culminated in PKG activation. I also showed that VASP is a target of PKG after Tat exposure. However, the mechanism by which

PKG can suppress synapse recovery is still not known. PKG has a number of putative targets in the hippocampus that could mediate synapse recovery, including CaMKII, the small GTPase RhoA, and α-synuclein (Liu et al., 2004b; Ninan and Arancio, 2004). Downstream of NMDA receptor activation, PKG activity increases CaMKII gene expression in the hippocampus and modulates induction of long-term potentiation (LTP) (Johnston and Morris, 1995). Thus, CaMKII downstream of PKG is implicated in synaptic plasticity, and could contribute to the suppression of synapse recovery mediated by PKG. Much of the work illuminating PKG and its effectors has been performed in the context of LTP, and has been shown to operate presynaptically (Ko and Kelly, 1999; Wang et al., 2005). The findings in the studies outlined here are consistent with Tat-induced synapse loss and recovery being driven by postsynaptic mechanisms (Shin et al., 2012). A postsynaptic role for CaMKII in Tat-induced synapse loss has also been established, consistent with these studies and providing a contrast with mechanisms of LTP (N.J. Hargus and S.A. Thayer, unpublished observations). Another substrate of PKG, RhoA has also been shown to inhibit dendritic spine formation in hippocampal neurons (Tashiro et al., 2000), making it a tantalizing target for future mechanistic studies downstream of PKG.

The initial observation that led to the studies in this dissertation was the exciting discovery that Tat-induced synapse loss was reversed by RAP. While not a primary subject of this dissertation, the mechanisms of RAP as an agent of synapse recovery are currently unknown. RAP was identified as a chaperone protein and competitive antagonist of LRP (Bu and Rennke, 1996). Consistent with this mechanism of action, pretreatment with RAP prior to Tat exposure prevents synapse loss (Kim et al., 2008). However after 16 h Tat exposure, Tat has presumably been internalized via LRP into neurons, and at this point competitive antagonism by RAP cannot explain the reversal

of synapse loss. However, RAP could induce recovery by an alternate mechanism. As outlined in Chapter Four, nNOS associates with PSD95 to couple cell surface GluN2B-mediated signaling to a downstream pathway. Another protein that has been shown to associate with nNOS is the carboxy-terminal PDZ ligand of nNOS (CAPON). As its name suggests, CAPON interacts with nNOS at its PDZ domain, competing with PSD95 for nNOS binding (Jaffrey et al., 1998). Based on these findings, CAPON presumably binds to nNOS to reduce complex formation of NMDAR/PSD95/nNOS, thereby downregulating the signaling capacity of NMDA receptors via nNOS. Intriguingly, CAPON has also been shown to associate with LRP (Gotthardt et al., 2000). Perhaps RAP induces synapse recovery by binding to LRP and influencing the protein interactions of CAPON, either to LRP directly or by mediating CAPON's interaction with nNOS.

The *in vitro* studies thus far have identified GluN2B-containing NMDA receptors as a key mediator of Tat-induced neuronal death, and suppressor of synapse recovery. The next step in determining the relevance of these *in vitro* findings and relating it to cognitive deficits in HAND patients is to translate the current knowledge into a behavioral output. Inhibition of GluN2B-containing NMDA receptors with ifenprodil induces synapse recovery *in vitro*; perhaps ifenprodil treatment can improve learning and memory in behavioral paradigms. A transgenic mouse model with inducible Tat expression has recently been generated (Bruce-Keller et al., 2008), and is a good system to study the *in vivo* correlates of the work outlined in this dissertation. Correlating the findings in this dissertation with *in vivo* models is the logical first step to developing therapeutic strategies for treatment of HAND.

IV. Synapse loss and recovery: a perspective

HIV Tat induces excitotoxic synapse loss between hippocampal neurons *in*

vitro, a process that can be reversed by selective inhibition of GluN2B-containing NMDA receptors. Neuronal injuries such as synapse loss correlate to cognitive decline in HAND; *in vivo* studies of Tat in the CNS imply that it participates in the neuropathologies of HAND. The mechanisms of synapse recovery may prove to be better therapeutic targets rather than the initial inhibition of synapse loss. Furthermore, reversing the existing damage might improve cognition and be more relevant in a clinical setting. Thus, it is paramount to understand the mechanisms that underlie Tat's neurotoxic effects, in particular the pathways that mediate synapse recovery, in order to provide a framework for designing treatments for HAND.

The mechanisms highlighted in this dissertation are common to many pathways of neurodegeneration. NMDA receptor overactivation is well characterized as a mechanism of neurodegeneration not only in HAND, but other cognitive disorders such as Alzheimer's disease (Hardingham and Bading, 2003). Moreover LRP, the neuronal receptor for Tat, is implicated in clearance of the amyloid-beta (Aβ) peptide from the brain, a hallmark of Alzheimer's disease (Deane et al., 2004). Thus, disorders with different etiologies share common pathways that produce cognitive decline; targeting these common pathways can result in treatment strategies for multiple disorders. Understanding the molecular mechanisms of neuronal injury induced by HIV, and the exciting process of synapse recovery, may improve the treatment of HAND.

Chapter Six:

Bibliography

Adle-Biassette H, Chretien F, Wingertsmann L, Hery C, Ereau T, Scaravilli F, Tardieu M, Gray F (1999) Neuronal apoptosis does not correlate with dementia in HIV infection but is related to microglial activation and axonal damage. Neuropathol Appl Neurobiol 25:123-133.

Aksenov MY, Aksenova MV, Mactutus CF, Booze RM (2009) Attenuated neurotoxicity of the transactivation-defective HIV-1 Tat protein in hippocampal cell cultures. Exp Neurol 219:586-590.

Aksenova MV, Aksenov MY, Adams SM, Mactutus CF, Booze RM (2008) Neuronal survival and resistance to HIV-1 Tat toxicity in the primary culture of rat fetal neurons. Exp Neurol.

Antinori A, Arendt G, Becker JT, Brew BJ, Byrd DA, Cherner M, Clifford DB, Cinque P, Epstein LG, Goodkin K, Gisslen M, Grant I, Heaton RK, Joseph J, Marder K, Marra CM, MCArthur JC, Nunn M, Price RW, Pulliam L, Roberston KR, Sacktor N, Valcour V, Wojna VE (2007) Updated research nosology for HIV-associated neurocognitive disorders. Neurology 69:1789-1799.

Arancio O, Kiebler M, Lee CJ, Lev-Ram V, Tsien RY, Kandel ER, Hawkins RD (1996) Nitric oxide acts directly in the presynaptic neuron to produce long-term potentiation in cultured hippocampal neurons. Cell 87:1025-1035.

Areosa SA, Sherriff F, McShane R (2005) Memantine for dementia. Cochrane Database Syst Rev:CD003154.

Arnold DB, Clapham DE (1999) Molecular determinants for subcellular localization of PSD-95 with an interacting K+ channel. Neuron 23:149-157.

Avenet P, Leonardon J, Besnard F, Graham D, Frost J, Depoortere H, Langer SZ, Scatton B (1996) Antagonist properties of the sterioisomers of ifenprodil at NR1A/NR2A and NR1A/NR2B subtypes of the NMDA receptor expressed in

Xenopos oocytes. Eur J Pharmacol 296:209-213.

Bansal AK, Mactutus CF, Nath A, Maragos W, Hauser KF, Booze RM (2000) Neurotoxicity of HIV-1 proteins gp120 and Tat in the rat striatum. Brain Res 879:42-49.

Berger EA, Murphy PM, Farber JM (1999) Chemokine receptors as HIV-1 coreceptors: roles in viral entry, tropism, and disease. Annu Rev Immunol 17:657-700.

Bettini E, Sava A, Griffante C, Carignani C, Buson A, Capelli AM, Negri M, Andreetta F, Senar-Sancho SA, Guiral L, Cardullo F (2010) Identification and characterization of novel NMDA receptor antagonists selective for NR2A- over NR2B-containing receptors. J Pharmacol Exp Ther 335:636-644.

Bianchetta MJ, Lam TT, Jones SN, Morabito MA (2011) Cyclin-Dependent Kinase 5 Regulates PSD-95 Ubiquitination in Neurons. The Journal of Neuroscience 31:12029-12035.

Black M, Lanthorn T, Small D, Mealing G, Lam V, Morley P (1996) Study of potency, kinetics of block and toxicity of NMDA receptor antagonists using fura-2. Eur J Pharmacol 317:377-381.

Bonavia R, Bajetto A, Barbero S, Albini A, Noonan DM, Schettini G (2001) HIV-1 Tat causes apoptotic death and calcium homeostasis alterations in rat neurons. Biochem Biophys Res Commun 288:301-308.

Boyce-Rustay JM, Holmes A (2006) Genetic Inactivation of the NMDA Receptor NR2A Subunit has Anxiolytic- and Antidepressant-Like Effects in Mice. Neuropsychopharmacology 31:2405-2414.

Brake DA, Debouck C, Biesecker G (1990) Identification of an Arg-Gly-Asp (RGD) cell adhesion site in human immunodeficiency virus type 1 transactivation protein, tat. J Cell Biol 111:1275-1281.

Bruce-Keller AJ, Chauhan A, Dimayuga FO, Gee J, Keller JN, Nath A (2003) Synaptic Transport of Human Immunodeficiency Virus-Tat Protein Causes Neurotoxicity and Gliosis in Rat Brain. J Neurosci 23:8417-8422.

Bruce-Keller AJ, Turchan-Cholewo J, Smart EJ, Geurin T, Chauhan A, Reid R, Xu R, Nath A, Knapp PE, Hauser KF (2008) Morphine causes rapid increases in glial activation and neuronal injury in the striatum of inducible HIV-1 Tat transgenic mice. Glia 56:1414-1427.

Bu G, Rennke S (1996) Receptor-associated protein is a folding chaperone for low density lipoprotein receptor-related protein. J Biol Chem 271:22218-22224.

Burette A, Zabel U, Weinberg RJ, Schmidt HHHW, Valtschanoff JG (2002) Synaptic Localization of Nitric Oxide Synthase and Soluble Guanylyl Cyclase in the Hippocampus. J Neurosci 22:8961-8970.

Butt E, Abel K, Krieger M, Palm D, Hoppe V, Hoppe J, Walter U (1994) cAMP- and cGMP-dependent protein kinase phosphorylation sites of the focal adhesion vasodilator-stimulated phosphoprotein (VASP) in vitro and in intact human platelets. J Biol Chem 269:14509-14517.

Carpenter CC, Cooper DA, Fischl MA, Gatell JM, Gazzard BG, Hammer SM, Hirsch MS, Jacobsen DM, Katzenstein DA, Montaner JS, Richman DD, Saag MS, Schechter M, Schooley RT, Thompson MA, Vella S, Yeni PG, Volberding PA (2000) Antiretroviral therapy in adults: updated recommendations of the International AIDS Society-USA Panel. Jama 283:381-390.

Chan DC, Kim PS (1998) HIV entry and its inhibition. Cell 93:681-684.

Chavis P, Westbrook G (2001) Integrins mediate functional pre- and postsynaptic maturation at a hippocampal synapse. Nature 411:317-321.

Chen HSV, Lipton SA (1997) Mechanism of memantine block of NMDA-activated

channels in rat retinal ganglion cells: uncompetitive antagonism. J Physiol 499:27-46.

Cheng J, Nath A, Knudsen B, Hochman S, Geiger JD, Ma M, Magnuson DS (1998) Neuronal excitatory properties of human immunodeficiency virus type 1 Tat protein. Neuroscience 82:97-106.

Chin CL, Tovcimak AE, Hradil VP, Seifert TR, Hollingsworth PR, Chandran P, Zhu CZ, Gauvin D, Pai M, Wetter J, Hsieh GC, Honore P, Frost JM, Dart MJ, Meyer MD, Yao BB, Cox BF, Fox GB (2007) Differential effects of cannabinoid receptor agonists on regional brain activity using pharmacological MRI. Br J Pharmacol.

Chin J, Ascher MS, eds (2000) Control of Communicable Diseases Manual, 17 Edition. Baltimore, MD: United Book Press, Inc.

Cho KO, Hunt CA, Kennedy MB (1992) The rat brain postsynaptic density fraction contains a homolog of the Drosophila discs-large tumor suppressor protein. Neuron 9:929-942.

Christopherson KS, Hillier BJ, Lim WA, Bredt DS (1999) PSD-95 Assembles a Ternary Complex with the N-Methyl-D-aspartic Acid Receptor and a Bivalent Neuronal NO Synthase PDZ Domain. J Biol Chem 274:27467-27473.

Coan EJ, Saywood W, Collingridge GL (1987) MK-801 blocks NMDA receptor-mediated synaptic transmission and long term potentiation in rat hippocampals slices. Neurosci Lett 80:111-114.

Cohen EA, Terwilliger EF, Jalinoos Y, Proulx J, Sodroski JG, Haseltine WA (1990) Identification of HIV-1 vpr product and function. J Acquir Immune Defic Syndr 3:11-18.

Colledge M, Snyder EM, Crozier RA, Soderling JA, Jin Y, Langeberg LK, Lu H, Bear MF, Scott JD (2003) Ubiquitination regulates PSD-95 degradation and AMPA

receptor surface expression. Neuron 40:595-607.

Cui H, Hayashi A, Sun H-S, Belmares MP, Cobey C, Phan T, Schweizer J, Salter MW, Wang YT, Tasker RA, Garman D, Rabinowitz J, Lu PS, Tymianski M (2007) PDZ Protein Interactions Underlying NMDA Receptor-Mediated Excitotoxicity and Neuroprotection by PSD-95 Inhibitors. J Neurosci 27:9901-9915.

Cull-Candy S, Brickley S, Farrant M (2001) NMDA receptor subunits: diversity, development and disease. Curr Opin Neurobiol 11:327-335.

Cysique LA, Maruff P, Brew BJ (2004) Prevalence and pattern of neuropsychological impairment in human immunodeficiency virus–infected/acquired immunodeficiency syndrome (HIV/AIDS) patients across pre- and post-highly active antiretroviral therapy eras: A combined study of two cohorts. J Neurovirol 10:350-357.

Dayton AI, Sodroski JG, Rosen CA, Goh WC, Haseltine WA (1986) The trans-activator gene of the human T cell lymphotropic virus type III is required for replication. Cell 44:941-947.

Deane R, Wu Z, Sagare A, Davis J, Du Yan S, Hamm K, Xu F, Parisi M, LaRue B, Hu HW, Spijkers P, Guo H, Song X, Lenting PJ, Van Nostrand WE, Zlokovic BV (2004) LRP/amyloid beta-peptide interaction mediates differential brain efflux of Abeta isoforms. Neuron 43:333-344.

Del Valle L, Croul S, Morgello S, Amini S, Rappaport J, Khalili K (2000) Detection of HIV-1 Tat and JCV capsid protein, VP1, in AIDS brain with progressive multifocal leukoencephalopathy. J Neurovirol 6:221-228.

Dou H, Ellison B, Bradley J, Kasiyanov A, Poluektova LY, Xiong H, Maggirwar S, Dewhurst S, Gelbard HA, Gendelman HE (2005) Neuroprotective mechanisms of lithium in murine human immunodeficiency virus-1 encephalitis. J Neurosci

25:8375-8385.

El-Husseini AE, Schnell E, Chetkovich DM, Nicoll RA, Bredt DS (2000) PSD-95 involvement in maturation of excitatory synapses. Science 290:1364-1368.

Ellis R, Langford D, Masliah E (2007) HIV and antiretroviral therapy in the brain: neuronal injury and repair. Nat Rev Neurosci 8:33-44.

Ensoli B, Barillari G, Salahuddin SZ, Gallo RC, Wong-Staal F (1990) Tat protein of HIV-1 stimulates growth of cells derived from Kaposi's sarcoma lesions of AIDS patients. Nature 345:84-86.

Ensoli B, Buonaguro L, Barillari G, Fiorelli V, Gendelman R, Morgan RA, Wingfield P, Gallo RC (1993) Release, uptake, and effects of extracellular human immunodeficiency virus type 1 Tat protein on cell growth and viral transactivation. J Virol 67:277-287.

Eugenin EA, King JE, Nath A, Calderon TM, Zukin RS, Bennett MV, Berman JW (2007) HIV-tat induces formation of an LRP-PSD-95- NMDAR-nNOS complex that promotes apoptosis in neurons and astrocytes. Proc Natl Acad Sci U S A 104:3438-3443.

Everall IP, Heaton RK, Marcotte TD, Ellis RJ, McCutchan JA, Atkinson JH, Grant I, Mallory M, Masliah E (1999) Cortical synaptic density is reduced in mild to moderate human immunodeficiency virus neurocognitive disorder. HNRC Group. HIV Neurobehavioral Research Center. Brain Pathol 9:209-217.

Feil R, Kleppisch T (2008) NO/cGMP-dependent modulation of synaptic transmission. Handb Exp Pharmacol:529-560.

Ferrando S, van Gorp W, McElhiney M, Goggin K, Sewell M, Rabkin J (1998) Highly active antiretroviral treatment in HIV infection: benefits for neuropsychological function. AIDS 12:F65-70.

Fitting S, Xu R, Bull C, Buch S, El-Hage N, Nath A, Knapp PE, Hauser KF (2010) Interactive Comorbidity between Opioid Drug Abuse and HIV-1 Tat: Chronic Exposure Augments Spine Loss and Sublethal Dendritic Pathology in Striatal Neurons. Am J Pathol 177:1397-1410.

Fletcher TL, Cameron P, De Camilli P, Banker G (1991) The distribution of synapsin I and synaptophysin in hippocampal neurons developing in culture. The Journal of Neuroscience 11:1617-1626.

Foster AC, Wong EHF (1987) The novel anticonvulsant MK-801 binds to the activated state of the N-methyl-D-aspartate receptor in rat brain. Br J Pharmacol 91:403-409.

Franco DL, Rezaval C, Caceres A, Schinder AF, Ceriani MF (2010) ENA/VASP downregulation triggers cell death by impairing axonal maintenance in hippocampal neurons. Mol Cell Neurosci 44:154-164.

Friebe A, Koesling D (2003) Regulation of nitric oxide-sensitive guanylyl cyclase. Circ Res 93:96-105.

Friedman HV, Bresler T, Garner CC, Ziv NE (2000) Assembly of new individual excitatory synapses: time course and temporal order of synaptic molecule recruitment. Neuron 27:57-69.

Furukawa H, Singh SK, Mancusso R, Gouaux E (2005) Subunit arrangement and function in NMDA receptors. Nature 438:185-192.

Fykse EM, Takei K, Walch-Solimena C, Geppert M, Jahn R, De Camilli P, Sudhof TC (1993) Relative properties and localizations of synaptic vesicle protein isoforms: the case of the synaptophysins. The Journal of Neuroscience 11:4997-5007.

Gambrill AC, Barria A (2011) NMDA receptor subunit composition controls synaptogenesis and synapse stabilization. Proc Natl Acad Sci U S A.

Garber ME, Wei P, KewalRamani VN, Mayall TP, Herrmann CH, Rice AP, Littman DR, Jones KA (1998) The interaction between HIV-1 Tat and human cyclin T1 requires zinc and a critical cysteine residue that is not conserved in the murine CycT1 protein. Genes Dev 12:3512-3527.

Garthwaite J, Southam E, Boulton CL, Nielsen EB, Schmidt K, Mayer B (1995) Potent and selective inhibition of nitric oxide-sensitive guanylyl cyclase by 1H-[1,2,4]oxadiazolo[4,3-a]quinoxalin-1-one. Mol Pharmacol 48:184-188.

Ge Y, Dong Z, Bagot RC, Howland JG, Phillips AG, Wong TP, Wang YT (2010) Hippocampal long-term depression is required for the consolidation of spatial memory. Proc Natl Acad Sci U S A 107:16697-16702.

Gendelman HE, Lipton SA, Tardieu M, Bukrinsky MI, Nottet HS (1994) The neuropathogenesis of HIV-1 infection. Journal of Leukocyte Biology 56:389-398.

Genis P, Jett M, Bernton EW, Boyle T, Gelbard HA, Dzenko K, Keane RW, Resnick L, Mizrachi Y, Volsky DJ, Epstein LG, Gendelman HE (1992) Cytokines and arachidonic metabolites produced during human immunodeficiency virus (HIV)-infected macrophage interactions: implications for the neuropathogenesis of HIV disease. J Exp Med 176:1703-1718.

Gill R, Foster AC, Woodruff G (1987) Systemic administration of MK-801 protects against ischemia-induced hippocampal neurodegeneration in the gerbil. The Journal of Neuroscience 7:3343-3349.

Goncalves J, Korin Y, Zack J, Gabuzda D (1996) Role of Vif in human immunodeficiency virus type 1 reverse transcription. J Virol 70:8701-8709.

Gotthardt M, Trommsdorff M, Nevitt MF, Shelton J, Richardson JA, Stockinger W, Nimpf J, Herz J (2000) Interactions of the low density lipoprotein receptor gene family with cytosolic adaptor and scaffold proteins suggest diverse biological functions

in cellular communication and signal transduction. J Biol Chem 275:25616-25624.

Gray JA, Shi Y, Usui H, During MJ, Sakimura K, Nicoll RA (2011) Distinct Modes of AMPA Receptor Suppression at Developing Synapses by GluN2A and GluN2B: Single-Cell NMDA Receptor Subunit Deletion In Vivo. Neuron 71:1085-1101.

Green M, Loewenstein PM (1988) Autonomous functional domains of chemically synthesized human immunodeficiency virus tat trans-activator protein. Cell 55:1179-1188.

Greene WC, Peterlin BM (2002) Charting HIV's remarkable voyage through the cell: Basic science as a passport to future therapy. Nature Medicine 8:673-680.

Hardingham GE, Bading H (2003) The yin and yang of NMDA receptor signalling. Trends in Neurosciences 26:81-89.

Hardingham GE, Fukunaga Y, Bading H (2002) Extrasynaptic NMDARs oppose synaptic NMDARs by triggering CREB shut-off and cell death pathways. Nat Neurosci 5:405-414.

Haughey NJ, Nath A, Mattson MP, Slevin JT, Geiger JD (2001) HIV-1 Tat through phosphorylation of NMDA receptors potentiates glutamate excitotoxicity. Journal of Neurochemistry 78:457-467.

Hayman M, Arbuthnott G, Harkiss G, Brace H, Filippi P, Philippon V, Thomson D, Vigne R, Wright A (1993) Neurotoxicity of peptide analogues of the transactivating protein tat from Maedi-Visna virus and human immunodeficiency virus. Neuroscience 53:1-6.

Heaton RK, Marcotte TD, Mindt MR, Sadek J, Moore DJ, Bentley H, McCutchan JA, Reicks C, Grant I (2004) The impact of HIV-associated neuropsychological impairment on everyday functioning. J Int Neuropsychol Soc 10:317-331.

Heaton RK, Clifford DB, Franklin DR, Jr., Woods SP, Ake C, Vaida F, Ellis RJ,

Letendre SL, Marcotte TD, Atkinson JH, Rivera-Mindt M, Vigil OR, Taylor MJ, Collier AC, Marra CM, Gelman BB, McArthur JC, Morgello S, Simpson DM, McCutchan JA, Abramson I, Gamst A, Fennema-Notestine C, Jernigan TL, Wong J, Grant I (2010) HIV-associated neurocognitive disorders persist in the era of potent antiretroviral therapy: CHARTER Study. Neurology 75:2087-2096.

Ho GP, Selvakumar B, Mukai J, Hester LD, Wang Y, Gogos JA, Snyder SH (2011) S-Nitrosylation and S-Palmitoylation Reciprocally Regulate Synaptic Targeting of PSD-95. Neuron 71:131-141.

Hofman FM, Dohadwala MM, Wright AD, Hinton DR, Walker SM (1994) Exogenous tat protein activates central nervous system-derived endothelial cells. J Neuroimmunol 54:19-28.

Hudson L, Liu J, Nath A, Jones M, Raghavan R, Narayan O, Male D, Everall I (2000) Detection of the human immunodeficiency virus regulatory protein tat in CNS tissues. J Neurovirol 6:145-155.

Huettner JE, Bean BP (1988) Block of N-methyl-D-aspartate-activated current by the anticonvulsant MK-801: Selective binding to open channels. Proc Natl Acad Sci U S A 85:1307-1311.

Hult B, Chana G, Masliah E, Everall I (2008) Neurobiology of HIV. Int Rev Psychiatry 20:3-13.

Hunt CA, Schenker LJ, Kennedy MB (1996) PSD-95 is associated with the postsynaptic density and not with the presynaptic membrane at forebrain synapses. J Neurosci 16:1380-1388.

Isel C, Karn J (1999) Direct evidence that HIV-1 Tat stimulates RNA polymerase II carboxyl-terminal domain hyperphosphorylation during transcriptional elongation. J Mol Biol 290:929-941.

Jaffrey SR, Snowman AM, Eliasson MJL, Cohen NA, Snyder SH (1998) Capon - a Protein Associated With Neuronal Nitric Oxide Synthase That Regulates Its Interactions With Psd95. Neuron 20:115-124.

Jeang KT, Xiao H, Rich EA (1999) Multifaceted activities of the HIV-1 transactivator of transcription, Tat. J Biol Chem 274:28837-28840.

Johnston HM, Morris BJ (1995) N-methyl-D-aspartate and nitric oxide regulate the expression of calcium/calmodulin-dependent kinase II in the hippocampal dentate gyrus. Brain Res Mol Brain Res 31:141-150.

Johnston PA, Sudhof TC (1990) The multisubunit structure of synaptophysin. J Biol Chem 265:8869-8873.

Kahn JO, Walker BD (1998) Acute Human Immunodeficiency Virus Type 1 Infection. N Engl J Med 336:33-39.

Kaplan JE, Hanson D, Dworkin MS, Frederick T, Bertolli J, Lindegren ML, Holmberg S, Jones JL (2000) Epidemiology of Human Immunodeficiency Virus–Associated Opportunistic Infections in the United States in the Era of Highly Active Antiretroviral Therapy. Clinical Infectious Diseases 30:S5-14.

Kaul M, Lipton SA (2006) Mechanisms of Neuronal Injury and Death in HIV-1 Associated Dementia. Curr HIV Res 4:307-318.

Kaul M, Garden GA, Lipton SA (2001) Pathways to neuronal injury and apoptosis in HIV-associated dementia. Nature 410:988-994.

Kim BO, Liu Y, Ruan Y, Xu ZC, Schantz L, He JJ (2003) Neuropathologies in transgenic mice expressing human immunodeficiency virus type 1 Tat protein under the regulation of the astrocyte-specific glial fibrillary acidic protein promoter and doxycycline. Am J Pathol 162:1693-1707.

Kim HJ, Thayer SA (2009) Lithium increases synapse formation between hippocampal

neurons by depleting phosphoinositides. Mol Pharmacol 75:1021-1030.

Kim HJ, Martemyanov KA, Thayer SA (2008) Human Immunodeficiency Virus Protein Tat Induces Synapse Loss via a Reversible Process That Is Distinct from Cell Death. J Neurosci 28:12604-12613.

Kim HJ, Shin AH, Thayer SA (2011) Activation of Cannabinoid Type 2 Receptors Inhibits HIV-1 Envelope Glycoprotein gp120-Induced Synapse Loss. Mol Pharmacol 80:357-366.

King JE, Eugenin EA, Buckner CM, Berman JW (2006) HIV tat and neurotoxicity. Microbes Infect 8:1347-1357.

Kleppisch T, Feil R (2009) cGMP signalling in the mammalian brain: role in synaptic plasticity and behaviour. Handb Exp Pharmacol:549-579.

Ko GY, Kelly PT (1999) Nitric oxide acts as a postsynaptic signaling molecule in calcium/calmodulin-induced synaptic potentiation in hippocampal CA1 pyramidal neurons. The Journal of Neuroscience 19:6784-6794.

Kruman II, Nath A, Mattson MP (1998) HIV-1 Protein Tat Induces Apoptosis of Hippocampal Neurons by a Mechanism Involving Caspase Activation, Calcium Overload, and Oxidative Stress. Experimental Neurology 154:276-288.

Kuppuswamy M, Subramanian T, Srinivasan A, Chinnadurai G (1989) Multiple functional domains of Tat, the trans-activator of HIV-1, defined by mutational analysis. Nucleic Acids Res 17:3551-3561.

Kwiatkowski AV, Rubinson DA, Dent EW, Edward van Veen J, Leslie JD, Zhang J, Mebane LM, Philippar U, Pinheiro EM, Burds AA, Bronson RT, Mori S, Fassler R, Gertler FB (2007) Ena/VASP Is Required for neuritogenesis in the developing cortex. Neuron 56:441-455.

Letendre SL, Woods SP, Ellis RJ, Atkinson JH, Masliah E, van den Brande G, Durelle

J, Grant I, Everall I (2006) Lithium improves HIV-associated neurocognitive impairment. Aids 20:1885-1888.

Li CJ, Ueda Y, Shi B, Borodyansky L, Huang L, Li YZ, Pardee AB (1997) Tat protein induces self-perpetuating permissivity for productive HIV-1 infection. Proc Natl Acad Sci U S A 94:8116-8120.

Li ST, Matsushita M, Moriwaki A, Saheki Y, Lu YF, Tomizawa K, Wu HY, Terada H, Matsui H (2004) HIV-1 Tat inhibits long-term potentiation and attenuates spatial learning. Ann Neurol 55:362-371.

Li W, Li G, Steiner J, Nath A (2009) Role of Tat Protein in HIV Neuropathogenesis. Neurotox Res 16:205-220.

Li W, Huang Y, Reid R, Steiner J, Malpica-Llanos T, Darden TA, Shankar SK, Mahadevan A, Satishchandra P, Nath A (2008) NMDA Receptor Activation by HIV-Tat Protein Is Clade Dependent. J Neurosci 28:12190-12198.

Lin WH, Nebhan CA, Anderson BR, Webb DJ (2010) Vasodilator-stimulated phosphoprotein (VASP) induces actin assembly in dendritic spines to promote their development and potentiate synaptic strength. J Biol Chem 285:36010-36020.

Liner KJ, 2nd, Hall CD, Robertson KR (2007) Impact of human immunodeficiency virus (HIV) subtypes on HIV-associated neurological disease. J Neurovirol 13:291-304.

Lipton SA, Choi YB, Pan ZH, Lei SZ, Chen HSV, Sucher NJ, Loscalzo J, Singel DJ, Stamler JS (1993) A redox-based mechanism for the neuroprotective and neurodestructive effects of nitric oxide and related nitroso-compounds. Nature 364:626-632.

Liu L, Wong TP, Pozza MF, Lingenhoehl K, Wang Y, Sheng M, Auberson YP, Wang YT (2004a) Role of NMDA Receptor Subtypes in Governing the Direction of

Hippocampal Synaptic Plasticity. Science 304:1021-1024.

Liu S, Ninan I, Antonova I, Battaglia F, Trinchese F, Narasanna A, Kolodilov N, Dauer W, Hawkins RD, Arancio O (2004b) alpha-Synuclein produces a long-lasting increase in neurotransmitter release. Embo J 23:4506-4516.

Liu Y, Jones M, Hingtgen CM, Bu G, Laribee N, Tanzi RE, Moir RD, Nath A, He JJ (2000) Uptake of HIV-1 tat protein mediated by low-density lipoprotein receptor-related protein disrupts the neuronal metabolic balance of the receptor ligands. Nat Med 6:1380-1387.

Liu Y, Wong TP, Aarts M, Rooyakkers A, Liu L, Lai TW, Wu DC, Lu J, Tymianski M, Craig AM, Wang YT (2007) NMDA Receptor Subunits Have Differential Roles in Mediating Excitotoxic Neuronal Death Both In Vitro and In Vivo. J Neurosci 27:2846-2857.

Ma M, Nath A (1997) Molecular determinants for cellular uptake of Tat protein of human immunodeficiency virus type 1 in brain cells. J Virol 71:2495-2499.

Magnuson DS, Knudsen BE, Geiger JD, Brownstone RM, Nath A (1995) Human immunodeficiency virus type 1 tat activates non-N-methyl-D-aspartate excitatory amino acid receptors and causes neurotoxicity. Ann Neurol 37:373-380.

Manahan-Vaughan D, von Haebler D, Winter C, Juckel G, Heinemann U (2008) A single application of MK801 causes symptoms of acute psychosis, deficits in spatial memory, and impairment of synaptic plasticity in rats. Hippocampus 18:125-134.

Maragos WF, Tillman P, Jones M, Bruce-Keller AJ, Roth S, Bell JE, Nath A (2003) Neuronal injury in hippocampus with human immunodeficiency virus transactivating protein, Tat. Neuroscience 117:43-53.

Martel MA, Ryan TJ, Bell KF, Fowler JH, McMahon A, Al-Mubarak B, Komiyama NH, Horsburgh K, Kind PC, Grant SG, Wyllie DJ, Hardingham GE (2012) The

Subtype of GluN2 C-terminal Domain Determines the Response to Excitotoxic Insults. Neuron 74:543-556.

Masliah E, Heaton RK, Marcotte TD, Ellis RJ, Wiley CA, Mallory M, Achim CL, McCutchan JA, Nelson JA, Atkinson JH, Grant I (1997) Dendritic injury is a pathological substrate for human immunodeficiency virus-related cognitive disorders. HNRC Group. The HIV Neurobehavioral Research Center. Ann Neurol 42:963-972.

Massey PV, Johnson BE, Moult PR, Auberson YP, Brown MW, Molnar E, Collingridge GL, Bashir ZI (2004) Differential roles of NR2A and NR2B-containing NMDA receptors in cortical long-term potentiation and long-term depression. J Neurosci 24:7821-7828.

May P, Woldt E, Matz RL, Boucher P (2007) The LDL receptor-related protein (LRP) family: an old family of proteins with new physiological functions. Ann Med 39:219-228.

McArthur JC (2004) HIV dementia: an evolving disease. J Neuroimmunol 157:3-10.

McArthur JC, Steiner J, Sacktor N, Nath A (2010) Human Immunodeficiency Virus-Associated Neurocognitive Disorders Mind the Gap. Ann Neurol 67:699-714.

McMahon HT, Bolshakov VY, Janz R, Hammer RE, Siegelbaum SA, Sudof TC (1996) Synaptophysin, a major synaptic vesicle protein, is not essential for neurotransmitter release. Proc Natl Acad Sci U S A 93:4760-4764.

Meyer G, Varoqueaux F, Neeb A, Oschlies M, Brose N (2004) The complexity of PDZ domain-mediated interactions at glutamatergic synapses: a case study on neuroligin. Neuropharmacology 47:724-733.

Midde N, Gomez A, Zhu J (2012) HIV-1 Tat protein decreases dopamine transporter cell surface expression and vesicular monoamine transporter-2 function in rat

striatal synaptosomes. J Neuroimmune Pharmacol 7:629-639.

Minagar A, Shapshak P, Fujimura R, Ownby R, Heyes M, Eisdorfer C (2002) The role of macrophage/microglia and astrocytes in the pathogenesis of three neurologic disorders: HIV-associated dementia, Alzheimer disease, and multiple sclerosis. J Neurol Sci 202:13-23.

Minagar A, Commins D, Alexander JS, Hoque R, Chiappelli F, Singer EJ, Nikbin B, Shapshak P (2008) NeuroAIDS: Characteristics and Diagnosis of the Neurological Complications of AIDS. Mol Diagn Ther 12:25-43.

Mishra A, Kim HJ, Shin AH, Thayer SA (2012) Synapse Loss Induced by Interleukin-1β Requires Pre- and Post-synaptic Mechanisms. J Neuroimmune Pharmacol DOI: 10.1007/s11481-012-9342-7.

Monyer H, Burnashev N, Laurie DJ, Sakmann B, Seeburg PH (1994) Developmental and regional expression in the rat brain and functional properties of four NMDA receptors. Neuron 12:529-540.

Moore DJ, Masliah E, Rippeth JD, Gonzalez R, Carey CL, Cherner M, Ellis RJ, Achim CL, Marcotte TD, Heaton RK, Grant I (2006) Cortical and subcortical neurodegeneration is associated with HIV neurocognitive impairment. AIDS 20:879-887.

Morse SA, Ballard RC, Holmes KK, Moreland AA, eds (2003) Atlas of Sexually Transmitted Diseases and AIDS, 3rd Edition. Edinburgh: Mosby - Elsevier Science Limited.

Mount C, Downton C (2006) Alzheimer disease: progress or profit? Nat Med 12:780-784.

Muir KW, Lees KR (1995) Clinical experience with excitatory amino acid antagonist drugs. Stroke 26:503-513.

Mustafa AK, Kumar M, Selvakumar B, Ho GP, Ehmsen JT, Barrow RK, Amzel LM,

Snyder SH (2007) Nitric oxide S-nitrosylates serine racemase, mediating feedback inhibition of D-serine formation. Proc Natl Acad Sci U S A 104:2950-2955.

Nath A, Conant K, Chen P, Scott C, Major EO (1999) Transient exposure to HIV-1 Tat protein results in cytokine production in macrophages and astrocytes. A hit and run phenomenon. J Biol Chem 274:17098-17102.

Nath A, Psooy K, Martin C, Knudsen B, Magnuson DS, Haughey N, Geiger JD (1996) Identification of a human immunodeficiency virus type 1 Tat epitope that is neuroexcitatory and neurotoxic. J Virol 70:1475-1480.

Ninan I, Arancio O (2004) Presynaptic CaMKII is necessary for synaptic plasticity in cultured hippocampal neurons. Neuron 42:129-141.

Nong Y, Huang YQ, Ju W, Kalia LV, Ahmadian G, Wang YT, Salter MW (2003) Glycine binding primes NMDA receptor internalization. Nature 422:302-307.

OARAC HPoAGfAaAAWGotOoARAC- (2013) Panel on Antiretroviral Guidelines for Adults and Adolescents. Guidelines for the use of antiretroviral agents in HIV-1-infected adults and adolescents. In: (Services DoHaH, ed), pp E1-24; F21-29.

Parent A, Schrader K, Munger SD, Reed RR, Linden DJ, Ronnett GV (1998) Synaptic transmission and hippocampal long-term potentiation in olfactory cyclic nucleotide-gated channel type 1 null mouse. J Neurophysiol 79:3295-3301.

Parsons CG, Gruner R, Rozental J, Millar J, Lodge D (1993) Patch Clamp Studies on the Kinetics and Selectivity of N-Methyl-D-Aspartate Receptor Antagonism by Memantine (1-Amino-3,5-Dimethyladamantan). Neuropharmacology 32:1337-1350.

Pasti L, Zonta M, Pozzan T, Vicini S, Carmignoto G (2001) Cytosolic calcium oscillations in astrocytes may regulate exocytotic release of glutamate. J Neurosci 21:477-

484.

Perelson AS, Neumann AU, Markowitz M, Leonard JM, Ho DD (1996) HIV-1 dynamics in vivo: virion clearance rate, infected cell life-span, and viral generation time. Science 271:1582-1586.

Perry S, Barbieri J, Tong N, Polesskaya O, Pudasaini S, Stout A, Lu RK, M, Maggirwar S, Gelbard H (2010) Human immunodeficiency virus-1 Tat activates calpain proteases via the ryanodine receptor to enhance surface dopamine transporter levels and increase transporter-specific uptake and Vmax. The Journal of Neuroscience 30:14153-14164.

Philippon V, Vellutini C, Gambarelli D, Harkiss G, Arbuthnott G, Metzger D, Roubin R, Filippi P (1994) The basic domain of the lentiviral Tat protein is responsible for damages in mouse brain: involvement of cytokines. Virology 205:519-529.

Pulliam L, Herndier B, Tang N, McGrath M (1991) Human immunodeficiency virus-infected macrophages produce soluble factors that cause histological and neurochemical alterations in cultured human brains. J Clinic Invest 87:503-512.

Rao VR, Sas AR, Eugenin EA, Siddappa NB, Bimonte-Nelson H, Berman JW, Ranga U, Tyor WR, Prasad VR (2008) HIV-1 Clade-Specific Differences in the Induction of Neuropathogenesis. J Neurosci 28:10010-10016.

Rehm H, Wiedenmann B, Betz H (1986) Molecular characterization of synaptophysin, a major calcium-binding protein of the synaptic vesicle membrane. Embo J 5:535-541.

Reisberg B, Doody R, Stoffler A, Schmitt F, Ferris S, Mobius HJ (2003) Memantine in moderate-to-severe Alzheimer's disease. N Engl J Med 348:1333-1341.

Repaske DR, Corbin JG, Conti M, Goy MF (1993) A cyclic GMP-stimulated cyclic nucleotide phosphodiesterase gene is highly expressed in the limbic system of

the rat brain. Neuroscience 56:673-686.

Robertson KR, Robertson WT, Ford S, Watson D, Fiscus S, Harp AG, Hall CD (2004) Highly active antiretroviral therapy improves neurocognitive functioning. J Acquir Immune Defic Syndr 36:562-566.

Roche KW, Standley S, McCallum J, Ly CD, Ehlers MD, Wenthold RJ (2001) Molecular determinants of NMDA receptor internalization. Nature Neuroscience 4:794-802.

Rusakov DA, Kullmann DM (1998) Extrasynaptic Glutamate Diffusion in the Hippocampus - Ultrastructural Constraints, Uptake, and Receptor Activation. Journal of Neuroscience 18:3158-3170.

Sa MJ, Madeira MD, Ruela C, Volk B, Mota-Miranda A, Paula-Barbosa MM (2004) Dendritic changes in the hippocampal formation of AIDS patients: a quantitative Golgi study. Acta Neuropathol (Berl) 107:97-110.

Sabatier J-M, Vives E, Mabrouk K, Benjouad A, Rochat H, Duval A, Hue B, Bahraout E (1991) Evidence for neurotoxic activity of *tat* from human immunodeficiency virus type 1. J Virol 65:961-967.

Sacktor N, Nakasujja N, Robertson K, Clifford DB (2007) HIV-associated cognitive impairment in sub-Saharan Africa--the potential effect of clade diversity. Nat Clin Pract Neurol 3:436-443.

Sacktor N, McDermott MP, Marder K, Schifitto G, Selnes OA, McArthur JC, Stern Y, Albert S, Palumbo D, Kieburtz K, De Marcaida JA, Cohen B, Epstein L (2002) HIV-associated cognitive impairment before and after the advent of combination therapy. J Neurovirol 8:136-142.

Sastry KJ, Reddy HR, Pandita R, Totpal K, Aggarwal BB (1990) HIV-1 tat gene induces tumor necrosis factor-beta (lymphotoxin) in a human B-lymphoblastoid cell line. J Biol Chem 265:20091-20093.

Scheiffele P, Fan J, Choih J, Fetter R, Serafini T (2000) Neuroligin expressed in nonneuronal cells triggers presynaptic development in contacting axons. Cell 101:657-669.

Schifitto G, Zhang J, Evans SR, Sacktor N, Simpson D, Millar LL, Hung VL, Miller EN, Smith E, Ellis RJ, Valcour V, Singer E, Marra CM, Kolson D, Weihe J, Remmel R, Katzenstein D, Clifford DB (2007a) A multicenter trial of selegiline transdermal system for HIV-associated cognitive impairment. Neurology 69:1314-1321.

Schifitto G, Navia BA, Yiannoutsos CT, Marra CM, Chang L, Ernst T, Jarvik JG, Miller EN, Singer EJ, Ellis RJ, Kolson DL, Simpson D, Nath A, Berger J, Shriver SL, Millar LL, Colquhoun D, Lenkinski R, Gonzalez RG, Lipton SA (2007b) Memantine and HIV-associated cognitive impairment: a neuropsychological and proton magnetic resonance spectroscopy study. Aids 21:1877-1886.

Shen M, Thayer SA (1998) The cannabinoid agonist Win55,212-2 inhibits calcium channels by receptor-mediated and direct pathways in cultured rat hippocampal neurons. Brain Res 783:77-84.

Shi Y, Ethell IM (2006) Integrins Control Dendritic Spine Plasticity in Hippocampal Neurons through NMDA Receptor and Ca2+/Calmodulin-Dependent Protein Kinase II-Mediated Actin Reorganization. The Journal of Neuroscience 26:1813-1822.

Shin AH, Thayer SA (2013) Human immunodeficiency virus-1 protein Tat induces excitotoxic loss of presynaptic terminals in hippocampal cultures. Molecular and Cellular Neuroscience 54:22-29.

Shin AH, Kim HJ, Thayer SA (2012) Subtype selective NMDA receptor antagonists induce recovery of synapses lost following exposure to HIV-1 Tat. Br J Pharmacol 166:1002-1017.

Sodroski J, Rosen C, Wong-Staal F, Salahuddin SZ, Popovic M, Arya S, Gallo RC, Haseltine WA (1985) Trans-acting transcriptional regulation of human T-cell leukemia virus type III long terminal repeat. Science 227:171-173.

Speth C, Stockl G, Mohsenipour I, Wurzner R, Stoiber H, Lass-Florl C, Dierich MP (2001) Human immunodeficiency virus type 1 induces expression of complement factors in human astrocytes. J Virol 75:2604-2615.

Stevenson M (2003) HIV-1 pathogenesis. Nature Medicine 9:853-860.

Suarez S, Baril L, Stankoff B, Khellaf M, Dubois B, Lubetzki C, Bricaire F, Hauw JJ (2001) Outcome of patients with HIV-1-related cognitive impairment on highly active antiretroviral therapy. AIDS 15:195-200.

Tashiro A, Minden A, Yuste R (2000) Regulation of dendritic spine morphology by the rho family of small GTPases: antagonistic roles of Rac and Rho. Cereb Cortex 10:927-938.

Theodore S, Cass W, Dwoskin L, Maragos W (2012) HIV-1 protein Tat inhibits vesicular monoamine transporter-2 activity in rat striatum. Synapse 66:755-757.

Thyagarajan A, Ting AY (2010) Imaging Activity-Dependent Regulation of Neurexin-Neuroligin Interactions Using trans-Synaptic Enzymatic Biotinylation. Cell.

Togashi H, Abe K, Mizoguchi A, Takaoka K, Chisaka O, Masatoshi T (2002) Cadherin Regulates Dendritic Spine Morphogenesis. Neuron 35:77-89.

tom Dieck S, Sanmarti-Vila L, Langnaese K, Richter K, Kindler S, Soyke A, Wex H, Smalla KH, Kampf U, Franzer J-T, Stumm M, Garner CC, Gundelfinger ED (1998) Bassoon, a Novel Zinc-finger CAG/Glutamine-repeat Protein Selectively Localized at the Active Zone of Presynaptic Nerve Terminals. J Cell Biol 142:499-409.

Tovar KR, Westbrook GL (1999) The incorporation of NMDA receptors with a distinct

subunit composition at nascent hippocampal synapses in vitro. J Neurosci 19:4180-4188.

Tovar KR, Westbrook GL (2002) Mobile NMDA receptors at hippocampal synapses. Neuron 34:253-264.

Tozzi V, Balestra P, Lorenzini P, Bellagamba R, Galgani S, Corpolongo A, Vlassi C, Larussa D, Zaccarelli M, Noto P, Visco-Comandini U, Giulianelli M, Ippolito G, Antinori A, Narciso P (2005a) Prevalence and risk factors for human immunodeficiency virus–associated neurocognitive impairment, 1996 to 2002: Results from an urban observational cohort. J Neurovirol 11:265-273

Tozzi V, Balestra P, Serraino D, Bellagamba R, Corpolongo A, Piselli P, Lorenzini P, Visco-Comandini U, Vlassi C, Quartuccio ME, Giulianelli M, Noto P, Galgani S, Ippolito G, Antinori A, Narciso P (2005b) Neurocognitive impairment and survival in a cohort of HIV-infected patients treated with HAART. AIDS Res Hum Retroviruses 21:706-713.

UNAIDS JUNPoHA- (2010) Global report: UNAIDS report on the global AIDS epidemic 2010. In: WHO Library.

van Staveren WC, Markerink-van Ittersum M, Steinbusch HW, Behrends S, de Vente J (2005) Localization and characterization of cGMP-immunoreactive structures in rat brain slices after NO-dependent and NO-independent stimulation of soluble guanylyl cyclase. Brain Res 1036:77-89.

Waataja JJ, Kim HJ, Roloff AM, Thayer SA (2008) Excitotoxic loss of post-synaptic sites is distinct temporally and mechanistically from neuronal death. J Neurochem 104:364-375.

Wang HG, Lu FM, Jin I, Udo H, Kandel ER, de Vente J, Walter U, Lohmann SM,

Hawkins RD, Antonova I (2005) Presynaptic and postsynaptic roles of NO, cGK, and RhoA in long-lasting potentiation and aggregation of synaptic proteins. Neuron 45:389-403.

Wei P, Garber ME, Fang SM, Fischer WH, Jones KA (1998) A novel CDK9-associated C-type cyclin interacts directly with HIV-1 Tat and mediates its high-affinity, loop-specific binding to TAR RNA. Cell 92:451-462.

Westendorp MO, Frank R, Ochsenbauer C, Stricker K, Dhein J, Walczak H, Debatin KM, Krammer PH (1995) Sensitization of T cells to CD95-mediated apoptosis by HIV-1 Tat and gp120. Nature 375:497-500.

Wiedenmann B, Franke W (1985) Identification and localization of synaptophysin, an integral membrane glycoprotein of Mr 38,000 characteristic of presynaptic vesicles. Cell 41:1017-1028.

Wiley CA, Baldwin M, Achim CL (1996) Expression of regulatory and structural mRNA in the central nervous system. AIDS 10:943-947.

Wiley CA, Masliah E, Achim CL (1999) Measurement of CNS HIV burden and its association with neurologic damage. Adv Neuroimmunol 4:319-325.

Williams K (1993) Ifenprodil Discriminates Subtypes of the N-Methyl-D-aspartate Receptor - Selectivity and Mechanisms at Recombinant Heteromeric Receptors. Mol Pharmacol 44:851-859.

Wong EHF, Kemp JA, Priestley T, Knight AR, Woodruff GN, Iverson LL (1986) The anticonvulsant MK-801 is a potent N-methyl-D-aspartate antagonist. Proc Natl Acad Sci USA 83:7104-7108.

Wyatt R, Kwong PD, Desjardins E, Sweet RW, Robinson J, Hendrickson WA, Sodroski JG (1998) The antigenic structure of the HIV gp120 envelope glycoprotein. Nature 393:705-711.

Xia P, Chen H-sV, Zhang D, Lipton SA (2010) Memantine Preferentially Blocks Extrasynaptic over Synaptic NMDA Receptor Currents in Hippocampal Autapses. J Neurosci 30:11246-11250.

Xiao H, Neuveut C, Lee H, Benkirane M, Rich EA, Murphy PM, Jeang K-T (2000) Selective CXCR4 antagonism by Tat: implications for in vivo expansion of coreceptor use by HIV-1. Proc Natl Acad Sci U S A 97:11466-11471.

Zauli G, Gibellini D, Caputo A, Bassini A, Negrini M, Monne M, Mazzoni M, Capitani S (1995) The human immunodeficiency virus type-1 Tat protein upregulates Bcl-2 gene expression in Jurkat T-cell lines and primary peripheral blood mononuclear cells. Blood 86:3823-3834.

Zhao Y, Navia BA, Marra CM, Singer EJ, Chang L, Berger J, Ellis RJ, Kolson DL, Simpson D, Miller EN, Lipton SA, Evans SR, Schifitto G (2010) Memantine for AIDS dementia complex: open-label report of ACTG 301. HIV Clin Trials 11:59-67.

Ziv NE (2001) Recruitment of Synaptic Molecules during Synaptogenesis. The Neuroscientist 7:365-370.

Ziv NE, Garner CC (2004) Cellular and molecular mechanisms of presynaptic assembly. Nat Rev Neurosci 5:385-399.